INVESTIGATING THE CONTRIBUTION OF ABERRANT SPHINGOSINE 1-PHOSPHATE SIGNALLING TO THE PATHOGENESIS OF DIFFUSE LARGE B-CELL LYMPHOMA

BY

LAUREN LUPINO

A thesis submitted to

The University of Birmingham

for the degree of

DOCTOR OF PHILOSOPHY

Institute of Cancer and Genomic Sciences
College of Medical and Dental Sciences
University of Birmingham
September 2016

ABSTRACT

There is an increasing body of evidence indicating an important role for the bioactive signalling lipid S1P (sphingosine 1-phosphate) in cancer. Sphingosine kinase-1 (SPHK1), one of the enzymes responsible for the synthesis of S1P, is reported to be overexpressed in many cancer types; in many cases correlating with increased tumour grade and reduced patient survival. However, the expression of SPHK1, and how it might contribute to lymphomagenesis, has not previously been explored in diffuse large B-cell lymphoma (DLBCL).

In chapter 3, I show that SPHK1 overexpression in DLBCL correlates with the expression of known tumour-angiogenic genes. I also describe the characterisation of human umbilical vein endothelial cells (HUVEC) as an *in vitro* model with which to study the impact of S1P on the endothelial cell transcriptome and to explore the extent to which these changes can be observed in primary DLBCL.

In chapter 4, I explore the effects of S1P on the transcription of endothelial cells with a focus on genes associated with leukocyte recruitment. I confirm the S1P-induced upregulation of chemokines and adhesion molecules in HUVEC and show that SPHK1 expression correlates with the expression of stromal cell gene signatures in primary DLBCL.

Finally, in chapter 5, I show that I can inhibit S1P-induced signalling in HUVEC with Sphingomab, a monoclonal antibody against S1P. Additionally, I validate the A20 syngeneic model of lymphoma as a relevant system which could be used to study the potential therapeutic targeting of SPHK1-S1P signalling in DLBCL.

ACKNOWLEDGMENTS

I would like to thank the Traynor Foundation who generously funded this project.

My deepest thanks to Professor Paul Murray for his supervision throughout my PhD. His guidance of my project, advice and teaching have been invaluable to me. I thank him for his patience and for always offering a listening ear to my new thoughts and ideas. His passion and enthusiasm for the work kept me motivated and positive. I would also like to thank Professor Martin Rowe and the late Professor Ciaran Woodman for their additional support and guidance. I have been very fortunate to work amongst some incredible minds and I will look back at the great discussions the four of us had together with fond memories.

I would also like to thank all past and present members of the PGM group, not only for their generous help in the lab but also for being such a kind and friendly group of people. I offer my appreciation to Dr Maha Ibrahim, for many an hour at the microscope assessing my slides and to Tracey for the animal work. A special mention to Kate Vrzalikova, my lab supervisor, who took me on as a fresh-faced new PhD student. She has given me practical support to develop my lab skills and also a fantastic friendship, sharing many laughs together.

I will be forever grateful to Dr Sally Roberts who first gave me the opportunity to realise my passion for this work. Without her, none of this would have been possible.

Personal thanks to my wonderful friends who always make me smile.

Lastly, I would like to thank my family for their unconditional love and encouragement. Throughout my life they have always offered immense support and without them I wouldn't be where I am today.

CONTENTS

LIST OF FIGURES

LIST OF TABLES

LIST OF ABBREVIATIONS

ABC DLBCL	activated B-cell like DLBCL
AID	activation-induced cytidine
BCL2	B-cell lymphoma 2
BCL6	B-cell lymphoma 6
BCR	B cell receptor
BLIMP1	B lymphocyte induced maturation protein 1
BLNK	B-cell linker
BTK	Bruton's tyrosine kinase
CARD11	caspase recruitment domain-containing protein 11
CBM	CARD11, BCL10 and MALT1
cDNA	complementary DNA
CPM	counts per million
CSR	class switch recombination
DLBCL	diffuse large B cell lymphoma
DMSO	dimethyl sulphoxide
ECGS	endothelial cell growth supplement
EDG	endothelial differentiation gene
ELISA	enzyme-linked immunosorbent assay
ERK	extracellular signal-regulated kinase
FBS	fetal bovine serum
FDC	follicular dendritic cell

FGF	fibroblast growth factor
GC	germinal centre
GCB DLBCL	germinal centre B-cell like DLBCL
GPCR	G protein coupled receptor
H&E	haematoxylin and eosin
HDAC	histone deacetylase
HIF	hypoxia-inducible factor
hpf	high power field
HUVEC	human umbilical vein endothelial cells
Ig	immunoglobulin
IHC	immunohistochemistry
IKK	NF-κB inhibitor kinase
IL6	interleukin 6
IL8	interleukin 8
IPI	International Prognostic Index
IRF	interferon regulatory factor
ITAM	immunoreceptor tyrosine-based activation motif
IκB	inhibitor of NF-κB
JAK	Janus-kinase
MAPK	mitogen activated protein kinase
mTOR	mechanistic target of rapamycin
NF-κB	nuclear factor-kappaB

NHL	non-Hodgkin lymphoma
P/S	penicillin/streptomycin
PARP	poly ADP-ribose polymerase
PBS	phosphate buffered saline
PDGF	platelet derived growth factor
pERK	phosphorylated ERK
PI3K	phosphoinositide 3-kinase
PKC	protein kinase C
PLC	phospholipase C
PRC2	polycomb repressive complex 2
PRDM1	PR domain zinc finger protein 1
pSPHK1	phosphorylated SPHK1
PTEN	phosphate and tensin homologue
qPCR	quantitative real time polymerase chain reaction
RCHOP	rituximab, cyclophosphamide, doxorubicin, vincristine and prednisone
RNAseq	RNA sequencing
S1P	sphingosine 1-phosphate
S1PR	sphingosine 1-phosphate receptor
SFK	SRC-family kinase
SHM	somatic hypermutation
SPHK	sphingosine kinase
STAT	signal transducer and activator of transcription

SYC	spleen tyrosine kinase
TBS	tris buffered saline
TNFα	tumour necrosis factor α
TRAF2	TNF receptor-associated factor 2
VEGF	vascular endothelial growth factor
WHO	World Health Organisation

CHAPTER ONE

INTRODUCTION

1.1 Diffuse large B cell lymphoma

1.1.1 Epidemiology

Non-Hodgkin lymphomas (NHL) are malignant cellular proliferations which arise from normal cells at different stages during the process of B cell development. Diffuse large B cell lymphoma (DLBCL) is the most common type of NHL accounting for approximately 30% of cases (Project, 1997). Men are slightly more susceptible than woman and the most common age of diagnosis is in the late 60s, although the disease can occur at any age (Novelli et al., 2013, Cancer Research UK, 2013). DLBCL is a highly heterogeneous disease both biologically and clinically. The disease can be nodal and/or extranodal and is defined by the World Health Organisation (WHO) as, "a diffuse proliferation of large B lymphoid cells whose nuclei are equal to or exceeding normal macrophage nuclei or more than twice the size of a normal lymphocyte" (Swerdlow, 2008).

The 2016 revision of the WHO classification of lymphoid neoplasms lists a large number of distinct DLBCL subentities, due to the presence of distinct clinical and/or molecular features or the propensity to affect distinct anatomical sites (Table 1.1) (Swerdlow et al., 2016). However, a significant proportion of DLBCL does not fit into these subgroups, which are referred to as DLBCL, not otherwise specified (DLBCL-NOS) (Table 1.1) (Swerdlow et al., 2016). Many studies have attempted to subdivide DLBCL-NOS based on molecular differences. Unless otherwise stated, DLBCL refers to DLBCL-NOS in this thesis.

Table 1.1: 2016 WHO classification of DLBCL. (Swerdlow et al., 2016). *=provisional entity

Diffuse large B-cell lymphoma, not otherwise specified DLBCL-NOS
Germinal centre B-cell type
Activated B-cell type
T-cell/histiocyte-rich large B-cell lymphoma
Primary DLBCL of the central nervous system (CNS)
Primary cutaneous DLBCL, leg type
EBV+ DLBCL, NOS
DLBCL associated with chronic inflammation
Primary mediastinal (thymic) large B-cell lymphoma
Intravascular large B-cell lymphoma
ALK+ large B-cell lymphoma
Plasmablastic lymphoma
Primary effusion lymphoma
HHV8+ DLBCL, NOS*
High-grade B-cell lymphoma, with MYC and BCL2 and/or BCL6 rearrangements
High-grade B-cell lymphoma, NOS
B-cell lymphoma, unclassifiable, with feature intermediate between DLBCL and classical Hodgkin lymphoma

1.1.2 Molecular subgroups of DLBCL

1.1.2.1 Introduction

Insights into the molecular biology of DLBCL were initially made possible through the use of gene expression microarrays, which provide a global profile of mRNA expression. From this, histologically indistinguishable molecular subtypes of DLBCL were identified that originate from lymphocytes at different developmental stages and use different oncogenic signalling pathways (Alizadeh et al., 2000). Before describing these molecular subgroups of DLBCL, it is first important to understand the process of normal B cell development and B cell receptor (BCR) signalling.

1.1.2.2 Normal B-cell development

B lymphocytes are produced in the bone marrow, and B cell development begins with rearrangement of the variable regions of the immunoglobulin (Ig) heavy and light chain genes to form a functional BCR. This requires double strand DNA breaks which are mediated by the recombination activating genes 1, 2 (RAG1 and RAG2) and resolved through the non-homologous end joining repair process (Fugmann S, 2000). This process is known as VDJ recombination and results in a highly diverse repertoire of Ig genes which encode the BCR of each B cell (Dudley et al., 2005). Once the BCR is expressed, the B cells leave the bone marrow and circulate through blood and lymphoid tissue as mature, naïve B cells where they can encounter antigen.

Upon binding of antigen to the BCR the naïve B cells migrate to secondary lymphoid organs such as lymph nodes, Peyer's patches, tonsils and spleen (MacLennan, 1994, Klein and Dalla-

Favera, 2008). First, naive B cells migrate to the T-cell-rich zone of secondary lymphoid organs where they become fully activated with the help of CD4+ T cells (MacLennan, 1994). These activated B cells move to the primary follicle, a structure made up of B cells within a network of follicular dendritic cells (FDCs). The B cells then enter the next stage of differentiation and start to rapidly proliferate leading to the development of the germinal centre (GC) (Figure 1.1).

In addition to B cell expansion, a process called somatic hypermutation (SHM) occurs in the GC. SHM involves modification of the Ig variable region through random point mutations and the introduction of insertions or deletions producing antibodies with a higher affinity for antigen (Goossens et al., 1998, Kocks and Rajewsky, 1989, Gearhart and Bogenhagen, 1983) (Figure 1.1). These reactions are mediated by the enzyme, activation-induced cytidine deaminase (AID) (Muramatsu et al., 2000). Cells with high affinity for antigen are selected by receiving survival signals from T helper cells and FDCs, whereas those with low affinity or deleterious mutations undergo apoptosis (Teng and Papavasiliou, 2007) (Figure 1.1). Surviving cells can go through another process known as class switch recombination (CSR), resulting in replacement of the IgM constant region with IgG, IgA or IgE. This process involves the generation of double strand breaks, deletion of unwanted sequence and the subsequent re-joining of the remaining gene segments within the heavy chain locus. As the variable region is not altered, this process does not affect the affinity of the Ig for antigen, but it can now interact with different effector molecules (Dudley et al., 2005). CSR also requires AID which is regulated by interferon regulatory factor 4 (IRF4) (Klein et al., 2006). IRF4 is induced by antigen receptor engagement and CD40 signalling through activation of the nuclear factor-kappaB (NF-κB) pathway leading to IRF4 promotor activation (Shaffer, 2009).

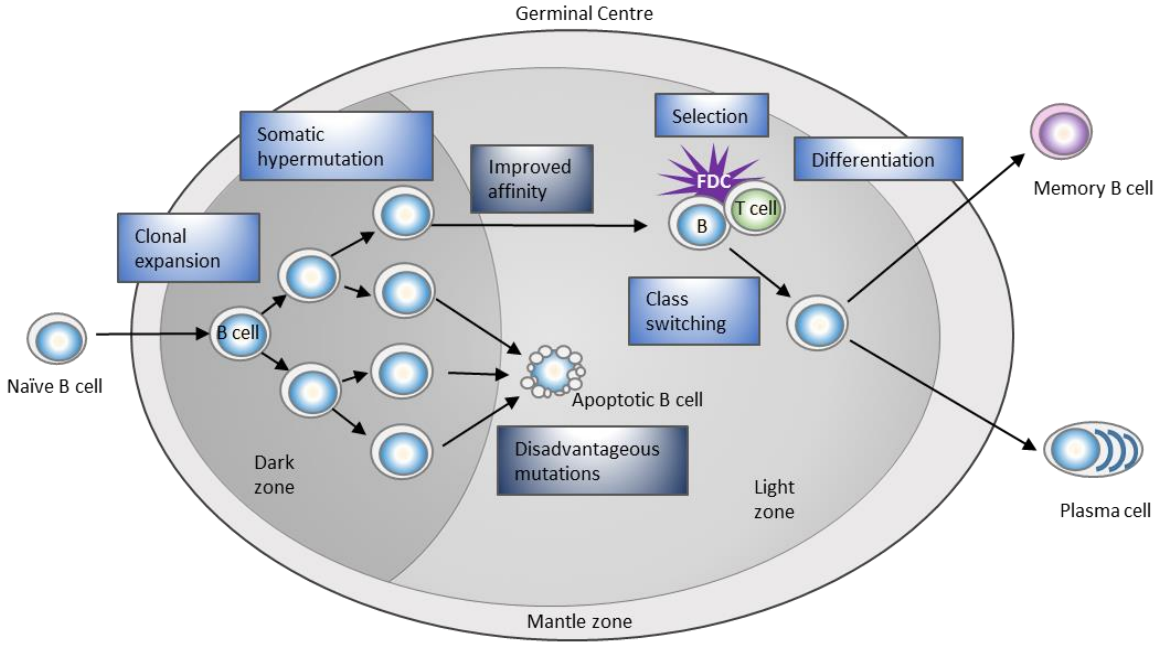

Figure 1.1: B cell development in the GC. A naïve B cell encounters antigen and then migrates to secondary lymphoid follicles. Following T cell stimulation, the B cells undergo clonal expansion and somatic hypermutation within the dark zone of the GC. The B cells then migrate to the light zone where they are selected for high affinity of their BCR through interaction with T helper cells and follicular dendritic cells, escaping the default apoptosis pathway of GC B cells. Selected GC B cells can then undergo class switching before differentiating into memory B cells or plasma cells.

Histologically, the GC can be divided into the dark zone made up of proliferating B cells undergoing SHM referred to as centroblasts, and a light zone in which negative selection and CSR of B cells, known as centrocytes, occurs. GC B cells traffic between the dark and light zones undergoing multiple rounds of proliferation and selection (Schwickert et al., 2007).

Cells that successfully emerge from the GC enter the final stage of B cell differentiation where they differentiate either into memory cells which provide a rapid response following subsequent antigen encounters, or plasma cells, which secrete antibody (Figure 1.1).

There are many transcription factors which are involved in establishing the GC phenotype such as B-cell lymphoma 6 (BCL6), OCT-binding factor 1 (OBF1), SPIB, BTB domain and CNC homolog 2 (BACH2) and interferon-regulatory factor 8 (IRF8). Of these, BCL6 has been referred to as the master transcriptional regulator of centroblasts as it is involved in the repression of multiple cellular processes to allow the hypermutation of centroblasts in the dark zone of the GC (Basso and Dalla-Favera, 2010, Basso and Dalla-Favera, 2012) (Figure 1.2A). The down regulation of BCL6 is required for GC exit (Shaffer et al., 2000). Signalling through the BCR leads to the downregulation of BCL6 expression via mitogen activated protein kinase (MAPK) phosphorylation which targets BCL6 for ubiquitin mediated proteosomal degradation (Niu et al., 1998). Signalling through CD40 also results in transcriptional silencing of BCL6 as a result of NF-κB mediated induction of IRF4, which represses BCL6 expression by binding to its promoter region (Saito et al., 2007). The downregulation of BCL6 derepresses B lymphocyte induced maturation protein 1 (BLIMP1) which is required for plasma cell development (Turner et al., 1994) (Figure 1.2B)

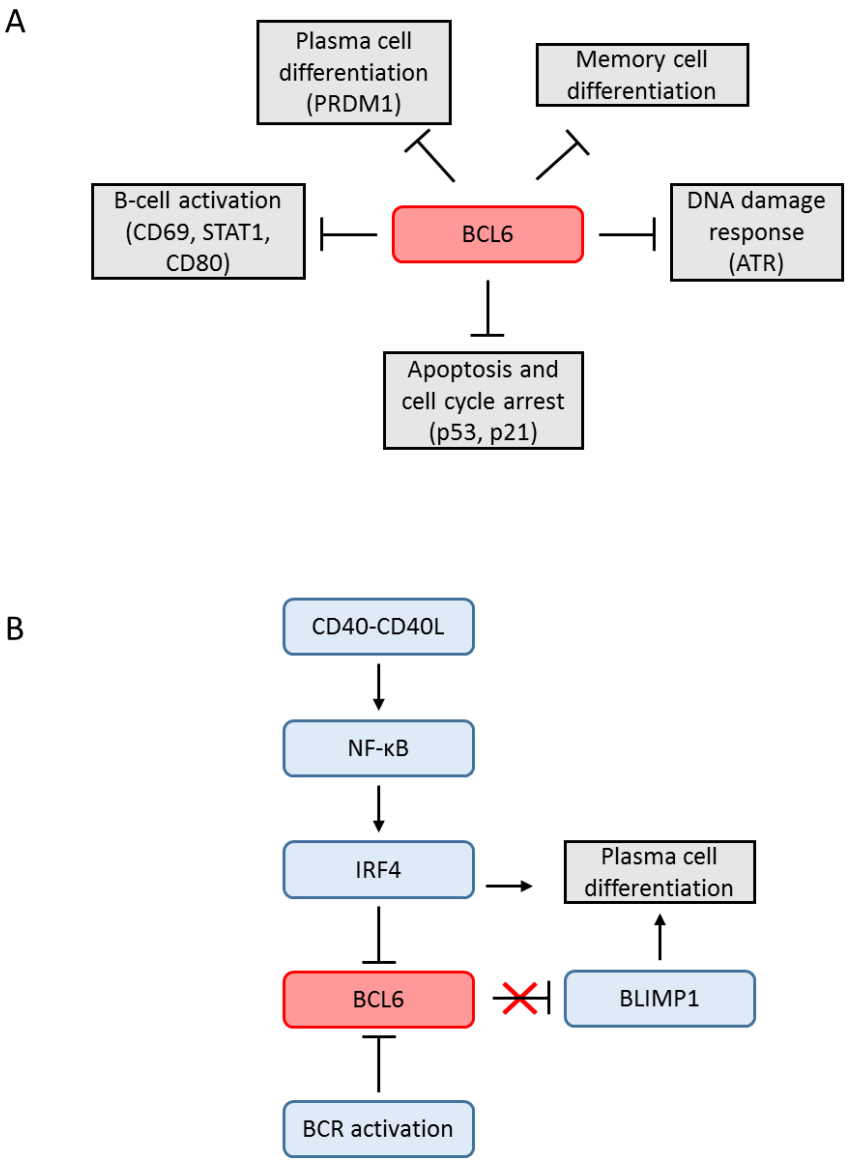

Figure 1.2: BCL6 in the GC: (A) BCL6 impairs premature B cell activation and differentiation and promotes tolerance of DNA damage in the GC centroblasts. (B) Down regulation of BCL6 is required for GC exit and differentiation to plasma cells. BCL6 is downregulated by transcriptional repression of BCL6 gene by IRF4 due to CD40 stimulation and post transcriptionally by ubiquitination mediated BCL6 degradation following BCR stimulation. BCL6 downregulation releases the gene which encodes BLIMP1 (PRDM1) from repression which is required for plasma cell differentiation.

The distinct modifications of B cell DNA during B cell development such as SHM and CSR are essential for the generation of a normal immune response but they also cause DNA damage which can lead to the development of lymphomas.

1.1.2.3 Normal BCR signalling

The BCR is a multimeric complex comprised of membrane-bound Ig associated with a disulphide linked heterodimer of CD79a and CD79b. BCR stimulation induces activation of SRC-family kinase (SFK) which phosphorylates immunoreceptor tyrosine-based activation motifs (ITAMs) in the cytoplasmic tails of CD79a and CD79b which leads to the recruitment of spleen tyrosine kinase (SYC). The signal is then transduced to early effectors of the signalling response such as Bruton's tyrosine kinase (BTK) and phospholipase C-gamma 2 (PLCγ), through the adaptor protein B-cell linker (BLNK) (reviewed in: Packard and Cambier, 2013, Rickert, 2013). BTK phosphorylates PLCγ2 leading to downstream responses including calcium signalling, protein kinase C (PKC), NF-κB and extracellular signal-regulated kinase (ERK) activation (Figure 1.3). NF-κB activation is due to PKCβ phosphorylation of caspase recruitment domain-containing protein 11 (CARD11), leading to the formation of the CBM signalling complex (CARD11, BCL10 and MALT1) (reviewed in: Packard and Cambier, 2013, Rickert, 2013) (Figure 1.3). The CBM signalling complex activates NF-κB inhibitor kinase (IKK) which leads to the phosphorylation and degradation of inhibitor of NF-κB (IκB). IκB masks the nuclear localisation signal of p50-p65 NF-κB transcription factors sequestering them in the cytoplasm. Following IκB degradation, p50-p65 NF-κB heterodimers accumulate in the nucleus and activate their target genes (Figure 1.3).

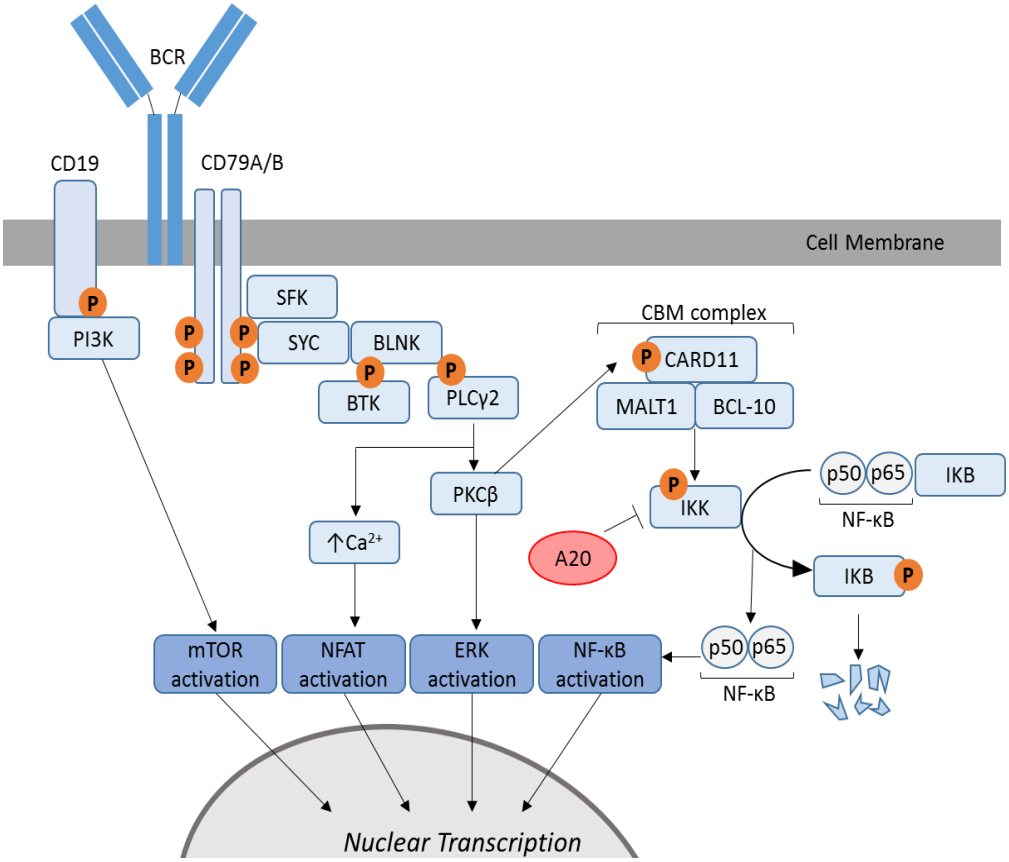

Figure 1.3: Overview of BCR signalling. Activation of the BCR leads to a signalling cascade which results in the activation of the NF-κB, mTOR, ERK and NFAT pathways. Signalling is initiated when a SRC-family kinase (SFK) phosphorylates ITAM motifs of the BCR subunits CD79A and CD79B which leads to the recruitment and activation of SYK. SYK activates the B cell linker (BLNK) adaptor protein, which serves as a scaffold for the Bruton's tyrosine kinase (BTK) mediated phosphorylation of phospholipase Cγ2 (PLCγ2). PLCγ2 in turn promotes the influx of calcium ions (Ca^{2+}) and activation of NFAT pathway; as well as activation of protein kinase Cβ (PKCβ) which initiates ERK signalling. Additionally PKCβ phosphorylates CARD11 causing it to recruit BCL10 and MALT1 into a multiprotein 'CBM' complex that activates the NF-κB inhibitor kinase (IKK). Activated IKK leads to the phosphorylation and the degradation of inhibitor of NF-κB (IκB) and the nuclear translocation of p50-p65 NF-κB heterodimer. In parallel, PI3K is activated by recruitment to the B-cell co-receptor CD19 activating the mTOR pathway. A20 is an NF-κB target gene and a negative regulator of the NF-κB signal.

In parallel, phosphoinositide 3-kinase (PI3K) is activated by recruitment to B cell co-receptor CD19 leading to the activation of the mechanistic target of rapamycin (mTOR) pathway. The activation of these many signalling pathways leads to B cell growth, proliferation and survival (reviewed in: Packard and Cambier, 2013, Rickert, 2013).

1.1.2.4 Cell of origin molecular subtypes

SHM is detected in DLBCL which suggests that DLBCL arises from B cells which have been through a GC reaction. Two molecularly distinct forms of DLBCL have been identified which have gene expression profiles indicative of different stages of B cell development. These are the germinal centre B-cell like DLBCL (GCB DLBCL) and the activated B-cell like DLBCL (ABC DLBCL) (Alizadeh et al., 2000, Rosenwald et al., 2003, Rosenwald et al., 2002).

GCB DLBCL

GCB DLBCLs are believed to be derived from GC B cells, as the genes expressed by this sub group, such as CD10, LMO2 and the transcriptional repressor BCL6, are highly expressed in normal GC B cells (Alizadeh et al., 2000, Rosenwald et al., 2002).

Many oncogenic signalling pathways are predominantly expressed by only one DLBCL subtype (Figure 1.4). A frequent genetic abnormality detected in GCB DLBCL is the t(14:18) translocation which deregulates the expression of the anti-apoptotic gene B-cell lymphoma 2 (BCL2). This translocation has been detected in approximately 45% of GCB DLBCL tumours but not in ABC DLBCL (Rosenwald et al., 2002).

Mutations exclusively found in GCB DLBCL include those affecting the methyltransferase, EZH2, detectable in approximately 20% of cases (Morin et al., 2010). EZH2 is the catalytic

subunit of the polycomb repressive complex 2 (PRC2) and mutation leads to a gain of function and increased methylation of histone 3, resulting in transcriptional silencing of key regulatory genes (Beguelin et al., 2013, Sneeringer et al., 2010). EZH2 is a master regulator of the GCB cell phenotype and co-operates with BCL6 to mediate lymphoma development in GCB DLBCL (Beguelin et al., 2013, Caganova et al., 2013).

Ten to fifteen percent of GCB DLBCL harbour deletions in the tumour suppressor gene PTEN (phosphate and tensin homologue) and a further 15% show amplification of microRNA cluster miR-17-92, which suppresses expression of PTEN (Xiao et al., 2008, Lenz et al., 2008c). The loss of PTEN expression was detected by immunohistochemistry (IHC) in 55% of GCB DLBCL cases compared to only 14% of non-GCB cases (Pfeifer et al., 2013). PTEN deletion results in constitutive activation of the PI3K/AKT/mTOR pathway indicating that deregulation of this pathway plays an important role in the progression of this subtype.

ABC DLBCL

The gene expression profile of the ABC subtype suggests that this type is derived from B cells that are in the process of differentiating into plasma cells, as they express genes characteristically expressed in plasma cells, such as the transcription factor XBP1 (X-box binding protein 1), the master regulator of Ig secretion (Wright et al., 2003, Shaffer et al., 2004). However, the full plasma cell differentiation is blocked. Inactivating mutations and deletions of PRDM1 (PR domain zinc finger protein 1), the gene which encodes BLIMP1 are present in approximately on quarter of ABC DLBCL patients (Tam et al., 2006). Furthermore, approximately one quarter of ABC DLBCL patients show BCL6 translocations and 26% show gain of SPIB, both of which repress the expression of BLIMP1 (Figure 1.4).

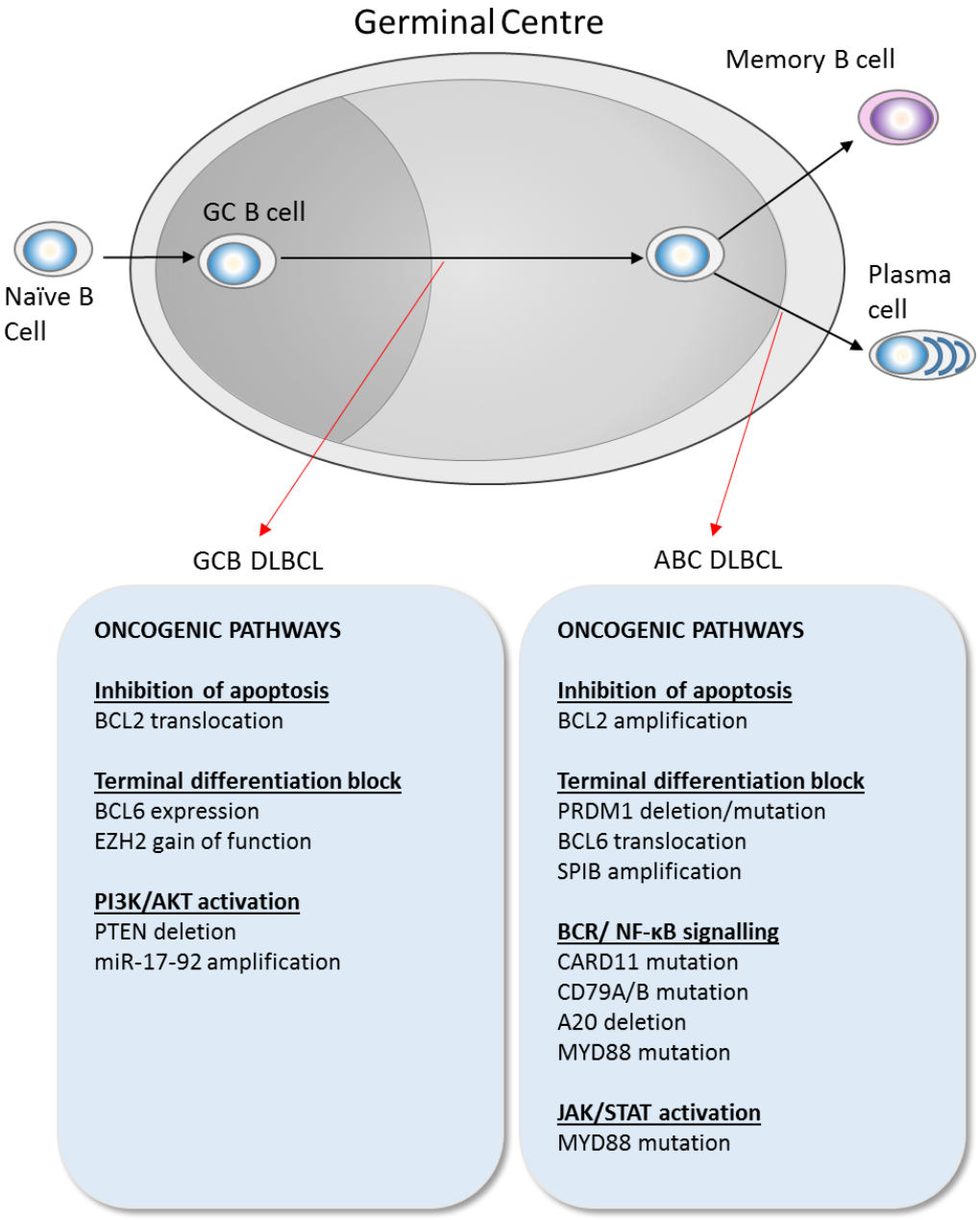

Figure 1.4: Molecular subtypes of DLBCL: On the basis of gene expression profiling, DLBCL can be divided into two molecular subtypes germinal centre B cell like (GCB DLBCL) and activated B cell like (ABC DLBCL). GCB DLBCL are believed to arise from GC B cells, whereas ABC DLBCL from post GC B cells in the process of differentiating in to plasma cells. The main oncogenic pathways are listed.

A hallmark of ABC DLBCL is the constitutive activation of the NF-κB pathway, which promotes cell survival, proliferation and inhibits apoptosis (Davis et al., 2010). Constitutive NF-κB activation is largely due to the constitutive formation of the CBM signalling complex which leads to IKK activation and degradation of IκB, as described earlier (Figure 1.3). In ABC DLBCL the CBM complex is constitutively activated by a number of mechanisms. Approximately 10% of ABC DLBCL patients harbour activating mutations of CARD11, whereas those with wildtype CARD11 have a chronic active form of BCR signalling (Lenz et al., 2008a). Mutations in CD79A and CD79B genes have been detected in approximately 20% of ABC DLBCL which result in a chronic active BCR signal (Davis et al., 2010). The importance of the constitutive activation of BCR signalling in ABC DLBCL with wild type CARD11 is highlighted by the dependence of ABC DLBCL cell lines upon the activation of SYC, BTK and PKCβ (Davis et al., 2010).

Inactivation of the NF-κB negative regulator A20 has been detected in around 30% of cases which results in loss of inhibition of NF-κB signalling (Figure 1.3). When A20 was reintroduced into cell lines carrying biallelic inactivation of the gene it caused apoptosis and cell growth arrest, indicating its role as a tumour suppressor (Compagno et al., 2009). The functional importance of the NF-κB pathway in ABC DLBCL was shown by Davis et al. (2001) who revealed that interference of the NF-κB signalling pathway, using small interfering molecules, was toxic to ABC DLBCL cell lines and but not to GCB DLBCL cell lines. These data strongly support the view that chronic active BCR signalling plays a vital role in the pathogenesis of the ABC subtype of DLBCL.

Mutations in MYD88 have been detected in >30% of ABC DLBCL tumours resulting in the upregulation of the NF-κB and Janus-kinase-signal transducer and activator of transcription (JAK-STAT) pathways (Ngo et al., 2011).

BCL2 overexpression is also detected in ABC DLBCL but by mechanisms distinct from those observed in GCB DLBCL, including transcriptional upregulation and gene amplification (Lenz et al., 2008c).

1.1.2.5 Identification of GCB DLBCL and ABC DLBCL subtypes

Due to the ongoing clinical trials to determine whether DLBCL subtype-specific therapies should be incorporated into clinical practice (discussed later; Section 1.1.3.4), the 2016 revision of the WHO classification of lymphoid neoplasms requires the identification of the GCB and ABC subtypes of DLBCL (Swerdlow et al., 2016). IHC algorithms are commonly used to subdivide DLBCL into subtypes. The most common is the Hans algorithm which uses CD10, BCL6 and IRF4 as markers (Hans et al., 2004) (Figure 1.5). Subgroups defined by IHC algorithms do not completely correlate with subgroups defined by gene expression profiling (~87% correlation, Hans algorithm), partly due to their oversimplification and the poor reproducibility of IHC (Meyer et al., 2011). Nevertheless, IHC algorithms will be considered acceptable according to the 2016 revision of the WHO classification of lymphoid neoplasms, due to the unavailability of gene expression profiling as a routine clinical test (Swerdlow et al., 2016). Newer methods based on quantification of RNA transcripts using paraffin-embedded tissue has proven to provide concordant results with gene expression profiling and capture the prognostic impact of cell-of-origin classification (Scott et al., 2014, Scott et al., 2015).

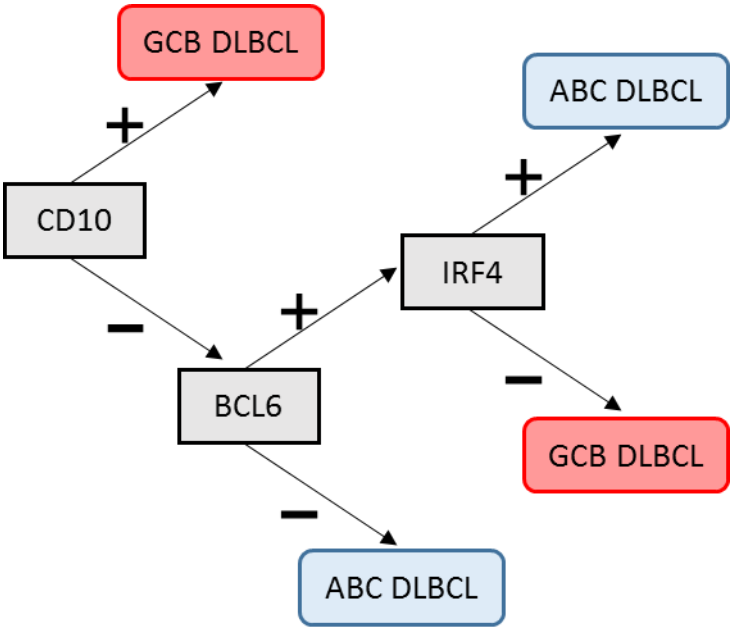

Figure 1.5: Hans algorithm for the determination of DLBCL subtypes. It is based on the IHC analysis of markers CD10, BCL6 and IRF4 (Hans et al,. 2004)

These methods are still not accessible to most laboratories, however, may represent a promising alternative to IHC algorithms in the future.

1.1.2.6 Differences in DLBCL survival

Overall survival is more favourable in those patients with GCB DLBCL compared to ABC DLBCL (3-year progression free survival of ~75% vs 40%, $p<0.001$, respectively) (Rosenwald et al., 2002, Rosenwald et al., 2003) (Figure 1.6).

Although the addition of the anti-CD20 antibody rituximab to standard chemotherapy combining cyclophosphamide, doxorubicin, vincristine and prednisone (R-CHOP) has greatly improved survival in patients, more than 50% of patients with ABC DLBCL will eventually succumb to their disease (Lenz et al., 2008b, Coiffier et al., 2002).

Lenz and colleagues (2008b) profiled gene expression in pre-treatment whole DLBCL biopsy specimens to identify gene expression signatures that correlated with differences in survival following treatment. They showed that the expression profiles were derived from CD19 negative non-malignant cells. These 'stromal signatures' were variably present in both GCB and ABC DLBCL which suggests that these signatures represent biological features of the tumour microenvironment which can be acquired during the pathogenesis of both DLBCL subtypes. This highlights that survival after treatment is influenced not only by the molecular signature of the tumour cells, but also by the composition of the tumour microenvironment.

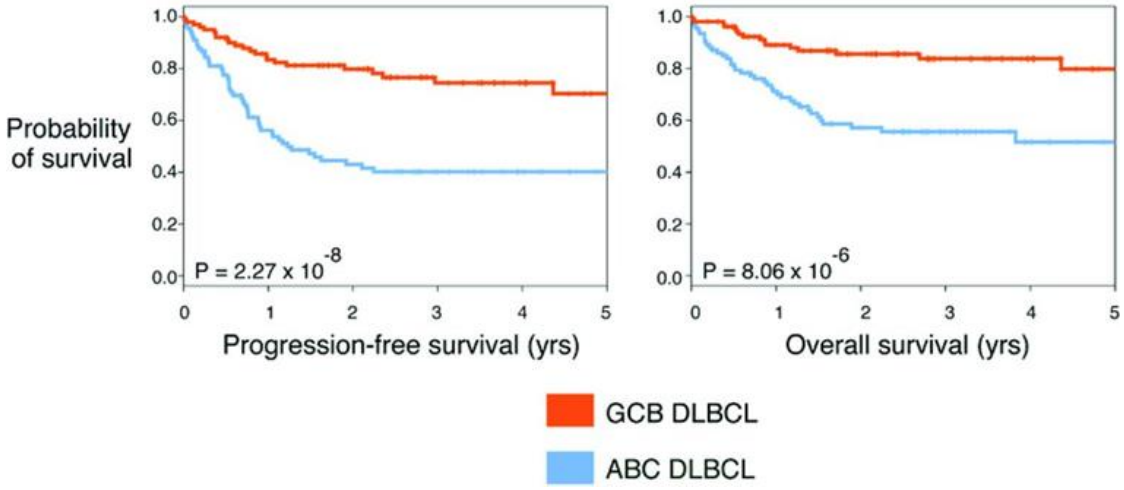

Figure 1.6: Differences in survival between GCB DLBCL and ABC DLBCL: Kaplan-Meier curves of survival rates for patients with a molecular diagnosis of the GCB or ABC DLBCL subtype after R-CHOP therapy. Patients with GCB DLBCL have a higher probability of progression free survival and overall survival than patients with ABC DLBCL (Reproduced from: Wilson, 2013).

1.1.2.7 Role of MYC and BCL2

MYC oncogene rearrangement is a hallmark of Burkitt lymphoma and can also be identified in approximately 5-15% of patients with DLBCL. MYC translocation is frequently associated with BCL2 and/or BCL6 translocation, referred to as “double-hit” and “triple-hit” lymphomas, respectively. Double-hit and triple-hit lymphomas have a very poor prognosis with a median overall survival of less than 12 months (Perry et al., 2014, Johnson et al., 2012). They are included in the updated 2016 WHO classification in the new category of, “high-grade B-cell lymphoma, with MYC and BCL2 and/or BCL6 rearrangements” (Table 1.1) (Swerdlow et al., 2016).

Overexpression of MYC protein can be detected by IHC in 30-50% of DLBCL patients and is associated with BCL2 expression in 20-35% of cases (Johnson et al., 2012, Green et al., 2012). The majority of these tumours do not carry MYC or BLC2 alterations and are referred to as “dual-expressers.” “Dual-expressers” have a significantly poorer outcome than patients who express only one or neither protein. MYC and BCL2 overexpression can be detected in both GCB and ABC DLBCL, although it is more common in ABC DLBCL and is suggested to contribute to its inferior survival (Hu et al., 2013).

1.1.3 Treatment of DLBCL

1.1.3.1 Prognostic factors

The identification of distinct molecular subtypes has not yet been translated into changes to clinical practice. The International Prognostic Index (IPI), developed prior to the addition of rituximab, remains the primary clinical tool to predict outcome of patients with aggressive

NHL (Shipp et al., 1993). This is based on the number of negative prognostic factors present at diagnosis which include:

- Age greater than 60
- Stage III or IV disease
- Elevated lactate dehydrogenase (LDH) serum level
- Eastern Cooperative Oncology Group (ECOG) performance status of 2 or more
- More than one extranodal site of disease

One point is assigned for each of these factors and the sum of the points classifies patients into one of four risk groups with predicted five-year overall survival rates ranging from 26% to 73% (Shipp et al., 1993). The IPI has been reassessed in patients treated with rituximab-based chemotherapy and has been shown to retain its prognostic usefulness (Ziepert et al., 2010). However, the IPI fails to identify high-risk patients, as all prognostic IPI categories have a higher than 50% chance of cure following treatment with R-CHOP. More recently, an enhanced IPI has been proposed using data from the National Comprehensive Cancer Network (NCCN-IPI), which was validated within a cohort of patients treated in British Colombia (Zhou et al., 2014). The NCCN-IPI uses the same five variables as the IPI, although the categories of age and LDH levels are further refined and the specific sites of extra nodal involvement, such as bone marrow, CNS, liver/gastrointestinal tract and lung are identified as negative factors, rather than the number of sites. The NCCN-IPI was better able to identify a high-risk group

with a 5 year overall survival of 33%; however this represented only 8-14% of patients (Zhou et al., 2014).

1.1.3.2 Front line therapy

Approximately 75% of DLBCL patients present with advanced stage disease which is defined as Ann Arbor stages 3 and 4 or stages 1 and 2 with B-symptoms or bulky disease (> 10 cm). The CHOP chemotherapy regimen remains the main treatment modality as more intensive combinations did not show additional benefit (Fisher et al., 1993). The addition of rituximab to the CHOP backbone dramatically improved outcomes in patients over 60 years of age resulting in a 16% improvement to the 10 year overall survival in the first trial (Coiffier et al., 2010, Coiffier et al., 2002). As a result of this study and of many additional trials, R-CHOP is now established as the standard of care (Habermann et al., 2006, Pfreundschuh et al., 2008, Pfreundschuh et al., 2006, Sehn et al., 2005). Consolidative radiation therapy following chemotherapy is frequently used in an attempt to eradicate potential residual disease. There have been no randomised trials assessing the role of this therapy in DLBCL patients in the rituximab era. However, retrospective analyses have indicated a benefit for radiation therapy following chemotherapy (Dorth et al., 2012, Phan et al., 2010, Held et al., 2014).

1.1.3.3 Salvage therapy

Although the standard therapy for many DLBCL patients is curative, approximately 10-15% of patients exhibit refractory disease and an additional 20-25% relapse following an initial response (Friedberg, 2011). The clinical approach to relapsed/refractory DLBCL includes high-dose therapy and autologous stem cell transplantation (HD-ASCT). However, due to co

morbidities and advanced age only around half of relapsed/refractory DLBCL patients are eligible for this intensive treatment. Of those eligible patients only half are sensitive to salvage therapy and receive transplant and of those, only half are cured. It was revealed that <10% of patients with primary refractory disease following R-CHOP treated at the British Colombia Cancer Agency achieved durable remissions with salvage therapies (Hitz et al., 2015). As a result, only very few patients are cured with secondary therapies. Due to the very low response rates seen in the salvage setting and the high proportion of patients ineligible for such treatments, novel agents are urgently required.

1.1.3.4 Novel therapies

Greater insights into the molecular heterogeneity of DLBCL uncovered by gene expression profiling have revealed unique therapeutic targets that have translated into the developments of novel agents.

Therapies targeting NF-KB and BCR signalling

Due to the constitutive activation of the NF-κB and BCR signalling pathways seen in ABC DLBCL, agents targeting these pathways are under evaluation in this subtype. For example, bortezomib, which prevents the degradation of IκB, has shown benefit when combined with chemotherapy in relapsed patients with ABC subtype (Dunleavy et al., 2009). An ongoing clinical trial, REMoDL-B, is evaluating the addition of bortezomib to R-CHOP as front line therapy in patients with ABC DLBCL. In a phase 1/2 clinical trial ibrutinib, an inhibitor of BTK, induced complete or partial responses in 37% of ABC DLBCL cases versus 5% of those with GCB DLBCL (Wilson et al., 2015). A phase 3 clinical trial, PHOENIX, is currently evaluating the

addition of ibrutinib to R-CHOP in non-GCB DLBCL. Additionally, idelalisib a selective inhibitor of PI3K, has indicated potential in chronic lymphocytic leukaemia (CLL) and indolent NHL, but has not been assessed in DLBCL (Gopal et al., 2014) (Furman et al., 2014). Although PI3K is an important component of the BCR pathway, due to the frequent activation of the PI3K pathway observed in GCB DLBCL, this drug may be of potential therapeutic benefit in this subtype as well as in ABC DLBCL (Pfeifer et al., 2013).

BCL2 targeting therapy

BCL2 is frequently overexpressed in both GCB and ABC DLBCL. This over expression has been shown to have a negative impact on the outcome for patients with GCB DLBCL and "dual expresser" lymphomas (Johnson et al., 2012, Iqbal et al., 2011). A potent selective inhibitor, known as ABT-199, showed responses in 38% of relapsed DLBCL patients in a phase I clinical study which has led to combination trials being investigated (Souers et al., 2013, Seymour et al., 2013).

Therapies targeting angiogenesis and the microenvironment

Due to the importance of the microenvironment in the pathogenesis of DLBCL, therapies that target this component are of great interest. One such agent, lenalidomide, has been shown to have pleiotropic activities including immunomodulatory, anti-angiogenic as well as direct tumour cell effects (reviewed in Kritharis et al., 2015). Lenalidomide treatment was well tolerated and demonstrated an overall response rate of 35% in a phase II clinical trial of relapsed/refractory aggressive B-cell NHLs (Witzig et al., 2011). It has been shown to be safely combined with R-CHOP in many studies and appears to overcome the negative prognostic

impact of ABC DLBCL versus GCB DLBCL (in patients treated with R-CHOP, progression free survival was 28% versus 64%; p< .001, in non-GCB DLBCL versus GCB DLBCL, respectively. In patients treated with R-CHOP plus lenalidomide there was no difference in progression free survival in GCB DLBCL versus ABC DLBCL, 60% versus 59%; p=.83) (Nowakowski et al., 2011, Vitolo et al., 2014, Nowakowski et al., 2015). As a result, a phase III clinical trial (ROBUST) is investigating the effects of lenalidomide plus R-CHOP in untreated patients with ABC DLBCL.

The results of clinical trials of anti-angiogenic therapies targeting the vascular endothelial growth factor (VEGF) signalling pathway have shown limited potential. The VEGF inhibitor, bevacizumab, showed only modest clinical activity in patients with relapsed NHL when delivered as a single agent or in combination with R-CHOP as first line treatment (Stopeck et al., 2009, Ganjoo et al., 2006). A phase III study of bevacizumab combined with R-CHOP in DLBCL patients (MAIN trial) was stopped early following a safety and efficacy analysis due to increased cardiotoxicity and without prolonging progression free survival (Seymour et al., 2014). Therefore, agents targeting alternative pathways are required to target angiogenesis in lymphoma patients. Alternatively, patients need to be selected for these therapies at diagnosis on the basis of an angiogenic phenotype.

1.2. SPHK1-S1P signalling

1.2.1 Introduction

Sphingolipids are one of the basic components of the biological membrane present in all eukaryotic cells. Sphingolipid metabolism leads to the formation of polar lipid mediators such as sphingosine 1-phosphate (S1P). Originally, S1P was believed to be an intermediate in the detoxification of sphingosine following its phosphorylation and degradation. However, S1P was later shown to regulate cell growth and suppress programmed cell death (Zhang et al., 1991, Cuvillier et al., 1996). S1P is now recognised as a potent, bioactive lipid mediator that regulates many cellular processes such as cell migration, proliferation and survival in both pathological and physiological settings.

1.2.2 S1P synthesis and release

S1P levels in cells are controlled by the balance between its formation and degradation. *De novo* synthesis of S1P occurs at the endoplasmic reticulum by condensation of serine and palmitate by serine palmitoyltransferase. S1P is also generated via sphingolipid turnover of the plasma membrane via the action of sphingomyelinase which generates the intermediate ceramide (Hannun and Obeid, 2008). Ceramide is further metabolised by ceramidase, which yields sphingosine. Subsequent production of S1P is via the phosphorylation of sphingosine by sphingosine kinases (SPHK1 and SPHK2). S1P is degraded via two separate pathways; it can either be dephosphorylated to sphingosine mediated by specific S1P phosphatases (SGPP1 and SGPP2) or irreversibly degraded to hexadecenal and phosphoethanolamine by S1P lyase (SGPL1) (Figure 1.7A).

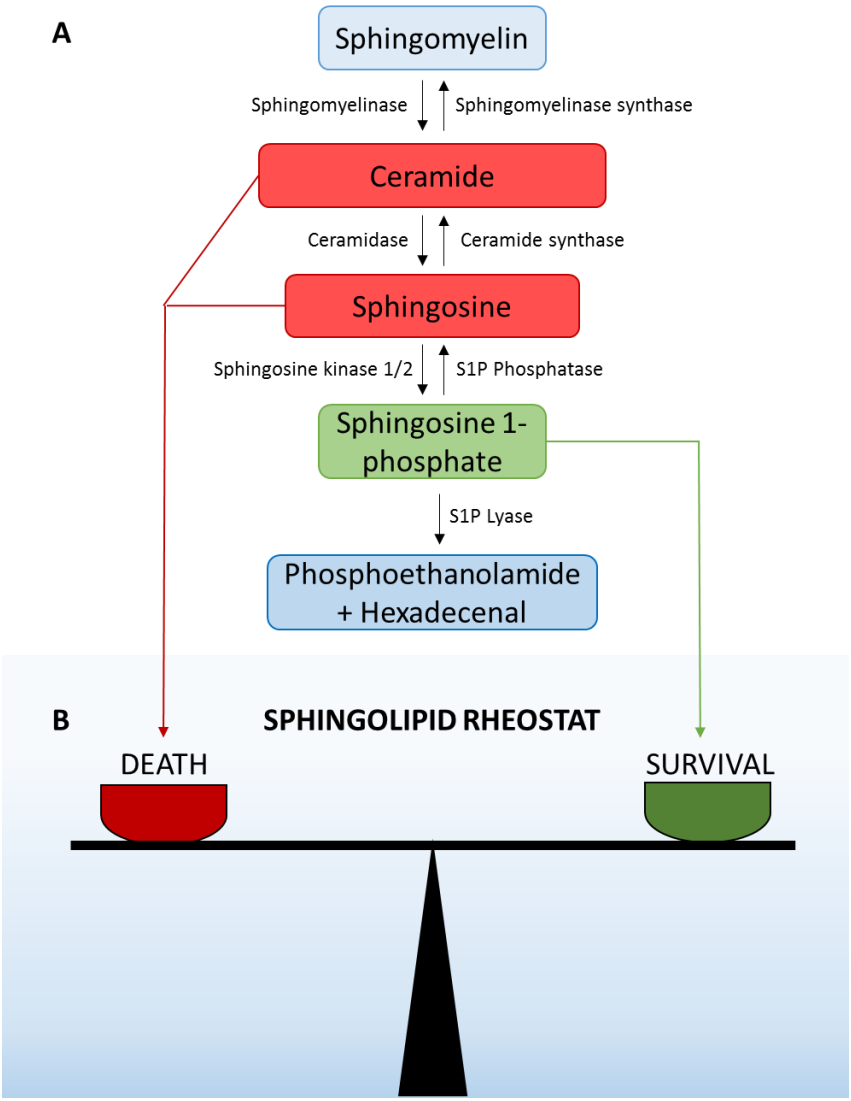

Figure 1.7: Sphingolipid metabolism. (A) The pathway of sphingolipid metabolism is shown. (B) S1P and ceramide have opposing functions, which makes their balance determine cell fate. This is referred to as the 'sphingolipid rheostat'.

Following its production, S1P can be exported out of the cell by adenosine triphosphate (ATP)-binding cassette multi-drug resistant transporters proteins such as ABCC1 and ABCA1 and the more recently identified transporter like protein SPNS2 (Mitra et al., 2006, Sato et al., 2007, Hisano et al., 2011). S1P is present in high concentrations in the circulation (between 0.1 – 4 μM) (Hanel et al., 2007). This S1P originates from different sources, with erythrocytes being the main blood cell store of S1P. S1P is also released from activated platelets and the vascular endothelium (Pappu et al., 2007, Venkataraman et al., 2008, Yatomi et al., 2001). Although S1P concentrations are high in blood and lymph, the concentrations are low in tissue interstitial fluids, this gives rise to an S1P gradient. This S1P gradient is essential for lymphocyte egress (discussed below; Section 1.2.9.4) (Cyster and Schwab, 2012, Schwab et al., 2005). Circulating S1P is bound to chaperone proteins including high density lipoprotein and albumin (Murata et al., 2000).

Extracellular S1P, produced by SPHK1, activates a family of G-protein-coupled receptors (GPCRs), a process known as “inside-out” signalling, whereas intracellular S1P, produced by SPHK2, acts as a second messenger by directly binding to intracellular protein targets (Spiegel, 1999, Takabe et al., 2008) (Figure 1.8).

1.2.3 Sphingolipid rheostat

S1P enhances growth and survival in diverse cell types (Spiegel and Milstien, 2003). By contrast, ceramide and sphingosine are important mediators of stress responses and induce apoptosis and cell cycle arrest (Cuvillier et al., 1996, Obeid et al., 1993). Death inducers such as tumour-necrosis factor α (TNFα), FAS/FAS ligand, growth factor withdrawal and increased levels of DNA damage all increase ceramide production (Ogretmen and Hannun, 2001).

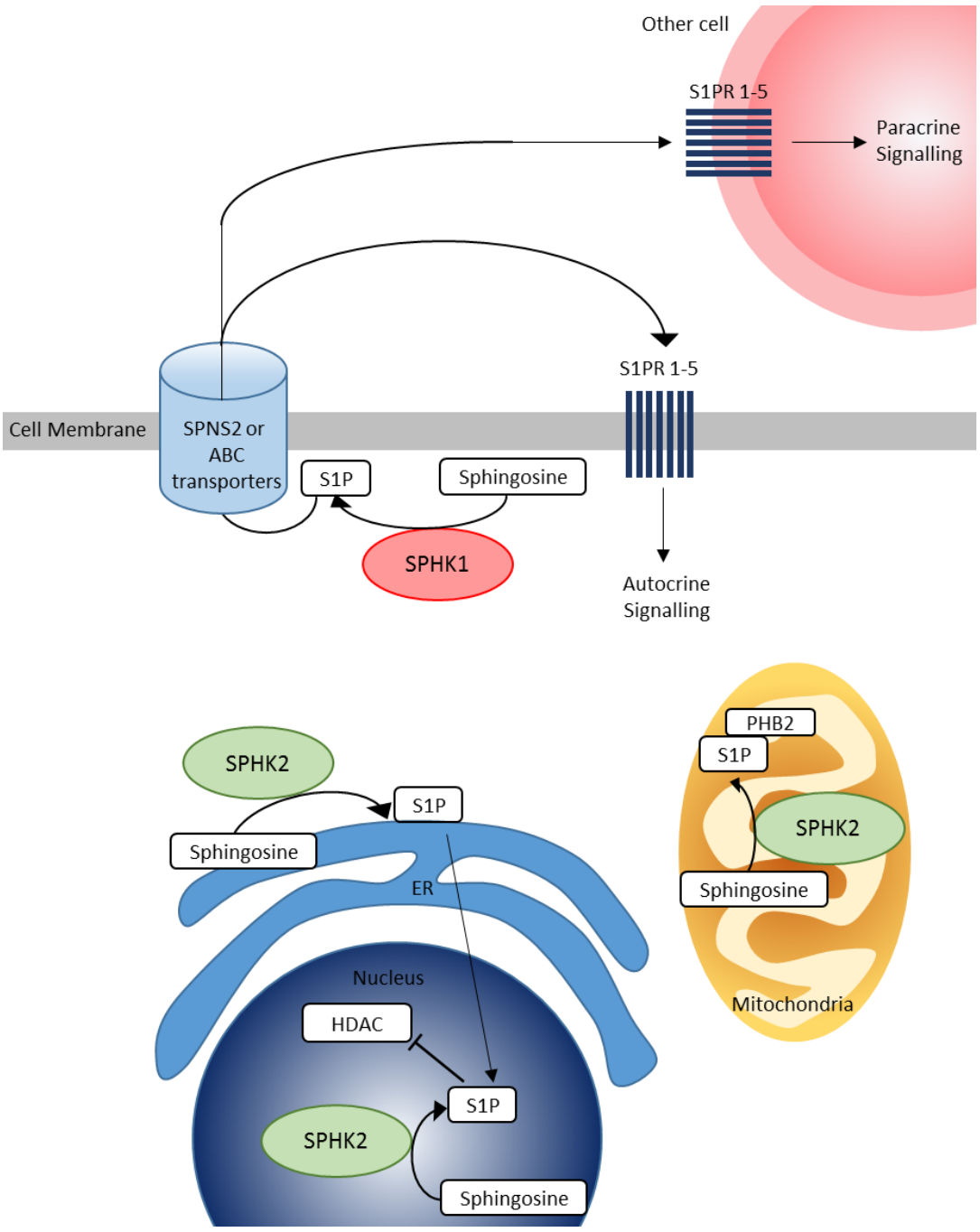

Figure 1.8: SPHKs localisation, S1P synthesis and signalling. SPHK1 is located in the cytoplasm and forms S1P from sphingosine at the plasma membrane, which can be exported out of the cell by specific transporters. Binding to S1P receptors (S1PR 1-5), extracellular S1P can initiate downstream signalling pathways in an autocrine or paracrine manner. SPHK2 is localised to the endoplasmic reticulum (ER), the mitochondrion and the nucleus. S1P produced in the nucleus and the mitochondria have direct intracellular targets which include histone deacetylases (HDACs) in the nucleus and prohibitin 2 (PHB2) in the mitochondria.

It is well established that ceramide has several targets which mediate its apoptotic function such as protein phosphatases 1, 2 (PP1 and PP2), cathepsin D and PKC (Heinrich et al., 2000, Wang et al., 2005).

These opposing roles between ceramide/sphingosine and S1P led to the concept of the "sphingolipid rheostat" whereby the dynamic balances between these metabolites can determine cell fate (Cuvillier et al., 1996) (Figure 1.7B).

1.2.4 Sphingosine kinase isoforms

SPHKs are evolutionary well conserved lipid kinases expressed in humans, mice, yeast and plants with homologues in worms and flies. Two mammalian SPHKs have been characterised, these are known as SPHK1 (43kDa) and SPHK2 (65kDa). The genes for SPHK1 and SPHK2 are located on different chromosomes, SPHK1 is present at 17q25.2 whereas SPHK1 is located at 19q13.2 (Kohama et al., 1998, Liu et al., 2000a). There are five highly conserved domains within SPHKs (C1-C5) with the catalytic domain located within C1-C3 and the ATP-binding site for S1P production is situated within the C2 domain (Takabe et al., 2008).

1.2.5 Localisation and activation of sphingosine kinases

SPHK1 and SPHK2 differ in their subcellular localisation, with SPHK1 being mainly cytosolic and SPHK2 mainly nuclear thereby creating distinct pools of S1P (Figure 1.8).

SPHK1 can be activated by multiple signals including GPCRs and tyrosine kinase agonists, proinflammatory cytokines, calcium and protein kinase activators, Ig receptors and small GTPases (Taha et al., 2006a, Maceyka et al., 2002). Following its activation, SPHK1 translocates

to the plasma membrane where it produces S1P from its substrate sphingosine. Additionally, this translocation results in localised production of S1P in the vicinity of membrane transport proteins and cell surface S1P receptors. SPHK1 translocation to the plasma membrane is dependent upon its phosphorylation on Ser225 by ERK1 and ERK2 (Pitson et al., 2003a). This dependency was highlighted by the inability of a phosphorylation deficient SPHK1 mutant to translocate to the plasma membrane and to increase proliferation and survival when over-expressed (Pitson et al., 2005). Recent studies have identified a critical role for the calcium-myristoyl switch protein, calcium and integrin binding protein 1 (CIB1), in the mechanism of SPHK1 translocation to the plasma membrane (Jarman et al., 2010). CIB1 interacts with SPHK1 in a calcium dependent manner at a calmodulin binding site of SPHK1. Following calcium binding, CIB1 translocates to the plasma membrane which provides a mechanism for active translocation of SPHK1 to this location (Jarman et al., 2010).

The regulation of SPHK2 is less well defined. SPHK2 is activated by a number of agonists including TNFα, interleukin 1β (IL1β) and epidermal growth factor (EGF) (Chun, 2013). Although the activating phosphorylation site of SPHK1 is not conserved in SPHK2, studies have also suggested that SPHK2 can be activated via its phosphorylation by ERK1 and ERK2, although the exact site(s) of phosphorylation are yet to be elucidated (Hait et al., 2007). Phosphorylation of SPHK2 also appears to play a role in its subcellular localisation. SPHK2 is located mainly in the nucleus or at the endoplasmic reticulum, however upon phosphorylation by PKD, SPHK2 is exported from the nucleus to the cytoplasm (Maceyka et al., 2005, Igarashi et al., 2003, Ding et al., 2007).

Although SPHK1 and SPHK2 produce distinct pools of S1P, SPHK1 and SPHK2 single knockout mice develop and reproduce normally. However, the double knockout is embryonically lethal due to severely disturbed neurogenesis and angiogenesis (Mizugishi et al., 2005).

1.2.6 Role of intracellular S1P

Although there is an abundance of evidence that "inside out" SPHK1 derived S1P signalling regulates many cellular processes, much less is known about the functions of intracellular S1P produced by SPHK2. Recent reports have demonstrated that intracellular S1P binds to and inhibits histone deacetylases (HDAC1 and HDAC2) (Figure 1.8). SPHK2 was also detected at the promotors of the transcriptional regulator c-fos and the cyclin dependent kinase inhibitor p21, leading to the S1P-mediated regulation of histone acetylation resulting in their enhanced transcription (Hait et al., 2009).

Intracellular S1P also plays a role in TNFα induced activation of NF-κB signalling and is a co-factor required for the ligase activity of TNF receptor-associated factor 2 (TRAF2) (Alvarez et al., 2010). TRAF2 is an adaptor protein that is involved in the ubiquitination of RIP1, a critical event in the activation of NF-κB in response to TNFα.

Intracellular S1P has suggested roles in mitochondrial respiration via binding to prohibitin 2 (PHB2), a protein which regulates mitochondrial assembly and function. SPHK2 knockout mice have reduced mitochondrial respiration due to defective assembly and activity of cytochrome oxidase, suggesting that the interaction of S1P with PHB2 is important for these processes (Strub et al., 2011).

1.2.7 Effects of SPHK2 expression

There are conflicting reports of SPHK2 functions. Early reports indicated that overexpression of SPHK2 causes the suppression of cell growth and cell cycle arrest via inhibition of DNA synthesis (Igarashi et al., 2003). Apoptosis following mitochondrial release of cytochrome c and activation of caspase 3 has also been shown to follow SPHK2 overexpression (Liu et al., 2003). These effects were shown to be the result of the SPHK2 Bcl-2 homology 3 (BH3) binding domain which sequesters the anti-apoptotic protein BCL2L1 inhibiting its function (Liu et al., 2003).

However, other studies suggest pro-survival functions for SPHK2. For example, SPHK2 knockdown increases the sensitivity of breast and colon cancer cells to doxorubicin- induced apoptosis (Sankala et al., 2007). Furthermore, knockdown of SPHK2 in glioblastoma cells inhibits their proliferation (Van Brocklyn et al., 2005).

1.2.8 S1P receptor signalling

Five high-affinity S1P GPCRs have been described: S1PR1 (EDG1), S1PR2 (EDG5), S1PR3 (EDG3), S1PR4 (EDG6) and S1PR5 (EDG), encoded by endothelial differentiation genes (EDG). Signalling through these receptors, S1P can mediate both paracrine and autocrine signalling (Alvarez et al., 2007) (Figure 1.8). S1P receptors are 7 transmembrane proteins that couple to a variety of heterotrimeric G proteins. A schematic representation of the binding specificities can be seen in (Figure 1.9).

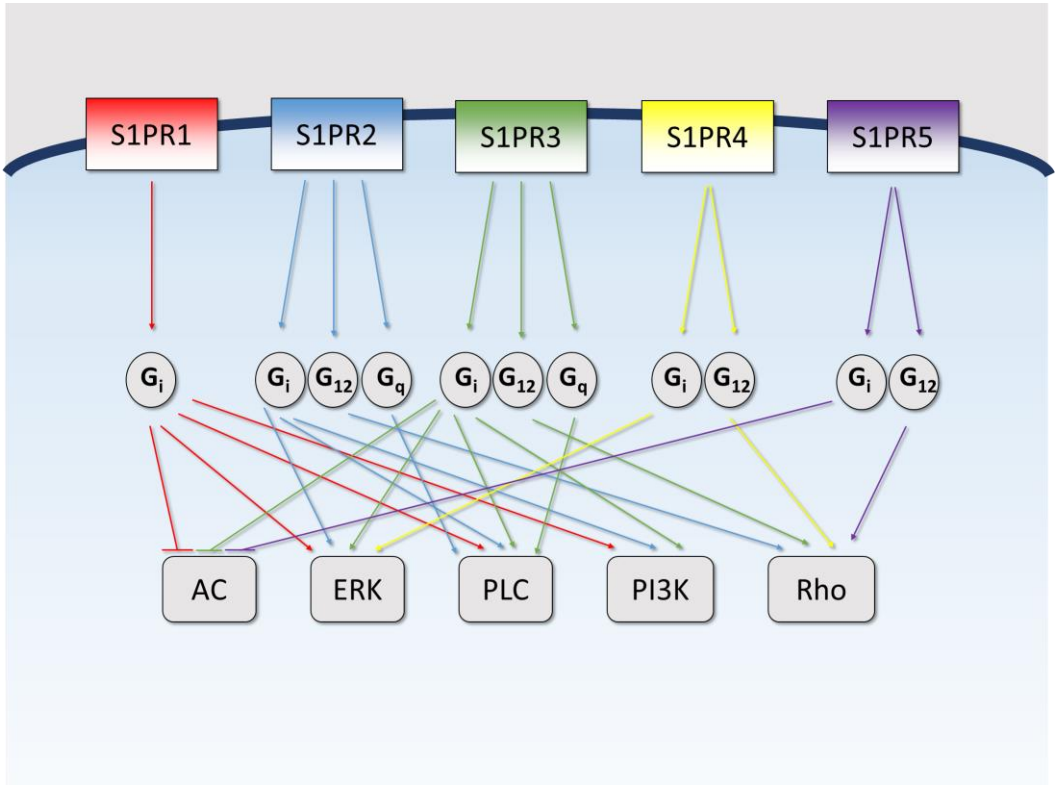

Figure 1.9: Downstream signalling pathways of S1P receptors. S1P is a ligand for five receptors S1PR1-5. Each S1P receptor is coupled to different G proteins which activate different signalling pathways.

S1PR1, S1PR2 and S1PR3 are widely expressed in most mammalian tissues, whereas S1PR4 and S1PR5 are mainly expressed in lymphoid cells and brain, respectively (Brinkmann, 2007, Chun et al., 2010). The response to S1P is governed by the mix of these different receptors on the cell surface.

S1PR1

S1PR1 was cloned in 1990 when it was discovered that one of the immediate early response genes induced during angiogenesis in human umbilical vein endothelial cells (HUVEC) encoded a GPCR, and it was named endothelial differentiation gene-1 (EDG1) (Hla and Maciag, 1990). The ubiquitous expression of S1PR1 is observed in many tissues and cell types (Chun, 2013). S1PR1 is abundant in endothelial cells but has also been shown to be expressed by many other cells including vascular smooth muscle cells, fibroblasts and epithelial cells as well as cells of the immune system such as T and B cells, macrophages, dendritic cells and natural killer cells (Goetzl et al., 2004, Chun, 2013). Following S1P binding, S1PR1 exclusively couples to G_i protein which leads to ERK and PI3K/AKT pathway activation, resulting in prosurvival and mitogenic signalling (Figure 1.10). Additionally, S1PR1 signalling leads to the activation of the Rho family small GTPase Rac, which is essential for cell migration and lamellipodia formation. This results in S1PR1 directed cell migration towards S1P. Moreover, S1PR1 activates phospholipase C (PLC) and Ca^{2+} mobilisation via G_i (Okamoto et al., 1998, Rivera and Chun, 2008).

S1PR2

S1PR2 was first cloned as a putative GPCR from a rat aortic cDNA library in an attempt to explore a novel signalling system in the vasculature (Okazaki et al., 1993). It was later identified by many groups as a high affinity S1P receptor (Gonda et al., 1999, Takuwa et al., 2011). Like S1PR1, S1PR2 is widely expressed. However, unlike S1PR1, S1PR2 couples to multiple heterotrimeric G proteins including G_i, G_q and $G_{12/13.}$ Of these, $G_{12/13}$ coupling to Rho activation is the most prominent (Windh et al., 1999, Okamoto et al., 2000, Takuwa, 2002). Contrary to the action of S1PR1, S1PR2 exerts an inhibitory effect on Rac, via downstream activation of Rho, which results in inhibition of cell migration (Estrada et al., 2008, Takuwa, 2002) (Figure 1.10). Additionally, S1PR2 mediated Rho activation results in inhibition of AKT therefore inhibiting rather than promoting cell proliferation (Sanchez et al., 2005, Schuppel et al., 2008) (Figure 1.10). S1PR2 signalling also stimulates PLC and Ca^{2+} mobilisation through $G_{q,}$ and ERK and PI3K activation via G_i (Takuwa et al., 2001, Takuwa et al., 2002).

S1PR3

S1PR3 was isolated as an orphan GPCR gene with a high affinity to S1P. Like S1PR2, S1PR3 couples to multiple G proteins, activating PLC and Ca^{2+} via G_q and ERK, PI3K and Rac via G_i, predominantly inducing cell survival, proliferation and migration to S1P (Windh et al., 1999, Okamoto et al., 1999) (Figure 1.10). S1PR3 also couples to $G_{12/13}$ activating Rho, although this is to a much lower extent than S1PR2 (Okamoto et al., 2000).

S1PR4

S1PR4 was identified from murine and human dendritic cells as an orphan GPCR and later found to a high affinity receptor for S1P (Ishii et al., 2004). S1PR4 couples with G_i and $G_{12/13}$ mediating S1P-induced ERK, PLC and Rho activation as well as Ca^{2+} mobilisation, cytoskeleton rearrangement and cell migration (Ishii et al., 2004). In contrast to S1PR1-3, S1PR4 expression is restricted to lymphoid tissues indicating a role in regulation of the immune system

S1PR5

S1PR5 was isolated as an orphan GPCR from rat pheochromocytoma (PC12) cells and later found to be a high affinity S1P receptor (Malek et al., 2001, Glickman et al., 1999). S1PR5 can couple with G_i and $G_{12/13}$ and is highly expressed in white matter and cells of the oligodendrocyte lineage in the rat brain, suggesting a potential role in the maturation of oligodendrocytes (Terai et al., 2003).

.

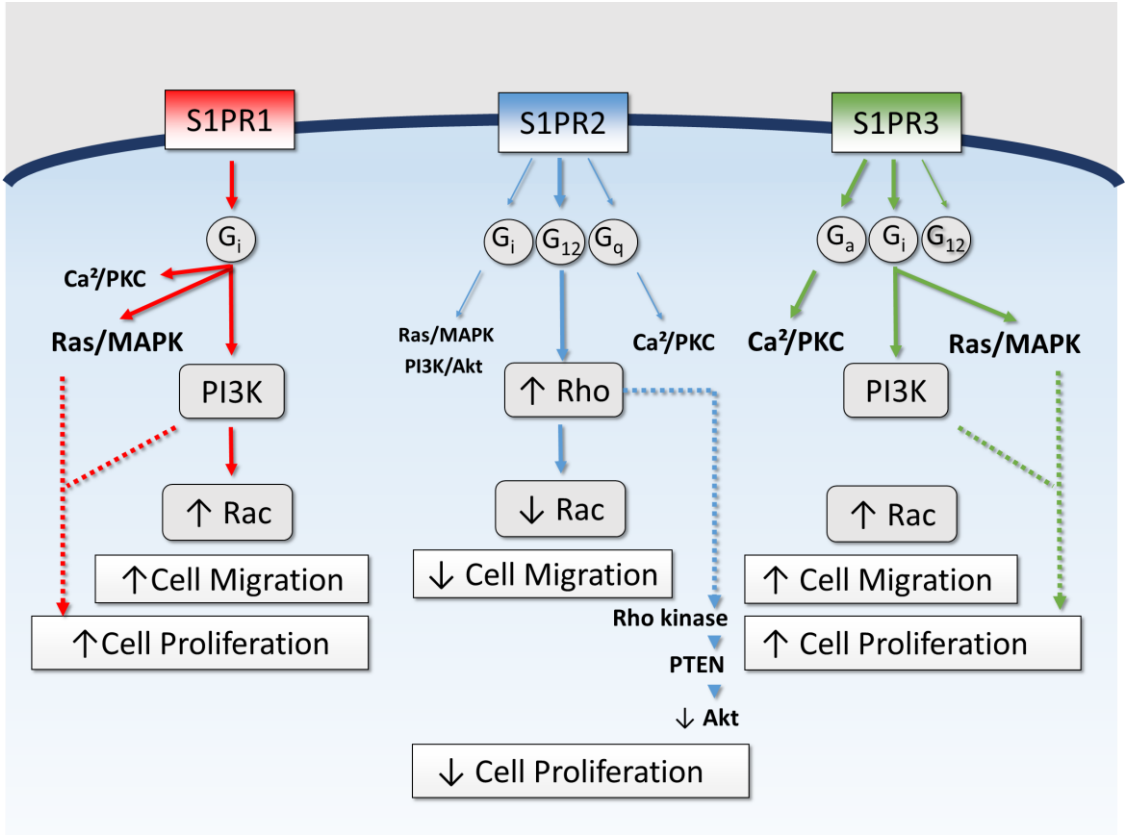

Figure 1.10: The differential effects of S1P receptor signalling: S1PR1 couples exclusively to Gi to activate ERK (MAPK) and PI3K/AKT/Rac pathways resulting in the stimulation of cell proliferation and migration. S1PR2 couples to multiple G proteins, especially to $G_{12/13}$ resulting in Rho activation, leading to the inhibition of Rac and cell migration as well as inhibition of cell proliferation due to the inhibition of AKT. S1PR3 activates the PLC- Ca^{2+} pathway via G_q and the ERK and PI3K pathways via $G_{i.}$ (Reproduced from: Takuwa et al. 2001)

1.2.9 Effects of SPHK1 expression

SPHK1 has been shown to increase cell survival, proliferation and migration. It also promotes angiogenesis and lymphocyte migration leading many to define SPHK1 as an oncogene (Pyne et al., 2012, Maceyka et al., 2002, Maceyka et al., 2012). Main findings are discussed below.

1.2.9.1 Expression of SPHK1 in cancer

In early studies, the overexpression of SPHK1 in NIH3T3 fibroblasts was shown to result in neoplastic transformation and the ability to form tumours when allografted into mice (Xia et al., 2000). This effect was not observed in NIH3T3 fibroblasts expressing a dominant negative kinase dead SPHK1 mutant or in the presence of an SPHK1 inhibitor (Xia et al., 2000). Subsequently, numerous studies showed SPHK1 expression is increased in many cancer types; in many cases correlating with increased tumour grade and reduced patient survival (summarised in Table 1.2).

Table 1.2: Increased SPHK1 expression in human tumours and clinical correlation

Tumour Location	mRNA or Protein	Number of Tumour Samples	Clinical correlation	References
Gastric	mRNA	27	undetermined	(French et al., 2003)
		4	undetermined	(Li et al., 2009)
	Protein	175	Increased expression of SPHK1 correlates with reduced patient survival	
Glioblastoma	mRNA	48	Increased expression of SPHK1 correlates with reduced patient survival	(Van Brocklyn et al., 2005)
Astrocytoma	Protein	243	Increased expression of SPHK1 correlates with reduced patient survival; expression increases with clinical grade	(Li et al., 2008a)
Breast	mRNA	1269	Increased expression of SPHK1 correlated with poor prognosis; higher expression in ER negative tumours	(Ruckhaberle et al., 2008)
Colon	mRNA	35	Undetermined	(French et al., 2003)
	Protein	47	Higher expression of SPHK1 in primary cancer with metastases than in those without metastases	(Kawamori et al., 2009)
Kidney	mRNA	20	undetermined	(French et al., 2003)
Lung	mRNA	21	undetermined	(French et al., 2003)
	Protein	25	undetermined	(Johnson et al., 2005)
Non-Hodgkin Lymphoma	mRNA	44	Increased expression of SPHK1 correlates with increased clinical grade	(Bayerl et al., 2008)
	Protein			
Ovary	mRNA	14	undetermined	(French et al., 2003)
Rectum	mRNA	18	undetermined	(French et al., 2003)
Uterus	mRNA	42	undetermined	(French et al., 2003)
Pancreas	Protein	60	undetermined	(Guillermet-Guibert et al., 2009)

Constitutively active mutant Ras has been shown to induce the transcriptional upregulation of SPHK1 (Xia et al., 2000). Similarly, v-Src expression has been shown to stabilise SPHK1 mRNA leading to increased SPHK1 mRNA levels and protein over expression (Sobue et al., 2008a). The degradation of SPHK1 is dependent upon p53, and loss of p53, which is frequently observed in human cancers, results in reduced SPHK1 degradation. SPHK1 is also proteolysed following genotoxic stress in a p53-dependent manner (Heffernan-Stroud et al., 2012).

Mice lacking both p53 alleles develop thymic lymphoma and were shown to display elevated levels of SPHK1/S1P and decreased levels of ceramide in the thymi. Notably, deletion of SPHK1 in p53 deficient mice completely abrogated thymic lymphomas and prolonged survival by 30% (Heffernan-Stroud et al., 2012). The SPHK1 gene has two hypoxia-inducible factor (HIF) responsive elements in its promotor region, through which HIF1α and HIF2α contribute to upregulate SPHK1 expression (Anelli et al., 2008, Schwalm et al., 2008).

1.2.9.2 Contribution of SPHK1-S1P signalling to cancer cell survival and treatment resistance

SPHK1 overexpression is protective against a diverse range of pro-apoptotic stimuli including TNFα, hydrogen peroxide, serum withdrawal, androgen depletion and amyloid β peptide in many biological settings (Cuvillier et al., 2010). Knockdown of SPHK1 has been shown to inhibit cell proliferation and/or trigger apoptosis in prostate, pancreatic, leukaemic, glioma and breast cancer cells (Akao et al., 2006, Pchejetski et al., 2005, Guillermet-Guibert et al., 2009, Baran et al., 2007, Kapitonov et al., 2009, Taha et al., 2006b). The mechanism for this function is likely to be as a result of enhanced SPHK1 activity reducing the levels of ceramide by driving ceramide metabolism towards the synthesis of growth promoting S1P. S1P has also been shown to inhibit caspase-dependent apoptosis by blocking cytochrome c release (Cuvillier and

Levade, 2001). S1P also increases the expression of the anti-apoptotic proteins BCL2 and induced myeloid leukaemia cell differentiation protein (MCL1), while downregulating the pro-apoptotic proteins, BCL2, associated agonist of cell death (BAD) and BCL2 associated X protein (BAX) (Sauer et al., 2005, Li et al., 2008c, Avery et al., 2008).

Due to these anti-apoptotic effects of S1P signalling, there are many reports that suggest that SPHK1 expression contributes to treatment resistance (Pchejetski et al., 2005, Baran et al., 2007, Sobue et al., 2008b). Many therapies against cancer utilise the apoptotic machinery of cells and the generation of ceramide. For example, taxol treatment of prostate cancer cells induces ceramide production whereas the inability to produce ceramide is linked to therapy resistance (Ogretmen and Hannun, 2001). Increased ceramide production following treatment may not be sufficient to push the cells towards apoptosis without also inhibiting S1P production as a result of SPHK1 expression. This was shown by the correlation observed between SPHK1 expression and resistance to irradiation in prostate cancer cells. In radiation resistant cells, SPHK1 activity was not altered following ionising radiation, whereas SPHK1 activity was greatly reduced in radiosensitive cells (Nava et al., 2000). The relationship between SPHK1 expression and resistance to chemotherapy has also been showed in prostate cancer cells; using an orthotopic model for prostate cancer, Pchejetski and colleagues (2005) demonstrated that animals injected with PC-3 cells overexpressing SPHK1 developed larger tumours which were resistant to docetaxel treatment. The increase in ceramide normally detected following docetaxel treatment was reduced in those animals implanted with PC-3 cells overexpressing SPHK1 compared to controls.

1.2.9.3 S1P signalling pathways in cancer

S1P signalling has also been identified as a crucial element involved in the persistent activation of STAT3 in tumour cells and the tumour microenvironment (Lee et al., 2010). Aberrant STAT3 activation in cancer cells has emerged as a major mechanism for cancer initiation and progression. It was shown that S1PR1 was elevated in STAT3 positive tumours and that STAT3 is a transcriptional regulator of S1PR1 expression. The enhanced S1PR1 expression activates STAT3 and upregulates interleukin-6 (IL6) production, a pro-inflammatory cytokine crucial for STAT3 activation. It was shown that silencing S1PR1 in tumour cells or immune cells inhibited tumour STAT3 activity, reducing tumour growth and metastasis (Lee et al., 2010). Therefore this feed-forward mechanism results in persistent STAT3 activation and is important in malignant progression (Lee et al., 2010). In ABC DLBCL, high levels of expression and activation of STAT3 have been reported (Ding et al., 2008). Consistent with these findings, it was shown that persistent activated STAT3 colocalises with high S1PR1 expression in ABC DLBCL. Inhibition of S1PR1 affected the downstream signalling of STAT3 involved in cell survival, proliferation and invasion (Liu et al., 2012).

1.2.9.4 Contribution of SPHK1-S1P signalling to cancer cell invasion and metastasis

S1P can also regulate cell migration, either negatively or positively, governed by the expression of different S1P receptors on the cell surface (Figure 1.10). This phenomenon is best demonstrated by the physiological role of S1P in the GC reaction and lymphocyte egress. The anti-migratory receptor S1PR2 is highly expressed by GC B cells. S1PR2 expression has been shown to be vital for GC B cell positioning and confinement to the GC; best demonstrated by S1PR2-deficient mice which display large GC outgrowths which lead to an expansion of the

lymph node and a loss of lymphoid architecture (Cattoretti et al., 2009, Green and Cyster, 2012).

Lymphocytes exit lymphoid structures into lymphatic vessels, a process known as lymphocyte egress. It has been demonstrated that lymphocyte egress is dependent upon the cellular expression of the pro-migratory receptor S1PR1 and increased concentrations of S1P in the blood and lymph compared to tissue (Cyster, 2005). The immunosuppressive S1P receptor agonist, FTY720, leads to lymphopenia in several animal models and in humans (discussed below; Section 1.2.10.2) (Chiba et al., 1998, Yagi et al., 2000, Mandala et al., 2002).

Through these activities, S1P signalling can stimulate the motility of cancer cells via S1PR1 or S1PR3; in contrast S1P inhibits cancer cell motility through S1PR2. This is illustrated by the S1P-induced migration of gastric tumour cells which exclusively express S1PR3 and the S1P-induced inhibition of migration of gastric tumour cells which predominantly express S1PR2 (Yamashita et al., 2006). Additionally S1P signalling can induce migration in many other cancer cell types (Pyne and Pyne, 2010, Park et al., 2007).

There are reports of the altered expression and or/ mutation of the S1P receptors in cancer. By two years of age, roughly half of S1PR2-deficient mice develop tumours that may be classified as DLBCL (Cattoretti et al., 2009). Furthermore, S1PR2 has been shown to be mutated in ~25% of patients with DLBCL (Cattoretti et al., 2009).

1.2.9.5 Contribution of SPHK1-S1P signalling to tumour angiogenesis

S1P has been shown to play a major role in vascular functions. In 1999, two papers were published which revealed that S1P played a potential role in angiogenesis (English et al., 1999,

Lee et al., 1999). It was shown that S1P stimulated DNA synthesis and the chemotactic motility of HUVEC in a dose dependent manner. The authors reported the S1P-induced tube formation of HUVEC in Matrigel. This observation was confirmed *in vivo* by a study which showed that S1P promotes angiogenesis in a Matrigel plug assay (Lee et al., 1999). S1P has also been shown to prevent apoptosis of endothelial cells induced by serum starvation and TNFα (Xia et al., 1999). The essential role of S1P signalling in vascular development is well demonstrated in S1PR1 knockout mice, which display impaired vascular maturation leading to embryonic haemorrhage and intrauterine death (Liu et al., 2000b). Additionally, as mentioned earlier, mice deficient for SPHK1 and SPHK2 show severe loss of vessel stability also leading to embryonic lethality (Mizugishi et al., 2005).

Tumour angiogenesis is essential for the survival and development of a tumour greater than 2 mm^3 in size (Folkman, 1971). Tumour blood vessels are a key part of the tumour microenvironment required for the delivery of nutrients and oxygen and essential for tumour growth and metastasis (Folkman, 1971). Tumour angiogenesis is a complex multistep process driven by cellular transformation and tumour-associated hypoxia (Tonini et al., 2003). Tumour cells secrete a number of pro-angiogenic growth factors including platelet derived growth factor (PDGF), VEGF and basic fibroblast growth factor (bFGF), which recruit endothelial cells and promote their proliferation and the formation of vessels (Carmeliet and Jain, 2000, Tonini et al., 2003). Furthermore, infiltrating stromal cells can also be stimulated to produce growth factors that support the angiogenic process (Murdoch et al., 2008).

As well as developmental angiogenesis, S1P signalling has been shown to play a role in tumour angiogenesis. Anelli et al. (2010) showed that S1P secreted from HEK cells and tumour cells

overexpressing SPHK1 induced endothelial cell migration and tube formation in a co-culture system. S1PR1 expression in vessels has been shown to be upregulated at the sites of tumour implantation in a Lewis lung carcinoma xenograft mouse model (Chae et al., 2004). Silencing of S1PR1 by repeated local injections of S1PR1 siRNA into established tumours suppressed tumour angiogenesis and vascular stabilisation with inhibition of tumour growth (Chae et al., 2004). Furthermore, it has been shown that targeting the S1P signalling pathway inhibits angiogenesis and tumour cell proliferation *in vivo*, to a greater extent than those observed with anti-VEGF antibodies; it has been shown that anti-S1P antibody suppresses VEGF and FGF induced angiogenesis in Matrigel plugs in mice, which suggests S1P plays a role in VEGF and FGF mediated angiogenesis (Visentin et al., 2006, LaMontagne et al., 2006, Azuma et al., 2002). These observations indicate that S1PR1 expressed in tumour-associated endothelium is crucial for tumour angiogenesis.

1.2.10 Targeting S1P signalling in cancer

Due to the aforementioned role of SPHK1-S1P signalling in cancer, much emphasis is now placed on the development of compounds that target this signalling pathway for treatment. Strategies which have been used to limit the effects of S1P signalling in cancer include sequestering released S1P, inhibition of SPHK1 and/or inhibition of specific S1P receptors.

1.2.10.1 S1P antibodies

Anti-S1P monoclonal antibody (Sphingomab) sequesters S1P preventing it from binding to its receptors. Sphingomab has been shown to have high specificity for S1P and does not cross react with other structurally related lipids such as lysophosphatidic acid (LPA) (O'Brien et al.,

2009). Sphingomab reduced tumour progression in murine xenograft models through inhibition of tumour angiogenesis, as shown by reduced microvessel density, and inhibition of S1P stimulated release of pro-angiogenic cytokines VEGF, IL6 and interleukin-8 (IL8) (Visentin et al., 2006). Sonepcizumab (humanised form of Sphingomab) has completed a Phase I clinical trial in cancer patients (ClinicalTrials.gov Identifier: NCT00661414). Sonepcizumab was administered as a single agent weekly to patients with refractory advanced solid tumours at doses between 1 and 24 mg/kg with the objectives to characterise the safety, tolerability and dose-limiting toxicities of the drug. Sonepcizumab was well tolerated across the range of doses tested and there were no dose-limiting toxicities observed. Of the 21 patients, 11 had stable disease for 2 months or longer, including one patient with an aggressive metastatic melanoma showing stable disease for 8 months, one patient with an adenoid cystic tumour treated for over 12 months without disease progression and another patient with a carcinoid tumour who was still being treated at the date of a report 26 months later (Sabbadini, 2011).

1.2.10.2 S1P receptor agonists

Several S1P receptor antagonists are available, in particular against S1PR1 and S1PR3. One such compound is the immunosuppressant FTY720 (fingolimod). FTY720 is an analogue of sphingosine, which is taken up by cells and phosphorylated by SPHK2 to yield biologically active FTY720-phosphate (FTY720-P) (Sanchez et al., 2003). FTY720-P binds to S1P receptors S1PR1, 3, 4 and 5. FTY720-P is an S1PR1 receptor agonist and FTY720-P binding induces S1PR1 internalisation and degradation resulting in prolonged receptor downregulation (Matloubian et al., 2004). In this way, lymphocytes are deprived of the signal necessary for their egress from secondary lymphoid organs resulting in lymphopenia following FTY720 treatment (Graler

and Goetzl, 2004, Matloubian et al., 2004, Cyster, 2005). These effects are advantageous for the treatment of autoimmune diseases and FTY720 has been approved by the Food and Drug Administration for the treatment of relapsing remitting multiple sclerosis. There have been many examples of the use effectiveness of FTY720 *in vivo* showing inhibition of tumour growth and angiogenesis in various mouse tumour models including renal, bladder, prostate, breast, hepatocellular carcinoma and melanoma (Ubai et al., 2007, Azuma et al., 2003, Chua et al., 2005, Azuma et al., 2002, Ho et al., 2005, LaMontagne et al., 2006). However, FTY720 has not been tested in a clinical trial of cancer patients.

1.2.10.3 Sphingosine kinase inhibitors

SPHK1 inhibitors might exert their effects not only by the reduction in S1P production but also by increasing the levels of pro-apoptotic ceramide and sphingosine. One of the first compounds identified as an inhibitor of SPHK activity was DHS (Saphingol). Later it was discovered that DMS, a methylated metabolite of sphingosine, was more potent that DHS. As a result DMS has been used most widely as a pharmacological inhibitor of sphingosine. However, neither DHS nor DMS are considered as specific kinase inhibitors as they inhibit both SPHK1 and SPHK2, ceramide kinase, PKC, protein dependent protein kinase, 3-phosphoinositide-dependent kinase and casein kinase II (reviewed in: Takabe et al., 2008). DHS and DMS have both been evaluated in pre-clinical trials in animal models and DMS was shown to reduce gastric and lung tumour growth *in vivo* and decrease lung metastasis of melanoma cells (Endo et al., 1991, Okoshi et al., 1991). Although DHS and DMS have shown to inhibit tumour growth *in vivo,* they cause significant haemolysis and hepatotoxicity (Kedderis et al., 1995).

Non-lipid SPHK1 inhibitors (compounds SPHK1 I-V) have also been identified with nanomolar potencies, which are non-competitive inhibitors at the ATP binding site of SPHK1. SPHK1-II, known as SPHKi, which does not inhibit other kinases, inhibits the proliferation and induces apoptosis in various cancer cell lines. Additionally, SPHKi was shown to inhibit tumour growth *in vivo* (French et al., 2003). However, SPHKi has not been tested in clinical trials of patients.

1.3 Study aims

SPHK1 has recently emerged as an important regulator of tumour cell growth, survival, metastasis and angiogenesis. These activities of SPHK1 are mainly a consequence of its ability to catalyse production of the bioactive signalling lipid, S1P. Importantly, new therapies targeting SPHK1-S1P signalling are being developed. This thesis explores the contribution of SPHK1-S1P signalling to the pathogenesis of DLBCL, and its potential therapeutic reversal, with a focus on tumour angiogenesis. The specific aims are to:

1. Investigate the expression of SPHK1 in primary DLBCL. Describe the association between SPHK1 expression and that of angiogenesis-associated genes in primary DLBCL.
2. Validate an *in vitro* model which can be used to study the effects of S1P signalling on the endothelial cell transcriptome. Use this model to define an S1P-induced endothelial cell gene signature and measure the extent to which this signature is expressed in primary DLBCL.
3. Explore the phenotypic effects of the S1P-induced endothelial cell gene signature.
4. Investigate the potential *in vitro* inhibition of S1P-induced signalling and gene expression in endothelial cells using SPHK1-S1P targeting drugs.
5. Establish an *in vivo* model of DLBCL which can be used to study the potential therapeutic efficacy of these SPHK1-S1P targeting drugs *in vivo*.

CHAPTER TWO

MATERIALS AND METHODS

2.1 HUVEC isolation

Endothelial cells were isolated from umbilical cords which were obtained from the Human Biomaterials Resource Centre (HBRC; University of Birmingham) with patient consent and ethical approval (No. RG_HBRC_14-180). The HUVEC were isolated using collagenase treatment as previously described (Jaffe et al., 1973). Briefly, the umbilical cords were sprayed with 70% ethanol and checked for needle holes. The vein of the umbilical cord was then cannulated at each end and phosphate-buffered saline (PBS) was flushed through to remove any residual blood. Collagenase (type 2; Sigma-Aldrich Ltd., Gillingham, UK) dissolved in PBS (1 mg/ml) was pushed through the vein until it became visible in both ends of the cannula. Both cannulae were then securely sealed and the cord was incubated at 37°C for 15 minutes. The collagenase solution containing the HUVEC was then removed and the cells were pelleted by centrifugation (Eppendorf Centrifuge 5810R) at 200 g for 10 minutes and resuspended in culture medium.

2.2 Cell culture

2.2.1 Maintenance of cell lines

All cells were maintained in the growth media detailed in Table 2.1 and incubated at 37 °C in a humidified atmosphere containing 5% carbon dioxide (Galaxy R CO_2 Incubator; RS Biotech). At between 70 and 80% confluency, as determined by visual inspection under a microscope, cells were passaged to prevent over growth. For adherent cells, media was aspirated using a VACUSAFE aspirator (INTEGRA Biosciences AG) and the cells were washed twice with PBS.

Table 2.1: Summary of cell lines and the culture media

Cell line name	Culture characteristics	Cell type	Culture Media
HUVEC	Adherent	Human endothelial cell	M199 (Sigma-Aldrich Ltd., Gillingham, UK) supplemented with 5% v/v foetal bovine serum (FBS), 5% endothelial cell growth supplement (ECGS; Caltag Medsystems), 1% v/v glutamine (Gibco, Life Technologies Ltd) and 1% v/v penicillin/streptomycin (P/S, Gibco, Life Technologies Ltd).
sEnd-1	Adherent	Murine endothelioma	DMEM (Gibco, Life Technologies Ltd) supplemented with 10% v/v FBS and 1% v/v P/S
HEK293	Adherent	Human embryonic kidney	DMEM supplemented with 10% v/v FBS and 1% v/v P/S
A20	Suspension	Murine B cell lymphoma	RPMI 1640 (Gibco, Life Technologies Ltd) supplemented with 10% v/v FBS and 0.05 mM 2-mercaptoethanol
L428	Suspension	Hodgkin lymphoma (human)	RPMI 1640, supplemented with 10% v/v FBS and 1% v/v P/S.
HT	Suspension	DLBCL (human)	RPMI 1640 supplemented with 10% v/v FBS and 1% v/v P/S.
Karpas 422	Suspension	DLBCL (human)	RPMI 1640 supplemented with 10% v/v FBS and 1% v/v P/S.
U2932	Suspension	DLBCL (human)	RPMI 1640 supplemented with 10% v/v FBS and 1% v/v P/S.
OCILY1	Suspension	DLBCL (human)	IMDM (Gibco, Life Technologies Ltd), supplemented with 10% v/v FBS and 1% v/v P/S.
OCILY3	Suspension	DLBCL (human)	IMDM supplemented with 10% v/v FBS and 1% v/v P/S.
OCILY7	Suspension	DLBCL (human)	IMDM supplemented with 10% v/v FBS and 1% v/v P/S.
SUDHL4	Suspension	DLBCL (human)	RPMI 1640 supplemented with 10% v/v FBS and 1% v/v P/S.
SUDHL5	Suspension	DLBCL (human)	RPMI 1640 supplemented with 10% v/v FBS and 1% v/v P/S.
FARAGE	Suspension	DLBCL (human)	RPMI 1640 supplemented with 10% v/v FBS and 1% v/v P/S.
THP-1	Suspension	Acute monocytic leukemia (human)	RPMI 1640 supplemented with 10% v/v FBS and 1% v/v P/S.

Trypsin solution (Gibco, Life Technologies Ltd) was added to the cells and incubated at 37°C for 3 minutes to allow the cells to detach from the culture flask. The trypsin was neutralised by addition of medium. Both adherent and suspensions cells were pelleted by centrifugation at 200 g for 10 minutes and resuspended in fresh culture media to obtain the desired concentration.

2.2.2 Cryopreservation of cells

Cells were pelleted by centrifugation at 200 g for 5 minutes and resuspended in chilled freezing solution (90% v/v FBS (PAA the cell culture company, Somerset, UK), 10% v/v dimethyl sulphoxide (DMSO; Sigma-Aldrich Ltd., Gillingham, UK)). Cells were transferred to cryopreservation tubes (Nunc® Cryo Tubes; Sigma-Aldrich Ltd., Gillingham, UK) and cooled overnight to -80°C in a cryo container (Nalgene® Mr. Frosty; Sigma-Aldrich Ltd., Gillingham, UK). Cells were transferred to the vapour phase of a -180°C liquid nitrogen freezer for storage.

2.3 Preparation of S1P

S1P (Sigma-Aldrich Ltd., Gillingham, UK) was dissolved by addition of methanol:water 95:5 to a final concentration of 0.5 mg/ml. The mixture was heated in a water bath at 65°C for 10 minutes and then briefly placed in an ultrasonic water bath. A 125 µM working solution was made by transferring 50 µl dissolved S1P to a glass vessel (Supelco; Sigma-Aldrich Ltd., Gillingham, UK) and the methanol:water solution allowed to evaporate. Low retention pipette tips (Plastibrand; Sigma-Aldrich Ltd., Gillingham, UK) were used to pipette S1P. To dissolve the S1P, 520 µl of 4 mg/ml fatty acid free bovine serum albumin (BSA; Sigma-Aldrich Ltd.,

Gillingham, UK) in water was added at 37°C and incubated for 30 minutes on a roller. S1P-BSA aliquots were stored at -20°C for a maximum of 3 months.

2.4 HUVEC stimulations

HUVEC were grown in normal growth conditions on 6 well dishes (Corning, Sigma-Aldrich Ltd., Gillingham, UK) until they reached confluence. Sixteen hours prior to S1P stimulation, HUVEC were washed twice with PBS and media changed to M199 supplemented with 5% v/v FBS and 1% v/v P/S, to deplete the HUVEC of ECGS. S1P was heated to 37°C and then pipetted directly into the HUVEC media of the 6 well dish.

Sphingomab and isotype control antibody (both LPath Inc., CA, USA) treatments were used at a concentration of 150 µg/ml per µM of S1P (O'Brien et al., 2009) unless otherwise stated, and were added to the medium at the same time as S1P.

For FTY720 treatment experiments, HUVEC were treated with FTY720 (Sigma-Aldrich Ltd., Gillingham, UK) for 1 hour prior to S1P treatments.

2.5 Transfection of HEK293 cells

HEK293 cells were grown on 9 mm multi-spot coated microscope slides (Hendley-Essex, Essex, UK) overnight to 70% confluency. The cells were then washed with Opti-MEM (Thermo Fisher Scientific Inc., Waltham, MA, USA) before 70 µl of Opti-MEM was pipetted onto each spot of cells. A transfection reaction mix was made up of: 100 µl Opti-MEM, 2 µl lipofectamine reagent (Thermo Fisher Scientific Inc, Waltham, MA, USA) and 1 µg plasmid DNA (pcDNA3.1, pcDNA3.1-S1PR1, pcDNA3.1-S1PR2 or pcDNA3.1-S1PR3) kindly provided by Dr Ian Paterson

(University of Malaya, Kuala Lumpur), and incubated for 15 minutes. Ten µl of transfection reaction mix was pipetted into the 70 µl of Opti-MEM on the HEK293 cells, incubated for 4 hours and then replaced with normal culture media. Twenty four hours later, the HEK293 cells were washed and fixed by submerging the microscope slide in PBS for 2 minutes followed by 10% formal-saline solution (Genta Medical, York, UK) for 10 minutes. The HEK293 cells were air-dried and the slides stored at -20˚C until required.

2.6 RNA analysis

2.6.1 RNA extraction

Total RNA was isolated using the QIAGEN RNeasy kits (QIAGEN Ltd., Manchester, UK) according to the manufacturer's protocol. Briefly, cells were lysed in RLT buffer and homogenized by vigorous vortexing. Samples were then mixed 1:1 v/v with 70% ethanol and loaded on RNeasy spin columns. The column was centrifuged at 8000 g and washed with kit buffers. The columns were incubated for 15 minutes with DNase solution (RNase-Free DNase Set; QIAGEN Ltd., Manchester, UK) at room temperature to degrade contaminating DNA in the samples. This was followed by several wash steps. Finally, the RNA was eluted by addition of nuclease-free water (Promega UK Ltd., Hampshire, UK) to the membrane. The RNA concentration of the samples was measured on a NanoDrop ND-1000 spectrophotometer (Thermo Fisher Scientific Inc, Waltham, MA, USA) and the RNA stored at -80°C.

2.6.2 Preparation of cDNA

Complementary DNA (cDNA) was synthesised from 500 ng of total RNA extracted from samples. Five hundred ng of RNA was added to 4 µl of qScript cDNA SuperMix (Quanta

Biosciences, MA, USA) and the volume was made up to 20 µl using nuclease free water in a sterile thin walled 0.2 ml PCR tube. The reaction mix was incubated in a Veriti Thermal Cycler (Applied Biosystems; Life Technologies Ltd, Paisley, UK) with the following protocol: 5 minutes at 25°C followed by 30 minutes at 42°C and then five minutes at 85°C. cDNA was stored at -20°C until required.

2.6.3 Quantitative real time polymerase chain reaction (qPCR)

All qPCR assays were performed using the ABI Prism 7700 sequence detection system (Applied Biosystems; Life Technologies Ltd, Paisley, UK). The qPCR reaction was set up as a multiplex reaction in a 20 µl volume of an optical 96 well reaction plate and covered with optical adhesive film (both Applied Biosystems; Life Technologies Ltd, Paisley, UK). Each reaction contained 5 µl of diluted cDNA (1:10 with nuclease-free water), 10 µl of FastStart Universal Probe Master Mix (Roche Diagnostics Limited), 1 µl of 20x primer/probe of gene of interest, 1 µl of 20x primer/probe endogenous control (Taqman, Applied Biosystems; Life Technologies Ltd, Paisley, UK) and 3 µl of nuclease free water. The primers and probes used are listed in Table 2.2. All reactions were run in triplicate and a water only (cDNA free) control was run for each primer-probe gene of interest. The samples were amplified using the standard relative quantification method using the following thermal-cycling conditions: enzyme activation at 50°C for 2 minutes, denaturation at 95°C for 10 minutes followed by 40 cycles of amplification, at 95°C for 15 s and extension at 60°C for 1 minute.

Table 2.2: List of Taqman primer/probe qPCR assays

Gene	Species	Assay ID
ICAM1	Mouse	Mm00516023_m1
SELE	Mouse	Mm00441278_m1
CXCL1	Mouse	Mm04207460_m1
GAPDH	Mouse	Mm99999915_g1
ANGPTL4	Human	Hs01101127_m1
CCL2	Human	Hs00234140_m1
CCL7	Human	Hs00171147_m1
CXCL1	Human	Hs00236937_m1
CXCL3	Human	Hs00171061_m1
CXCL8	Human	Hs00174103_m1
CXCL12	Human	Hs03676656_mH
ICAM1	Human	Hs00164932_m1
SELE	Human	Hs00174057_m1
SPHK1	Human	Hs01116530_g1
VCAM1	Human	Hs01003372_m1
GAPDH	Human	4310884E

2.6.4 qPCR data analysis

The delta-delta (ΔΔ) Ct method was used to quantify the relative levels of gene transcripts as previously reported (Livak and Schmittgen, 2001). Using amplification plots of fluorescent intensities generated by the ABI Prism 7700 sequence detection system, the threshold cycle (Ct) value was determined for each signal. Target gene values were normalised against an endogenous control (e.g. GAPDH) i.e. target Ct – endogenous control Ct. The resultant value was then expressed relative to an appropriate reference sample which was assigned an arbitrary value of 1.

2.6.5 RNA sequencing (RNAseq)

RNAseq was performed on 4 biological replicate pairs of HUVEC treated with S1P or vehicle control. Quality control check (RNA integrity number >7), library construction and sequencing was performed by BGI Tech Solutions (Hong Kong). RNA was hybridised to Illumina HiSeq 2000 platform and data obtained using 10 M clean reads. Data were analysed in-house (see Section 2.10).

2.7 Protein analysis

2.7.1 Western blotting

Protein Extraction

Suspension cells were pelleted by centrifugation at 200 g for five minutes. Cell pellets were washed in cold PBS and pelleted again in 1.5 ml eppendorfs prior to lysis. The medium of adherent cells was aspirated and the cells washed directly on the culture vessel with cold PBS prior to lysis. RIPA lysis buffer (140 mM NaCl, 10 mM Tris-HCl pH8, 1 mM EDTA, 1% Triton X-100, 0.1% SDS, 0.1% Sodium deoxycholate (deoxycholic acid)) supplemented with 1 mM of activated sodium vanadate and 4% v/v protease inhibitor (cOmplete Tablets, EDTA-free; Roche Diagnostics Limited, UK) was added to the eppendorfs (suspension cells) or directly to the culture vessel (adherent cells) and left on ice for 30 minutes. The lysates were centrifuged in 1.5 ml eppendorfs at full speed at 4°C for 15 minutes in a Heraeus Pico 17 Microcentrifuge (Thermo Fisher Scientific Inc, Waltham, MA, USA.). The protein supernatant was transferred to a new 1.5 ml eppendorf and stored at -20°C until required.

Determination of Protein Concentration

Protein concentration of samples was quantified using the Bio-Rad Protein Assay (Bio-Rad Laboratories Ltd., Hemel Hempstead, UK). Five standards of different concentrations of BSA (Sigma-Aldrich Ltd., Gillingham, UK): 0.1, 0.2, 0.3, 0.4 and 0.5 mg/ml were used. Each sample was diluted 1:10 with sterile distilled water. Ten µl of each standard and sample were plated in duplicate in a 96 well plate. Bio-Rad Protein Assay Reagent was diluted 1:5 in distilled water and 200 µl pipetted into each well. Absorbance was read on a Bio-Rad 680 microplate reader at 595 nm. The standards were used to plot a calibration curve from which the protein content of the samples was calculated.

Sodium dodecyl sulphate polyacrylamide gel electrophoresis (SDS-PAGE)

10% SDS-PAGE gels were made as per Lab FAQs booklet (Roche Diagnostics Limited, UK). Gels were submerged in Tris-Glycine-SDS PAGE Buffer (Geneflow Ltd., Litchfield, UK) in a Mini Trans-Blot Cell tank (Bio-Rad Laboratories Ltd., Hemel Hempstead, UK). Typically, 30 µg of protein lysates were mixed 1:4 v/v with 4x Laemmli sample buffer (Bio-Rad Laboratories Ltd., Hemel Hempstead, UK) and boiled at 95 °C for 5 minutes to denature proteins. Samples were loaded into the wells of the pre made gel along with Spectra Multicolor Broad Range Protein ladder (Thermo Fisher Scientific Inc, Waltham, MA, USA). Proteins were separated at 130 V for 1.5-2 hours depending on the size of the protein of interest.

Transfer of protein

Proteins were transferred from the gel to a polyvinylidene fluoride (PVDF) membrane using the ready-to-use Trans-Blot Turbo Mini PVDF Transfer Packs (Bio-Rad Laboratories Ltd., Hemel

Hempstead, UK) set up in Trans-Blot Turbo Transfer System (Bio-Rad Laboratories Ltd., Hemel Hempstead, UK). Proteins were transferred using the built in program of 1.3A, 25V for 7 minutes.

Table 2.3: List of antibodies used

Antibody	Species	Application	Company	Dilution
SPHK1	Rabbit	Western blotting	Cell signalling	1:1000
Phospho-SPHK1 (Ser-225)	Rabbit	Western blotting	ECM bioscience	1:1000
PARP	Rabbit	Western blotting	Cell signalling	1:1000
ERK	Rabbit	Western blotting	Cell signalling	1:1000
Phospho-ERK (Thr202/Tyr204)	Rabbit	Western blotting	Cell signalling	1:1000
SPHK1	Rabbit	IHC	Cell signalling	1:100
S1PR1 (H-60)	Rabbit	IHC	Santa cruz	1:600
S1PR2	Rabbit	IHC	Sigma-Aldrich	1:200
S1PR3	Rabbit	IHC	MyBioSource	1:600
CD15 (C3D-1)	Mouse	IHC	Dako	1:400
CD68 (PG-M1)	Mouse	IHC	Dako	1:200
CD31	Rabbit	IHC	Abcam	1:200
CD45-Pacific Blue (2D1)	Mouse	Flow cytometry	Ebioscience	1:100
CD144-APC (16B1)	Mouse	Flow cytometry	Ebioscience	1:100
CD31-PE (WM-59)	Mouse	Flow cytometry	Ebioscience	1:100

Immunoblotting

Non-specific protein binding was blocked by incubating the membrane for 1 hour at room temperature on a shaker in 5% dried milk dissolved in Tris buffered saline-0.1 % Tween-20 (TBST). Membranes were incubated with primary antibodies diluted to the appropriate concentrations (Table 2.3) in 5% w/v BSA/TBST on a rocker overnight at 4°C. The following day, membranes were washed 3 times, each for a total of 10 minutes, on a shaker in TBST prior to incubation for 1 hour in the appropriate HRP-conjugated secondary IgG antibodies

(Dako UK Ltd., Cambridgeshire, UK) which were diluted 1:1000 in 5% w/v milk/TBST. The membranes were washed again 3 times, each for a total of 10 minutes, on a shaker in TBST.

Proteins were visualised using Bio-Rad Clarity Western enhanced chemiluminescence (ECL) (Bio-Rad Laboratories Ltd., Hemel Hempstead, UK). Membranes were incubated with ECL mixture for 1 minute and then the excess liquid was drained off. The membrane was placed inside a plastic covering and developed on the ChemiDoc MP (Bio-Rad Laboratories Ltd., Hemel Hempstead, UK). Densitometry analysis was performed using ChemiDoc software.

Following the detection of the protein of interest, membranes were washed 3 times, each for a total of 10 minutes, in TBST and then re-probed for β-tubulin-HRP (Abcam, Cambridge, UK) diluted 1:1000 in 5% w/v milk/TBST for 1 hour at room temperature. Membrane was developed as described.

2.7.2 Immunohistochemistry (IHC)

Preparation of cells grown on microscope slides

HUVEC were grown on multi-spot coated microscope slides and then washed and fixed by submerging the slide in PBS for 2 minutes and 10% formal-saline solution for 10 minutes. Slides were then air-dried and stored at -20˚C until required.

Prepared slides of fixed HUVEC/HEK293 cells were thawed and then rinsed in running tap water for five minutes. The endogenous peroxidase activity was blocked by placing the slides in 0.3% hydrogen peroxidase (Sigma-Aldrich Ltd., Gillingham, UK) for 15 minutes.

Preparation of tissue sections

Paraffin-embedded blocks of DLBCL patient biopsy samples and reactive tonsil were obtained from the Queen Elizabeth Hospital, Birmingham, UK, with full ethical approval (No. RG_08-103). Paraffin embedded blocks of mouse tissue samples were processed by the Royal Orthopaedic Hospital (University of Birmingham). Sections were cut to a thickness of 4 µm onto X-tra Adhesive micro slides (Surgipath Europe, Peterborough, UK). The sections were de-waxed by immersing the slides in Histoclear (National Diagnostics, Hessel, UK) for 10 minutes and then rehydrated by immersing in 100% ethanol for 5 minutes (Sigma-Aldrich Ltd., Gillingham, UK) followed by tap water for a further 5 minutes. The endogenous peroxidase activity was blocked by placing the slides in 0.3% hydrogen peroxidase (Sigma-Aldrich Ltd., Gillingham, UK) for 15 minutes.

Antigen Retrieval

One litre of citrate buffer containing: 1.26 g sodium citrate, 0.25 g citric acid, 800 ml distilled water, pH adjusted to pH 6.0 with 0.1 M sodium hydroxide, was boiled in a glass beaker for 10 minutes on full power in a microwave prior to immersing the slides. The beaker containing the slides was then heated for 10 minutes at moderate power and then 10 minutes at low power. The buffer was then allowed to cool (approximately 30 minutes) before the slides were removed and rinsed in running tap water.

Detection of antigen

Following antigen retrieval, slides were placed in a metal microscope slide staining tray (Richardsons of Leicester Ltd., Leicester, UK) and washed with PBS-Tween-20 (0.1%) (PBST) for 5 minutes.

For human sections and fixed HUVEC/HEK293 cells: to reduce non-specific background staining, samples were blocked using 5X casein blocking solution (Vector Laboratories Ltd., Peterborough, UK) and incubated with diluted primary antibody in PBST overnight at 4°C (Table 2.3). Samples were washed with PBST for 5 minutes and incubated with DAKO Envision secondary antibody (Dako UK Ltd., Cambridgeshire, UK) for 30 minutes at room temperature. Samples were washed again with PBST for 5 minutes. Samples were incubated with diaminobenzidine (DAB) (Vector laboratories Ltd,. Peterborough, UK) which is converted to an insoluble brown product by the antigen-bound peroxidases allowing for visualisation of antigens bound to antibody.

For mouse sections: For CD15 and CD68 antibodies the M.O.M (mouse on mouse) detection kit (Vector laboratories Ltd,. Peterborough, UK) was used according to the manufacturer's protocol to reduce endogenous mouse Ig staining. For the SPHK1 and CD31 antibodies, the same process was carried out as the staining for human sections (above) but with incubation with anti-rabbit HRP-conjugated secondary IgG antibody diluted 1:200 in PBST (Dako UK. Ltd).

All sections were rinsed with distilled water and then counterstained with Mayer's haematoxylin (Sigma-Aldrich Ltd., Gillingham, UK) for 60 s and then rinsed again under running

warm tap water for 2 minutes. Stained sections were dehydrated by immersion in 100% ethanol for 5 minutes followed by Histoclear for 10 minutes and mounted with cover slips using DPX mounting medium (Sigma-Aldrich Ltd., Gillingham, UK) for microscopic examination. Slides were assessed by Dr Maha Ibrahim (University of Birmingham).

2.7.3 Flow cytometry

For flow cytometry, adherent cells were detached from the culture vessel by incubation with StemPro Accutase Cell Dissociation Reagent (Gibco, Life Technologies Ltd, Paisley, UK). Cells were counted and 1 x 10^6 cells pipetted into flow cytometry tubes for each stain required. Additionally, a tube of compensation beads (BD Biosciences, USA) was used for each antibody stain, each containing one drop of the relevant anti-species Ig and negative control. Cells and compensation beads were washed with 1% v/v FBS/PBS and then pelleted by centrifugation at 200 g for 5 minutes. The pellets were resuspended in 100 µl of 1% v/v FBS/PBS with antibody at the appropriate concentration (Table 2.3) and incubated at 4°C for 15 minutes in the dark. Following this, cells and compensation beads were washed in 1% v/v FBS/PBS and then fixed by resuspension in 200 µl of 1% paraformaldehyde. Cells were analysed using a BD LSR II Cell Analyzer (BD Biosciences, USA) and the data were analysed using Flowjo software (TreeStar Inc.).

2.7.4 Enzyme-linked immunosorbent assay (ELISA)

The production of chemokines by HUVEC was measured using a commercially available ELISA kit (DuoSet ELISA Development Systems; R&D Systems, Bio-Techne Ltd. Abingdon, UK.). For this assay, HUVEC were grown in normal growth conditions on 6 well dishes until they reached

confluency. The HUVEC were washed twice with PBS and culture media changed to M199 supplemented with 5% v/v FBS and 1% v/v P/S, to deplete the HUVEC of ECGS for 16 hours. The culture media was then changed for fresh M199 supplemented with 5% v/v FBS and 1% v/v P/S 1 hour prior to the treatment with S1P. S1P or vehicle control was then added directly to the medium which served as a 0 hours time point. HUVEC which received two S1P stimulations received the second S1P treatment at 6 hours. At 12 hours, the conditioned medium was collected and stored at -20°C until required. The ELISA was performed in accordance with the manufacturer's protocol and absorbance read at 450 nm. A calibration curve was calculated from the standards supplied in the kit using an online tool (www.elisaanalysis.com), which was then used to calculate the concentrations of the chemokines in the samples.

2.8 Migration assay

A transwell (Corning, Sigma-Aldrich Ltd., Gillingham, UK) was prepared by the addition of 600 µl of RPMI-1640 supplemented with 1% v/v FCS and chemokine (CXCL1 or MCP1; PeproTech, USA) or vehicle at the relevant concentration to the lower wells of a 24 well plate. 1 x 10^5 THP-1 cells or human CD14+ monocytes (provided by Tracey Perry) in 100 µl of RPMI-1640 supplemented with 1% v/v FCS were transferred into the transwell inserts (porse size 3 microns; Corning, Sigma-Aldrich Ltd., Gillingham, UK). Each treatment was run in triplicate. After 4 hours, transwell inserts were removed and all cells in the bottom wells pelleted and resuspended in 200 ul of 1% v/v FBS/PBS. Cells in each sample were counted on a BD LSR II Cell Analyzer for 60 s.

2.9 A20 syngeneic mouse model

A20 cells were injected at 3 x 10^6 cells/mouse intravenously into 6-9 week old female BALB/c mice (, USA) (carried out by) (Home office ethical approval, project no. PPL70_8280). At day 28, mice were killed by cervical dislocation and the spleens and livers were collected in RPMI-1640 (carried out by). A portion of liver and spleen was fixed in 10% formalin. Histology services at the Royal Orthopaedic Hospital, University of Birmingham, embedded the samples in paraffin wax and provided haematoxylin and eosin (H&E) stained sections. H&E sections were analysed by pathologist Dr Maha Ibrahim (University of Birmingham).

2.10 Statistical and bio-informatic analysis

Statistical analysis of data was performed using Graphpad Prism 7 software.

The reanalysis of published RNAseq data was performed by Dr Robert Hollows (University of Birmingham). The data for 32 ABC DLBCL and 54 GCB DLBCL were downloaded from the controlled access area of NIH database of genotypes and phenotypes (dbGap; http://www.ncbi.nlm.nih.gov/gap) using accession code phs000532.v5.p2 (Morin et al., 2013). The data for 4 GC B cell samples were downloaded from the Gene Expression Omnibus (GEO; http://www.ncbi.nlm.nih.gov/geo/) (accession GSE45982). The data for all samples were aligned to the hg19 human genome using Rsubread aligner (Liao et al., 2013) and assigned to individual genes using the featureCounts function. Read counts were then normalized between samples and converted to counts-per-million (CPM) reads for each gene using the edgeR package in R (Robinson et al., 2010).

The analysis of the S1P-treated HUVEC RNAseq data was performed by Dr Wenbin Wei (University of Birmingham). The same methodology was used as above to generate CPM values. Differentially expressed genes were identified using edgeR with $p<0.05$ and read CPM >1 in at least half of the sample list.

The reanalysis of microarray data was performed by Dr Wenbin Wei (University of Birmingham). The data for 11 DLBCL and 10 GC B cell samples was downloaded from the GEO (accession GSE12453) (Brune et al., 2008) and analysed using the MAS5 algorithm of the Affymetrix Expression Console to generate expression levels for each probe set (GCOS Signal). The MAS5 TGT was set to 100.

CHAPTER THREE

INVESTIGATING THE EFFECTS OF SPHK1 OVEREXPRESSION IN DLBCL AND DEFINING AN S1P GENE SIGNATURE PRESENT IN PRIMARY TUMOURS

3.1 Abstract

S1P is a small bioactive lipid, which through cellular signalling can induce many biological effects such as growth, survival and differentiation (Pyne and Pyne, 2000). In particular S1P has been shown to regulate vascular functions and angiogenesis. SPHK1, the main enzyme responsible for producing S1P, has been described as an oncogene and shown to be overexpressed in many cancers including NHL (Bayerl et al., 2008, Xia et al., 2000). However, our understanding of the contribution of SPHK1-S1P signalling to the pathogenesis of DLBCL, including its potential role in angiogenesis, remains unexplored.

In this chapter I show that SPHK1 is overexpressed in DLBCL and that SPHK1 expression correlates with the expression of known tumour-associated angiogenic genes. I also describe here the characterisation of HUVEC as a model which can be used to define an S1P-associated gene signature in primary DLBCL.

3.2 Results

3.2.1 SPHK1 is overexpressed in primary DLBCL and DLBCL cell lines

I first studied the expression of SPHK1 protein in tumour biopsy sections from 39 DLBCL patients. These samples were obtained from the Human Bioresource Resource Centre and the diagnosis of DLBCL was independently confirmed by three pathologists prior to analysis. To detect SPHK1 protein, I performed IHC. One case was excluded due to tissue being extensively crushed. Of the remaining 38 cases I observed SPHK1 staining in the tumour cells of 36/38 cases (Figure 3.1A). In one of the two negative cases, I observed staining in the squamous epithelium which served as an internal positive control. The other negative case was excluded due to the lack of an internal positive control (Appendix 1). As a consistent internal positive control was not present in all cases, I was unable to accurately assess the level of protein and determine whether SPHK1 was overexpressed. To overcome this I used available gene expression datasets to determine the level of SPHK1 mRNA in DLBCL cases compared to normal germinal centre B (GC B) cells (Brune et al., 2008, Morin et al., 2011). First, the reanalysis of a published RNAseq dataset showed a statistically significant increase in SPHK1 expression in both ABC DLBCL (n=32) and GCB DLBCL (n=54) compared to normal GC B cell samples (n=4) ($p<0.0001$, for both comparisons) (Figure 3.1B). Furthermore, the reanalysis of a published microarray dataset also revealed a statistically significant increase in SPHK1 expression when 11 primary DLBCL samples (subtypes unknown) were compared to 10 GC B cell samples ($p=0.002$) (Figure 3.1C)

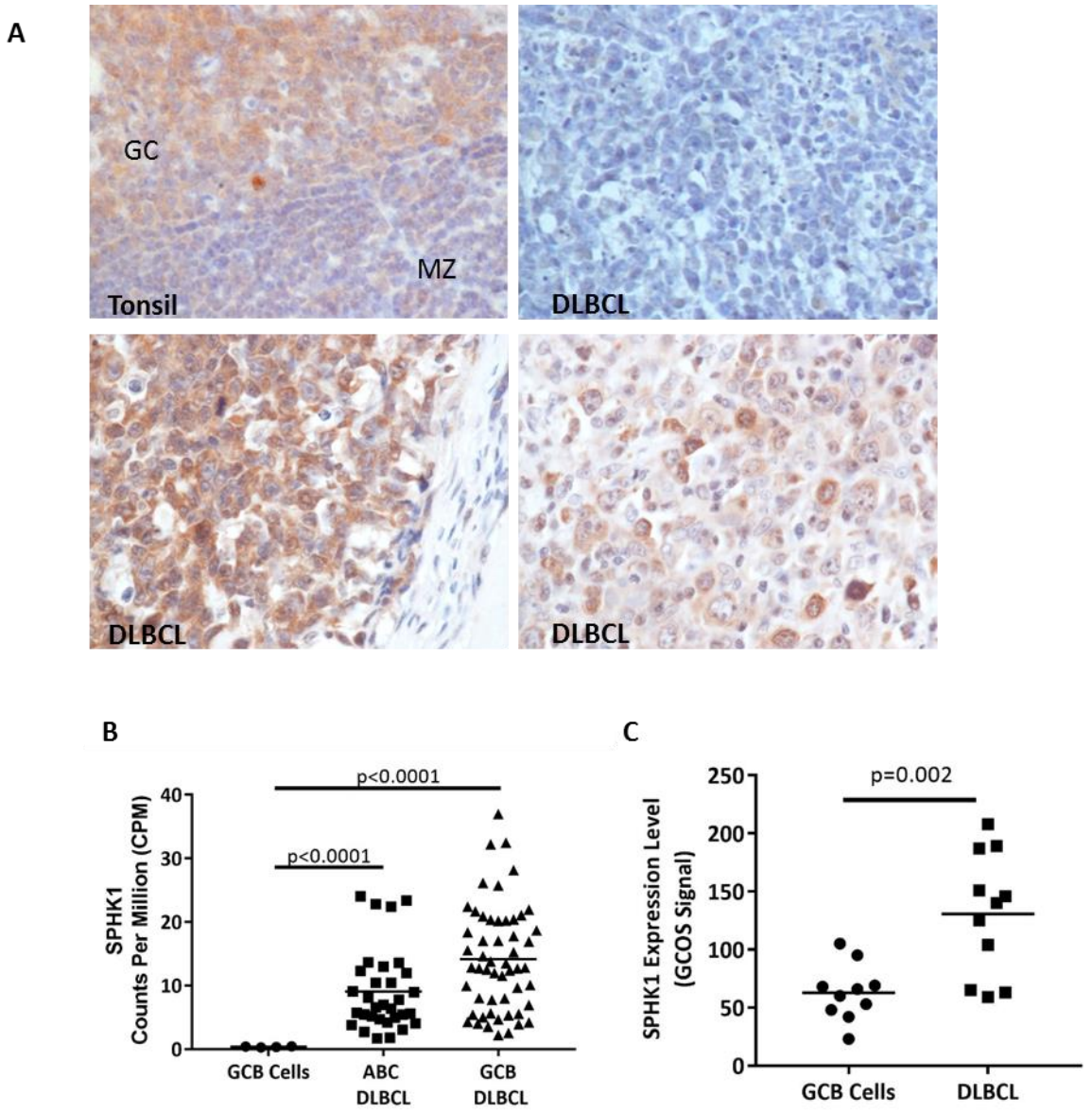

Figure 3.1: SPHK1 expression in primary DLBCL. (A) Representative IHC stains for SPHK1 expression. SPHK1 is expressed in normal GC cells of a tonsil (top left). SPHK1 negative DLBCL case 1/37 (top right). Two representative SPHK1 positive DLBCL cases from 36/37 (bottom panel). GC = germinal centre, MZ = mantle zone. (B) The reanalysis of RNAseq data shows a statistically significant increase in SPHK1 expression in 32 cases of ABC DLBCL and 54 cases of GCB DLBCL compared to 4 normal GCB cell samples. (C) Reanalysis of a published microarray dataset shows a statistically significant increase in SPHK1 expression in 11 primary DLBCL samples compared to 10 GC B cell samples. Students T-test.

Next, I compared the expression of SPHK1 mRNA in 9 DLBCL cell lines with that in CD10+ GC B cells isolated from three donors (provided by Dr Vrzalikova). SPHK1 expression was detected in all cell lines and, with the exception of SUDHL4, expression was the same or higher than in all three GC B cell samples (Figure 3.2A). Activation of SPHK1 and translocation to the plasma membrane where its substrate resides is mediated by phosphorylation at Serine 225 (Pitson et al., 2003b). Previous studies from our lab, (Abdullah et al; unpublished), have shown that available phospho-specific SPHK1 antibodies do not work in IHC. To ascertain the phosphorylation of SPHK1 in DLBCL cells I performed immunoblotting of the available DLBCL cell lines (Figure 3.2B). Consistent with the results of the qPCR analysis, I observed expression of SPHK1 in all cell lines. I detected phosphorylated SPHK1 in all cell lines, confirming the presence of the activated form of SPHK1.

3.2.2 SPHK1 expression is associated with angiogenic functions in primary DLBCL

Next, I identified a subset of genes that were co-expressed with SPHK1 in primary DLBCL using data provided by Dr Reuben Tooze (University of Leeds) in which a meta-analysis of ten different DLBCL gene expression datasets, including more than 2000 cases of whole tumour primary DLBCL, had been performed. Within each of the ten gene expression datasets, the Spearman's rank correlation was calculated for the expression of SPHK1 against all other genes individually (n=20,121). The resultant p values and correlations for each gene from all datasets were merged by taking the median values (Care et al., 2015). I identified 2236 genes that were significantly positively correlated, and 1658 genes that were significantly negatively correlated, with SPHK1 expression in primary DLBCL ($p<0.05$). Importantly, this gene signature included genes expressed from cells within the tumour microenvironment as well as the

tumour cells as it was generated using data from whole tumour biopsies. Using an online gene functional classification tool, DAVID (https://david.ncifcrf.gov/) (Dennis et al., 2003), I performed gene ontology analysis of the genes correlated with SPHK1 expression. This analysis identified a significant enrichment of vasculature related ontology terms in the significantly positively correlated gene set (Figure 3.3).

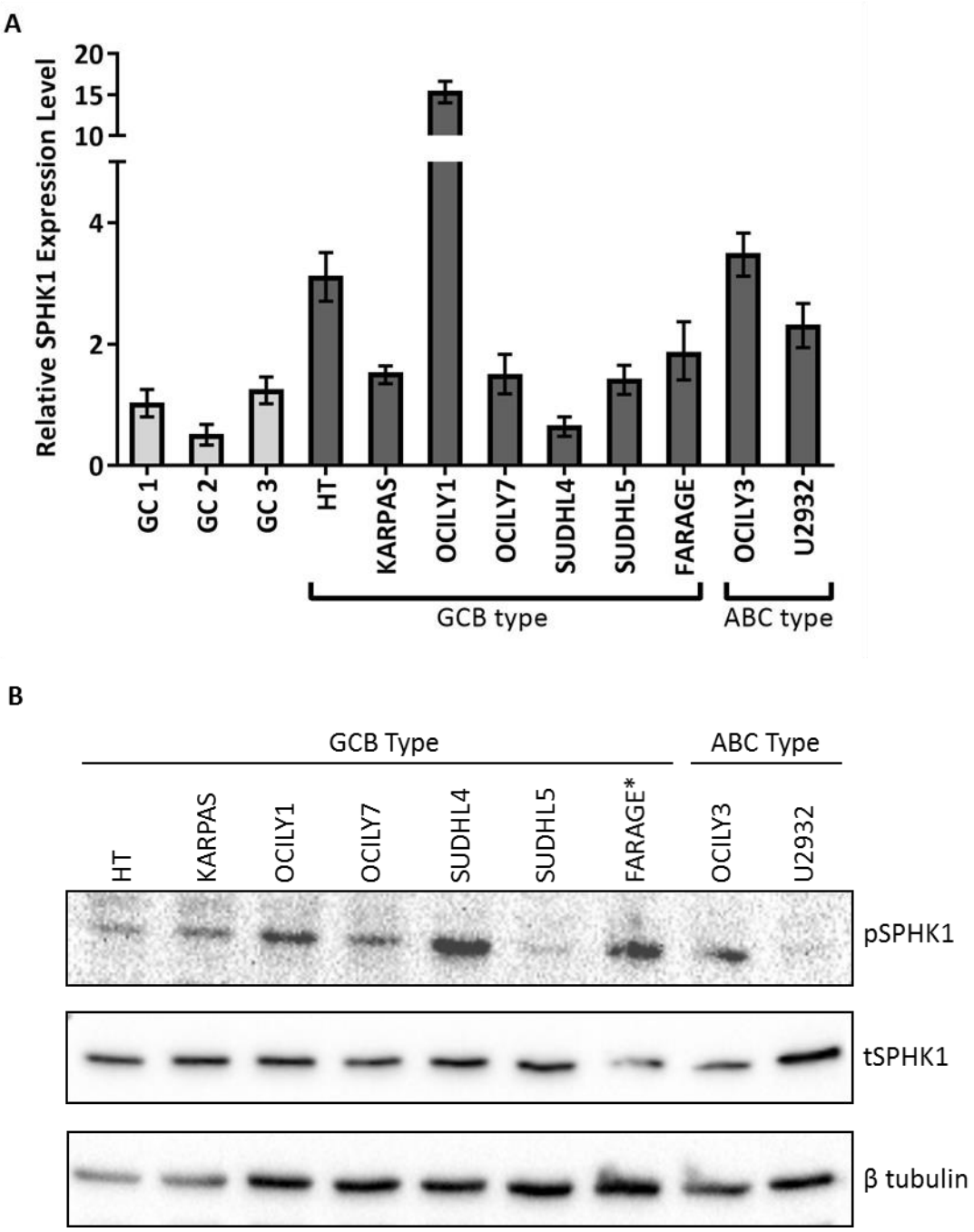

Figure 3.2: SPHK1 expression in DLBCL cell lines. (A) qPCR analysis for the expression of SPHK1 in DLBCL cell lines (dark grey bars) and GC B cell samples (light grey bars). Data are presented as $2^{-\Delta\Delta CT}$ and relative to one GCB sample. (B) Immunblotting analysis of DLBCL cell lines for phosphorylated and total SPHK1 (pSPHK1, tSPHK1, respectively). β-tubulin is a loading control. *= EBV+ cell line.

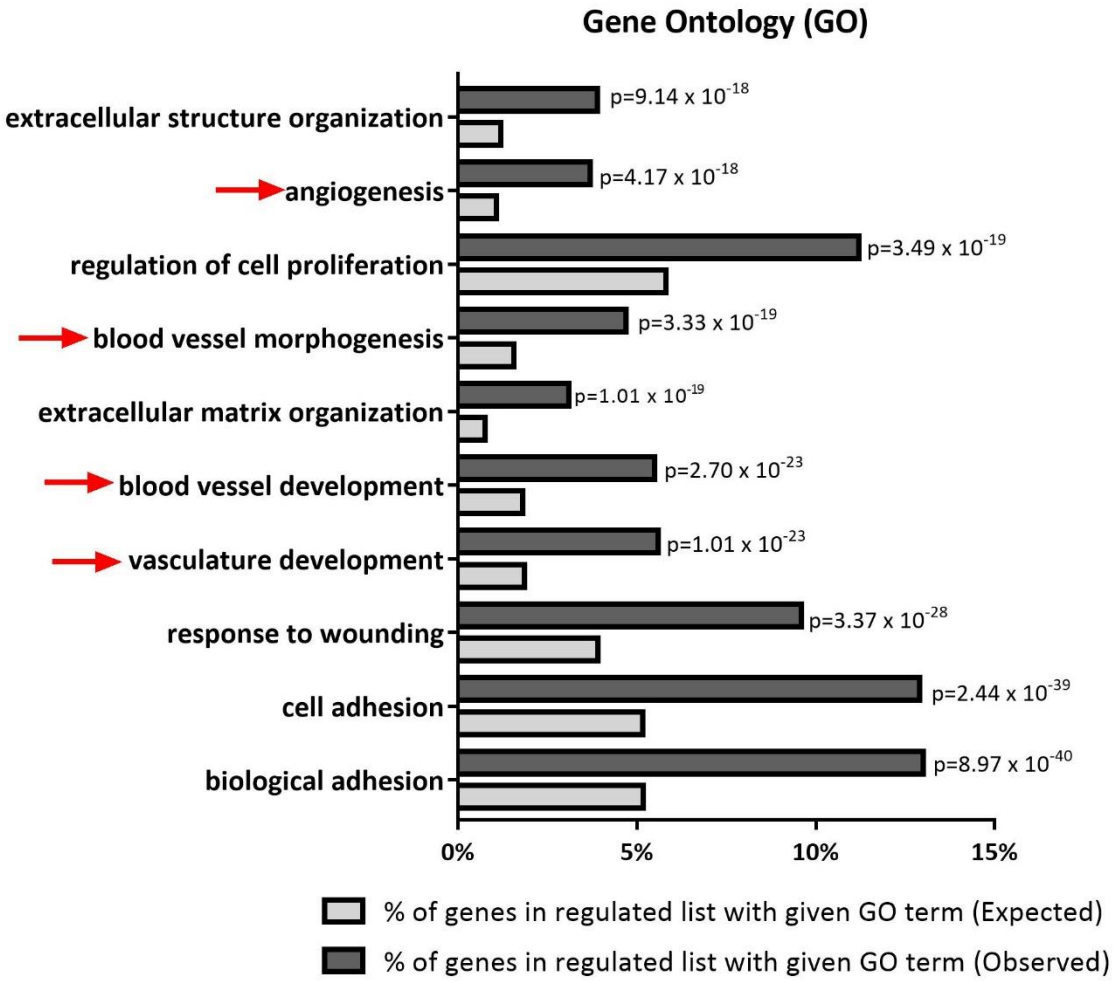

Figure 3.3: SPHK1 expression is associated with angiogenic functions in primary DLBCL. Gene ontology (GO) analysis of genes positively associated with the expression of SPHK1 in primary DLBCL ordered by p value. Analysis reveals GO terms associated with blood vessel function (red arrows). Dark grey bars represent the observed percentage of upregulated genes in a particular GO category. Light grey bars represent the expected percentage of upregulated genes in a particular GO category. P value of each term was determined using Fisher's exact test.

To provide further confirmation that angiogenesis related genes were enriched in the set of genes co-expressed with SPHK1 in DLBCL, I took advantage of the availability of a published 'tumour vascular gene signature.' This tumour vascular signature was generated from an integrative meta-analysis of more than 1000 primary human cancers and is comprised of genes the expression of which jointly correlates with that of many angiogenic genes or endothelial cell specific genes (Masiero et al., 2013). Using only genes present on both platforms (n= 17851; Table 3.1), I compared the genes significantly correlated with SPHK1 expression in primary DLBCL to this tumour vascular gene signature (Table 3.2). This analysis revealed that genes positively correlated with SPHK1 expression in primary DLBCL were significantly enriched for tumour vasculature signature genes (chi-square=560.18, odds ratio=7.9, $p<0.0001$; Table 3.3; Figure 3.4), whereas genes negatively correlated with SPHK1 in primary DLBCL were significantly depleted for tumour vascular signature genes (chi-square=14.42, odds ratio=0.37, $p<0.0001$; Table 3.3; Figure 3.4). Taken together, these results suggest that the overexpression of SPHK1, which would be expected to lead to the increased production of extracellular S1P, could promote angiogenesis in DLBCL.

Table 3.1: Number of genes positively and negatively correlated with SPHK1 expression in primary DLBCL and present in the tumour vascular signature including those used in the enrichment analyses.

	Total Number	Number of genes used in enrichment analysis (present on both DLBCL-SPHK1 correlated genes dataset and tumour vascular signature genes dataset n=17851)
Genes positively correlated with SPHK1 expression in primary DLBCL	2236	2150
Genes negatively correlated with SPHK1 expression in primary DLBCL	1658	1517
Tumour vascular signature genes	471	471

Table 3.2: Numbers of genes in the tumour vascular signature that were also found to be either positively or negatively correlated with the expression of SPHK1 in primary DLBCL

	Tumour Vascular Signature Genes (n=471)
Genes positively correlated with SPHK1 expression in primary DLBCL (n=2150)	235
Genes negatively correlated with SPHK1 expression in primary DLBCL (n=1517)	16

Table 3.3: Chi-square test of the overlap between genes correlated with the expression of SPHK1 in primary DLBCL and those present in the tumour vascular signature

	Observed (O)	Expected (E)	O-E	Chi square	Odds Ratio	P-Value
Tumour vascular signature genes and genes positively correlated with SPHK1 expression in primary DLBCL	235	56.73	178.27	560.18	7.9	<0.0001
Tumour vascular signature genes and genes negatively correlated with SPHK1 expression in primary DLBCL	16	40.03	-24.03	14.42	0.37	<0.0001

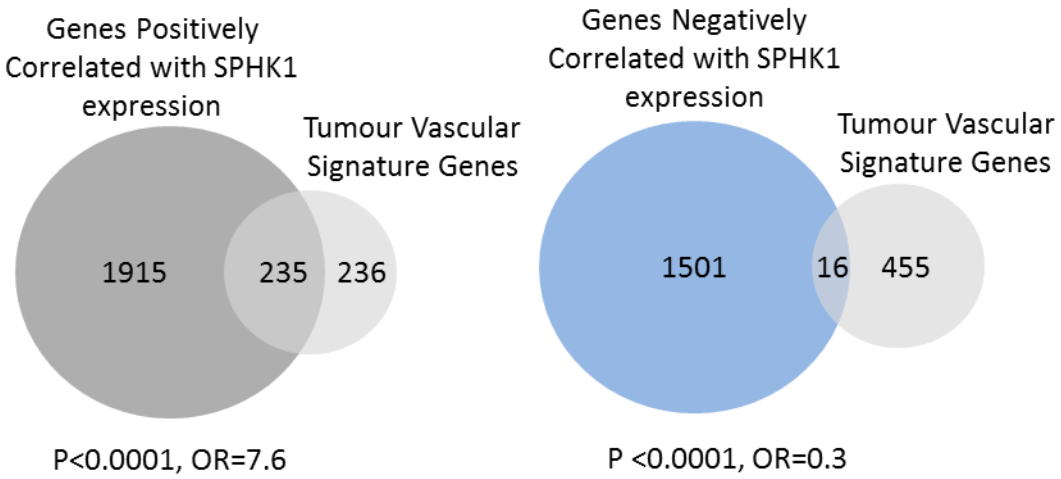

Figure 3.4: Genes co-expressed with SPHK1 in primary DLBCL are enriched for tumour vascular signature genes. Venn diagrams showing the overlap between genes positively or negatively correlated with SPHK1 in primary DLBCL (dark grey and blue circles respectively) with tumour vascular signature genes (light grey circles). Genes positively correlated with the expression of SPHK1 in primary DLBCL were significantly enriched for tumour vascular signature genes (chi square=560.18, odds ratio=7.6, p<0.0001). Genes negatively correlated with SPHK1 expression in primary DLBCL were significantly depleted for tumour vascular signature genes (chi-square=14.42, odds ratio=0.3, p<0.0001,) OR= odds ratio.

3.2.3 Establishing HUVEC as a model system to study the effects of S1P on DLBCL-associated endothelial cells

To further explore the potential impact of S1P on angiogenesis in DLBCL, I wanted to establish an *in vitro* model which would allow me to more directly study the impact of S1P signalling on the transcription of endothelial cells and, in turn, the extent to which this transcriptome could be observed in SPHK1 overexpressing DLBCL. To do this I used HUVEC, which are primary cells derived from the endothelium of veins from the umbilical cord that are extensively used as an *in vitro* endothelial cell model.

In this section I describe the isolation and characterisation of HUVEC, including the expression of S1P receptors, and show that this model is a useful one with which to study S1P activated signalling and resulting expression of angiogenesis-associated genes.

1. Identification and characterisation of HUVEC

HUVEC were isolated from the umbilical cords of four donors using collagenase treatment. As expected the cells were homogenous in morphology and exhibited a cobblestone growth pattern typical of endothelial cells (Figure 3.5A). Flow cytometry showed that over 97% of isolated cells were positive for CD31 and CD144, which are established biomarkers of endothelial cells, and negative for the leukocyte common antigen, CD45, indicating high purity without contamination from peripheral blood cells (Figure 3.5B).

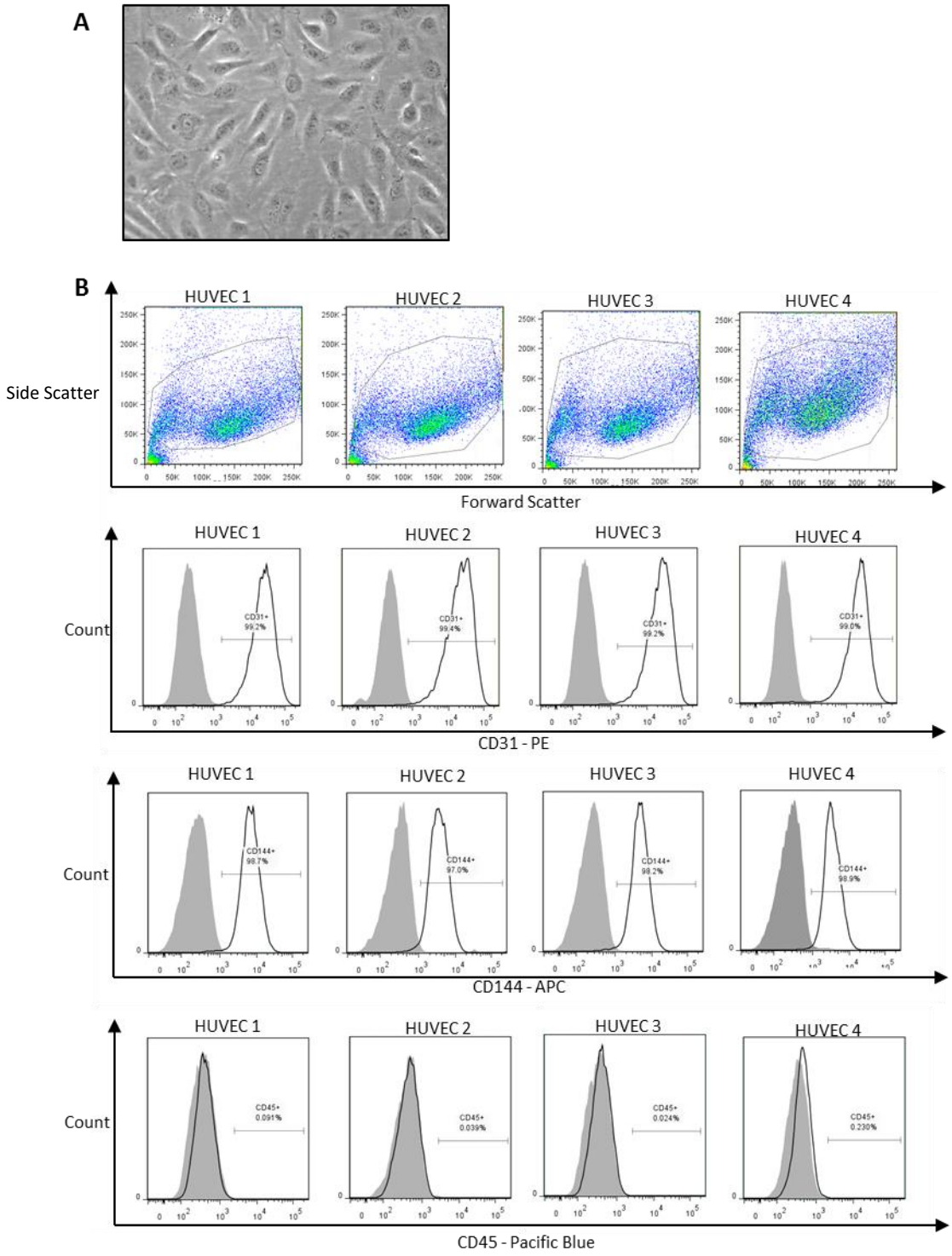

Figure 3.5: Purity of isolated HUVEC. (A) Representative image of cultured HUVEC showing cobblestone morphology typical of endothelial cells. (B) Isolated HUVEC samples were analysed by flow cytometry for expression of CD31, CD144 and CD45 in comparison to unstained cells (solid grey peak) to assess purity. Cells were gated by forward scatter and side scatter (top panel) to include all cells in the analysis. All four HUVEC samples were >97% positive for the endothelial markers CD31 and CD144 and negative for the leukocyte common antigen CD45.

2. S1P receptor expression in HUVEC is representative of that observed in DLBCL-associated endothelial cells

I next wanted to characterise the expression of the three major S1P receptors S1PR1, S1PR2 and S1PR3 in the tumour-associated endothelial cells of primary DLBCL and to ascertain if HUVEC recapitulate this expression profile. I first confirmed the specificity of the antibodies I was using by showing strong staining of S1PR1, S1PR2 and S1PR3 in plasmid transfected HEK293 cells but not in empty vector control transfected HEK293 cells (Figure 3.6). IHC with these antibodies revealed that the tumour-associated endothelial cells expressed S1PR1 in all cases of DLBCL (n=36). In contrast, S1PR2 was absent in endothelial cells in 35 cases, despite the strong expression of S1PR2 in red blood cells. Of the 36 cases stained for S1PR3, 17 cases were excluded due to the lack of an internal positive control (tumour cell positivity or squamous epithelial cell positivity). Of the remaining 19 cases S1PR3 was not expressed in the tumour-associated endothelial cells (Figure 3.7; Appendix 1).

I next characterised the expression of S1P receptors in isolated HUVEC. Figure 3.8 shows that S1PR1 was highly expressed whereas S1PR2 and S1PR3 protein was not detectable in HUVEC. Mantle zone, germinal centres and squamous epithelium of tonsil were used as positive controls (Figure 3.8).

Taken together, these results show that HUVEC are a suitable model in which to study the S1P signalling of DLBCL-associated endothelial cells.

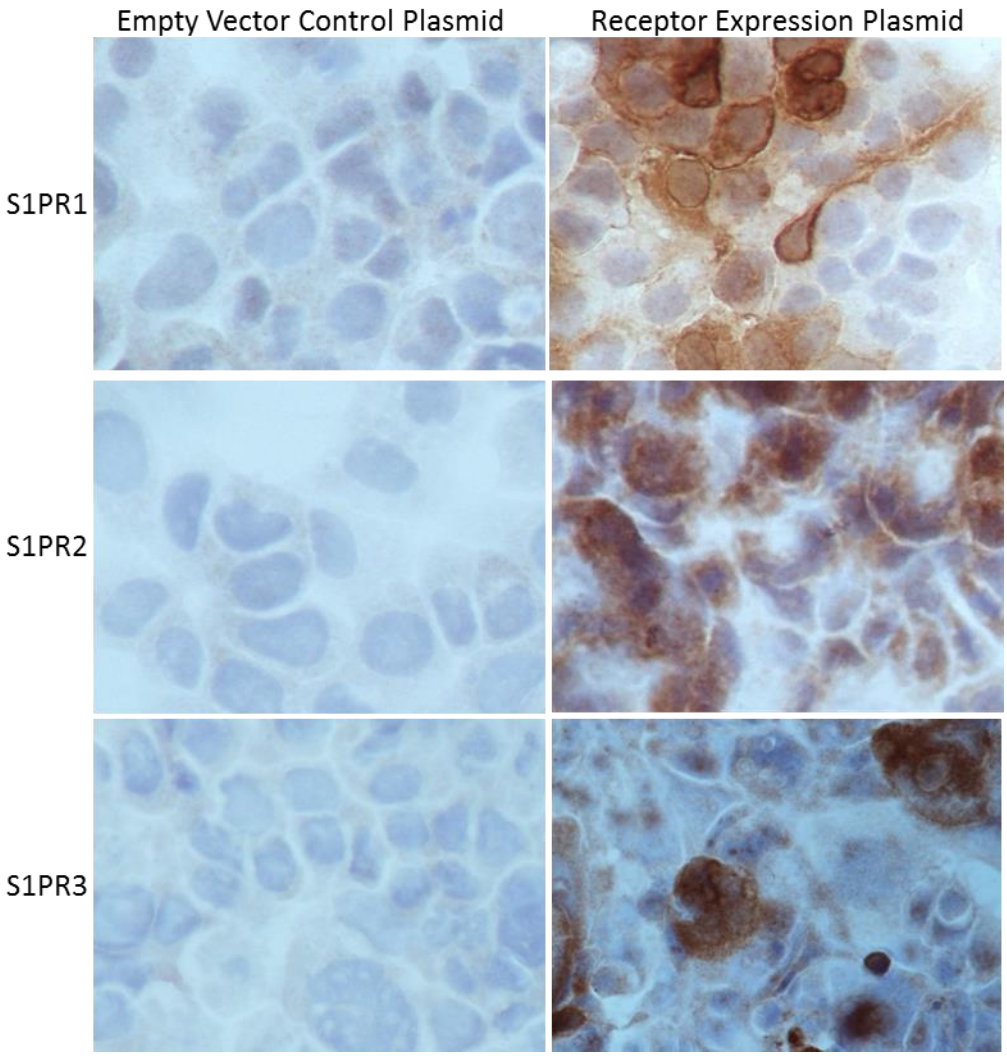

Figure 3.6: Validation of the specificity of S1P receptor antibodies. HEK293 cells were transfected with vector only control or S1P receptor expression plasmid. Receptor expression plasmid transfected cells shows strong specific staining compared to empty vector control transfected cells.

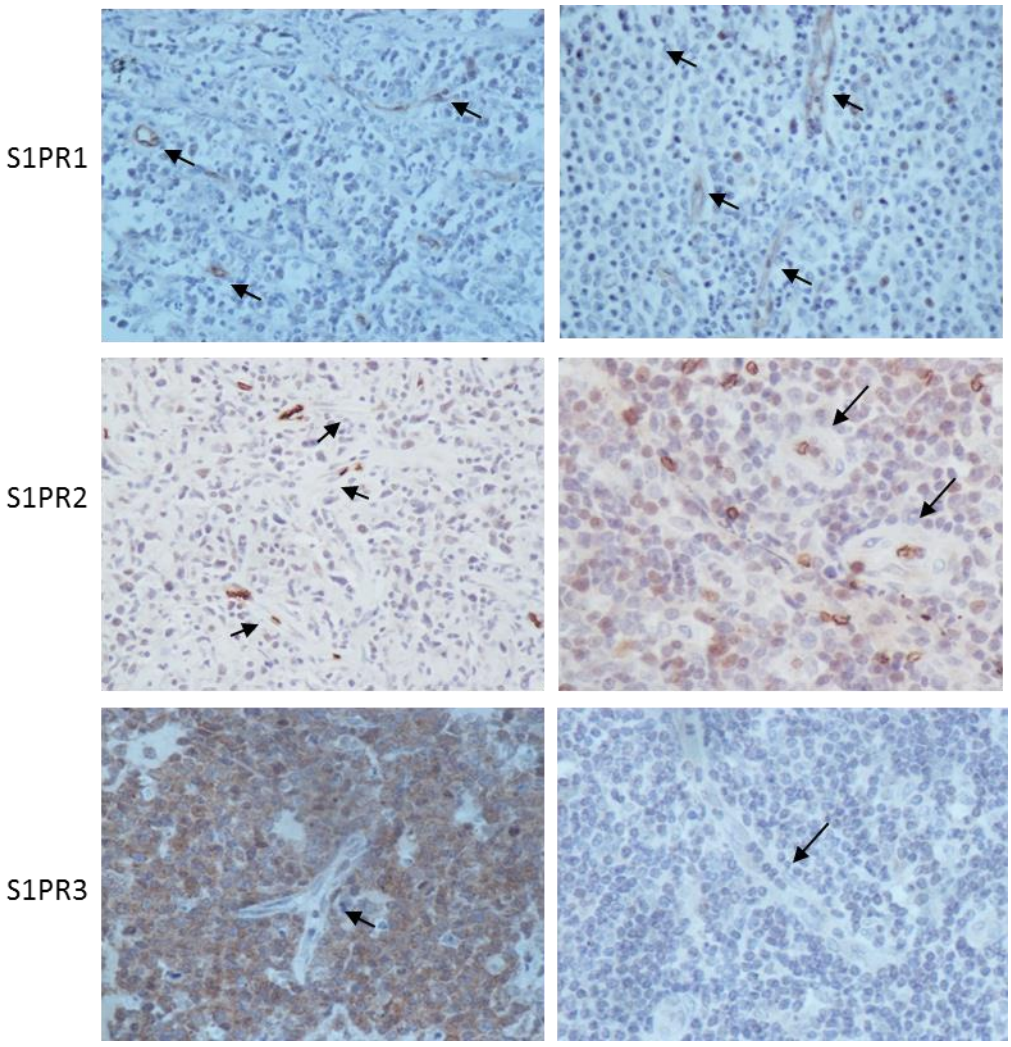

Figure 3.7: DLBCL-associated endothelial cells express S1PR1 but not S1PR2 or S1PR3. Representative IHC images of staining for S1PR1, S1PR2 and S1PR3 in DLBCL, endothelial cells were positive for S1PR1, but negative for S1PR2 and S1PR3 (black arrows). Bottom left shows S1PR3 positive tumour cells.

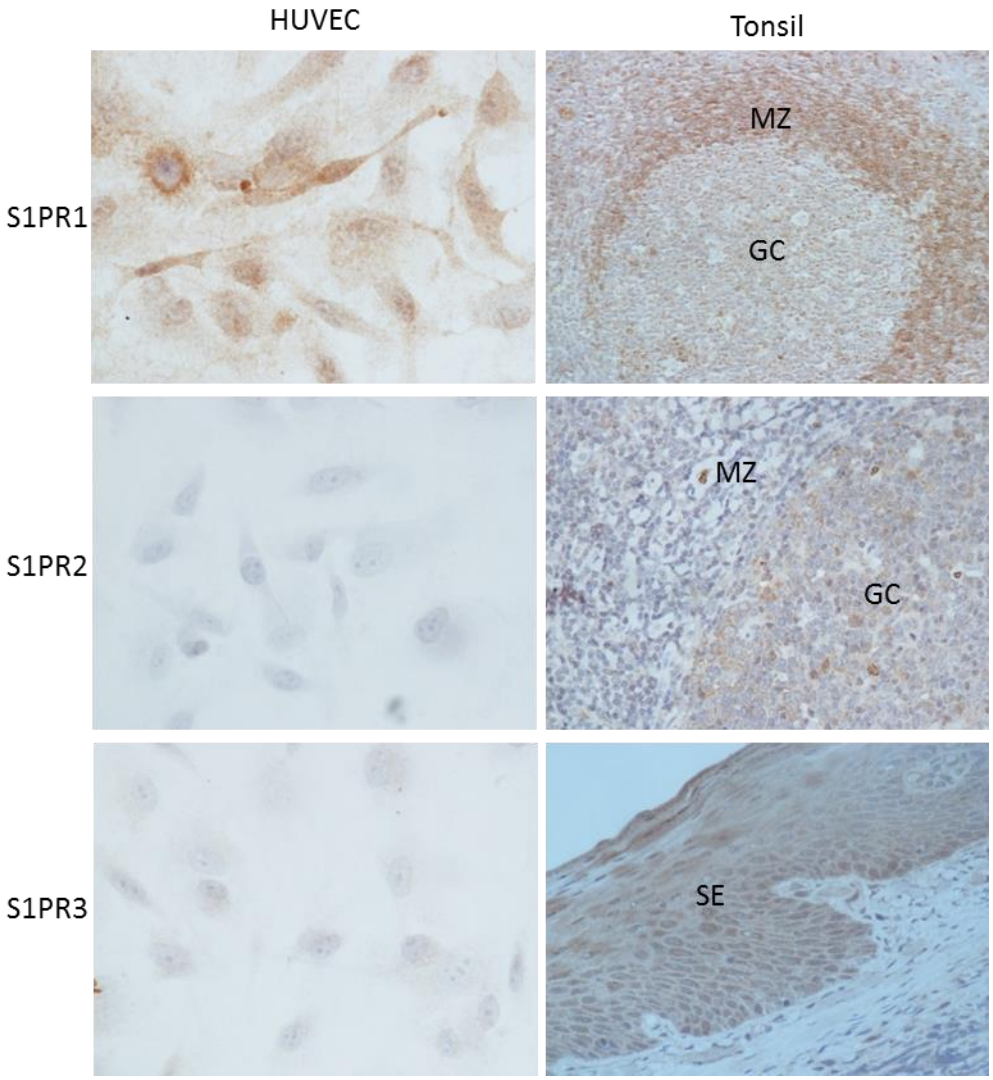

Figure 3.8: HUVEC express S1PR1, but not S1PR2 or S1PR3. S1P receptor expression was characterised by IHC. Tonsil was used as a positive control and showed S1PR1 expression in the mantle zone (MZ), S1PR2 expression in the germinal centre (GC) and S1PR3 expression in the squamous epithelium (SE).

3. S1P activates signalling pathways and the transcription of angiogenic genes in HUVEC

The cell culture medium of HUVEC contains commercially available endothelial cell growth supplement which contains angiogenic growth factors such as VEGF and FGF. As these growth factors could decrease the sensitivity of any signalling effects from S1P treatment, I first studied the effects of the removal of these growth factors from the cell culture medium. One possible outcome could be increased apoptosis. To study the effects of removal of these growth factors on cell survival I performed immunoblotting against poly ADP-ribose polymerase (PARP) as PARP cleavage by caspases is a marker of apoptosis. As a positive control, I used cells which had been serum starved for 24 hours. As expected I detected cleaved PARP (89kDa) in these cells (Figure 3.9). However, I did not detect cleaved PARP following the removal of growth factors from the media of HUVEC (Figure 3.9).

As the activation of ERK has been shown to be important for angiogenic functions in HUVEC induced by factors such as VEGF, I also studied the effects of growth factor removal on ERK activation (Rousseau, 1997). Removal of growth factors reduced the levels of phosphorylated ERK (pERK) (Figure 3.10).

Based on the results of these experiments I chose to deplete the HUVEC of endothelial cell growth supplement for 16 hours prior to S1P stimulation so as to increase the sensitivity of any observed S1P signalling effects.

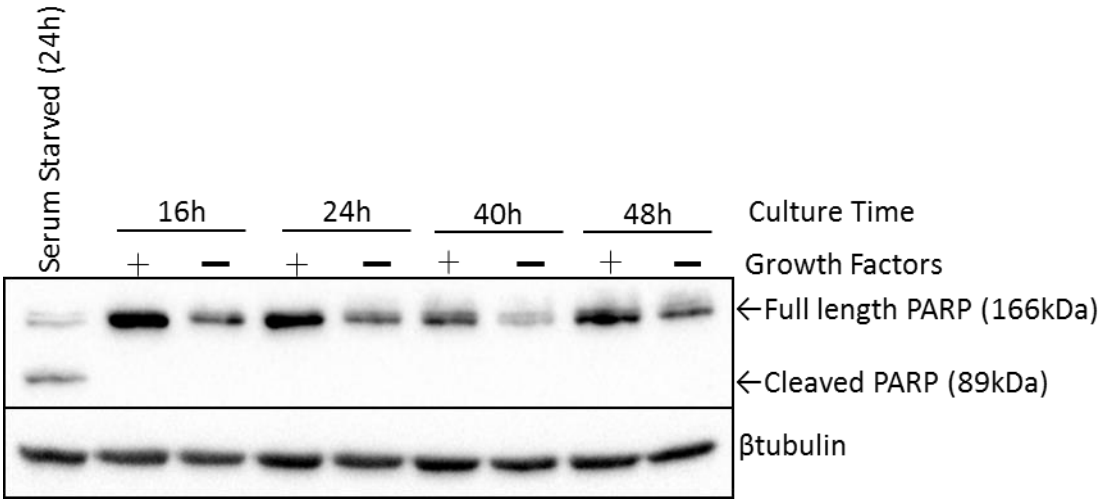

Figure 3.9: Detection of PARP in HUVEC following growth factor depletion. HUVEC were cultured in media either in the absence or presence of endothelial growth supplement (growth factors) and harvested at the indicated time points. Immunoblotting revealed no detectable PARP cleavage (89kDa) in cells cultured in media containing or not containing growth factor supplements at all time points. β-tubulin confirmed equal loading of samples. Data shown are representative of three independent experiments from three different HUVEC donors.

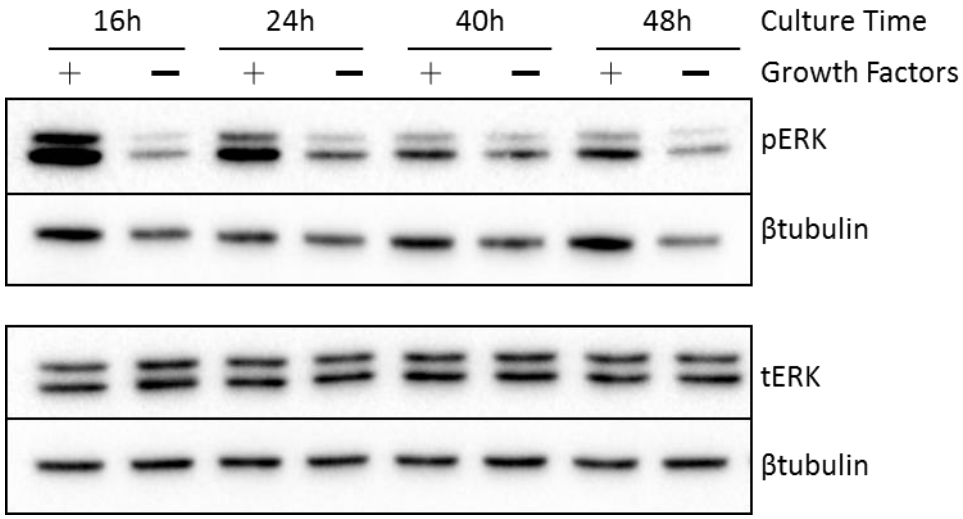

Figure 3.10: Detection of ERK in HUVEC following growth factor depletion. HUVEC were cultured in media either in the absence or presence of endothelial growth supplement (growth factors) and harvested at the indicated time points. Immunoblotting revealed higher levels of pERK in cells grown in media containing growth factor supplement compared to those grown in media without growth factor supplement. β-tubulin confirmed equal loading of samples. Data shown are representative of two independent experiments from two different HUVEC donors.

Next, I investigated ERK activation following the treatment of HUVEC with S1P. I performed immunoblotting against pERK on HUVEC treated with various concentrations of S1P for 5 minutes. S1P activated ERK at all concentrations reaching a maximum at 0.5 μM (Figure 3.11). For all subsequent stimulations I treated cells with 0.5 μM S1P.

Having shown that S1P activates ERK signalling in HUVEC, I next explored whether this is associated with changes in gene transcription in these cells. I chose three known target genes of S1P in endothelial cells, ICAM1, CXCL8 which encodes IL8, and SELE which encodes E-Selectin (Lin et al., 2006, Shimamura et al., 2004). I showed using qPCR that the expression of all three genes was upregulated in HUVEC from four different donors following treatment with S1P for 4 hours (Figure 3.12).

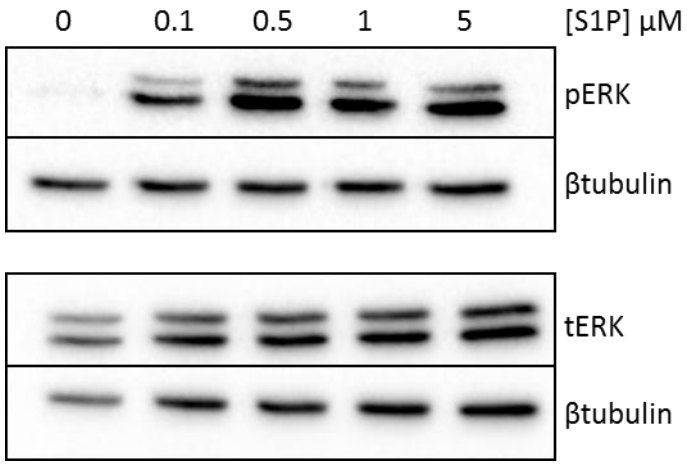

Figure 3.11: S1P treated HUVEC activate ERK in a dose dependent manner. HUVEC were treated with S1P at the indicated concentrations and harvested at 5 minutes. Immunoblotting revealed the dose dependent activation of ERK by S1P shown by increased levels of pERK compared to control. β-tubulin confirmed equal loading of samples. Data shown are representative of four independent experiments from four different HUVEC donors.

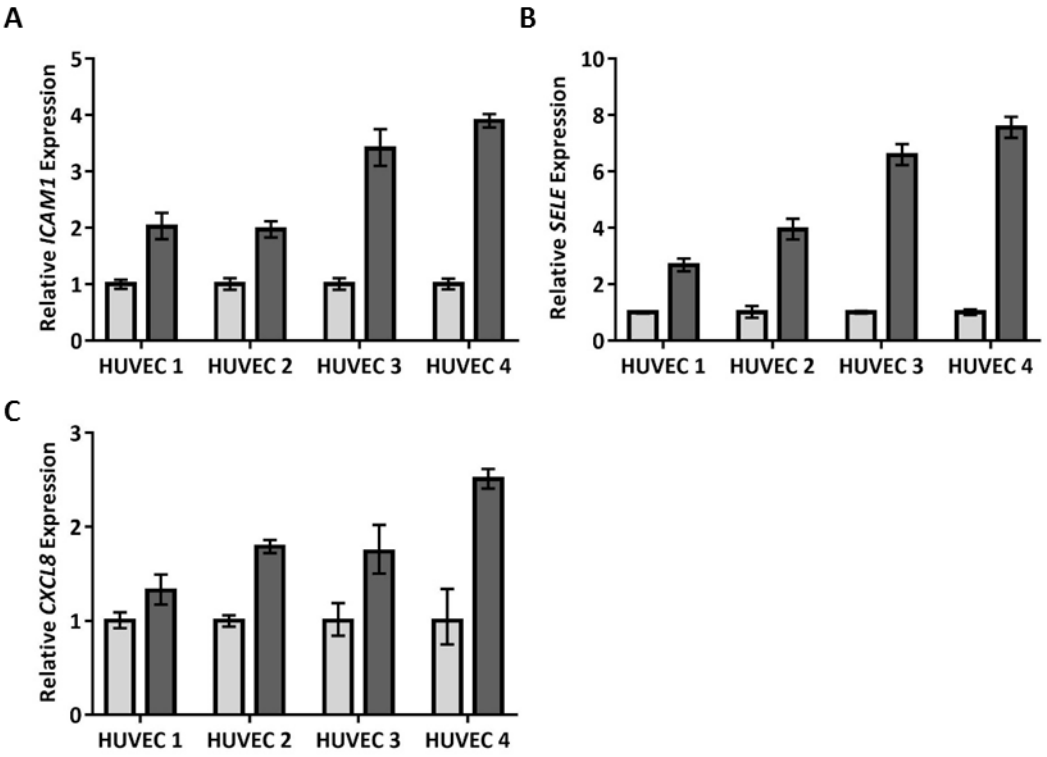

Figure 3.12: Upregulation of known S1P target genes in HUVEC. qPCR analysis shows the upregulation of ICAM1 (A), SELE (B) and CXCL8 (C) in HUVEC treated with S1P (dark grey bars) relative to untreated cells (light grey bars). Shown are the results from four separate donors (HUVEC 1-4). Samples were analysed in triplicate and are presented as $2^{-\Delta\Delta CT}$ values in comparison to corresponding control.

3.2.4 Optimisation of conditions and time point to study global gene expression changes in S1P treated HUVEC

S1P-mediated signalling pathway activation is transient in HUVEC

Having shown that HUVEC can be used to study the effects of S1P on the transcription of endothelial cells, I next wanted to optimise the conditions under which I could study global gene expression. The activation of ERK by S1P was further examined by treating HUVEC with S1P for various times. Fig 3.13 shows that the initial and rapid induction of ERK phosphorylation by S1P is transient, reaching a maximum at 5 minutes and declining back to basal levels from 1 hour.

Upregulation of S1P target genes following S1P treatment is transient

To choose an appropriate time point to study the global gene expression in S1P treated HUVEC, I performed a time course on S1P treated HUVEC using the expression of three S1P target genes, ICAM1, CXCL8 and SELE, as a read out. qPCR showed that the S1P-mediated upregulation of these genes is transient, with highest upregulation observed at 3h for CXCL8 and 4h for ICAM1 and SELE (Figure 3.14).

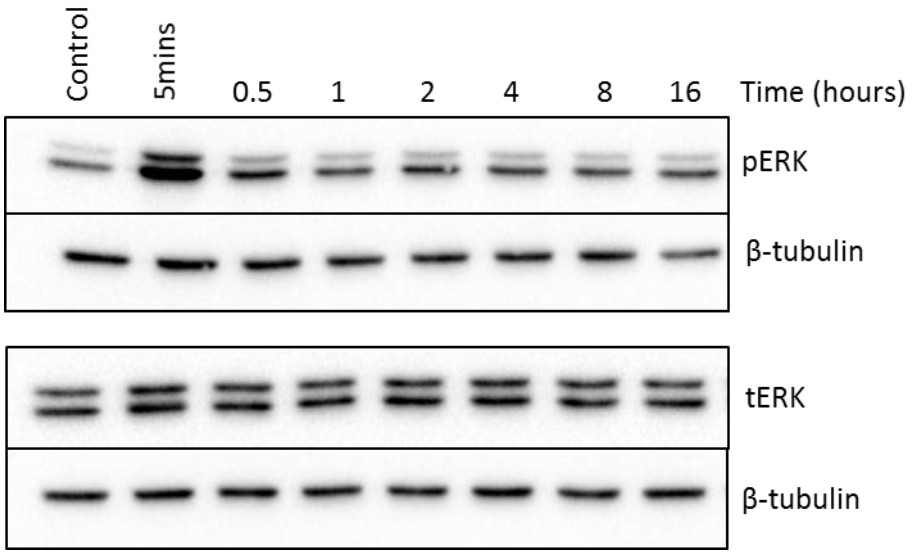

Figure 3.13: Activation of ERK is rapid and transient following S1P treatment of HUVEC. HUVEC were treated with S1P for the indicated time periods. Immunoblotting revealed that the activation of ERK by S1P is rapid, reaching maximum levels at 5 minutes and declining back to basal levels by 1 hour. β-tubulin confirmed equal loading of sample. Data shown are representative of four independent experiments from four different HUVEC donors.

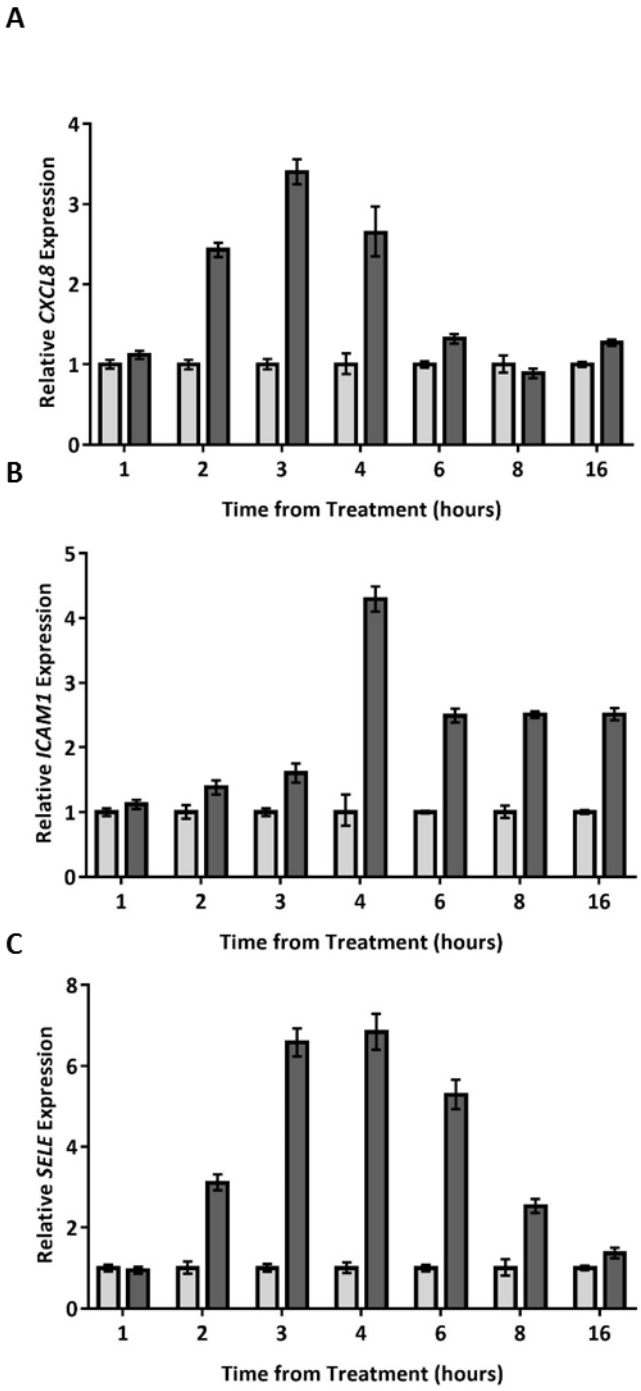

Figure 3.14: Time course of S1P target genes in HUVEC. qPCR analysis for the expression of CXCL8 (A), ICAM1 (B) and SELE (C) in HUVEC treated with S1P at indicated time points (light grey bars) relative to vehicle treated cells (dark grey bars). Analysis reveals the transient upregulation of genes reaches maximum expression levels for CXCL8 at 3 hours and ICAM1 and SELE at 4 hours. Samples were analysed in triplicate and are presented as $2^{-\Delta\Delta CT}$ values in comparison to corresponding control.

3.2.5 Identification of S1P target genes in HUVEC

I chose 4h as the optimum time point for a global gene expression analysis following S1P treatment of HUVEC. The upregulation of ICAM1, CXCL8 and SELE was confirmed in HUVEC from four different donors by qPCR prior to RNA sequencing analysis performed by BGI Tech Solutions (Hong Kong) (Figure 3.15). Following quality control checks, RNA was hybridised to Illumina Hiseq 2000 platform and data obtained using 10M reads per sample.

RNAseq data were mapped to 25,702 Entrez genes using criteria set out in the Materials and Methods (Section 2.10). Differentially expressed genes were identified using edgeR with $p < 0.05$ and read CPM > 1 in at least half of the samples. I found that S1P treatment of HUVEC was followed by the upregulation of 116 genes and the downregulation of 126 genes (Appendix 2).

3.2.6 Validation of S1P target genes identified in HUVEC

The RNAseq analysis identified the upregulation of ICAM1 and SELE, two genes I had previously shown to be upregulated by S1P (Figure 3.15). However, CXCL8 was not identified as an S1P target gene by RNAseq analysis. Fig 3.16 shows that RNAseq analysis revealed the upregulation of CXCL8 in 2 out of the 4 pairs of samples. As this gene has previously been identified as an S1P endothelial cell target gene and as I confirmed the upregulation of IL8 protein in HUVEC following S1P treatment (shown later; Figure 4.11) I chose to include CXCL8 in all subsequent analyses.

I used qPCR to validate the upregulation of three additional genes identified by RNAseq analysis which encode proteins of varying functions. These included the genes for SPHK1 itself,

the transmembrane adhesion molecule vascular cell adhesion protein-1 (VCAM1), the secreted chemokine C-C Motif ligand 2 (CCL2) and the glycosylated secreted protein angiopoietin-like 4 (ANGPTL4) (Figure 3.17).

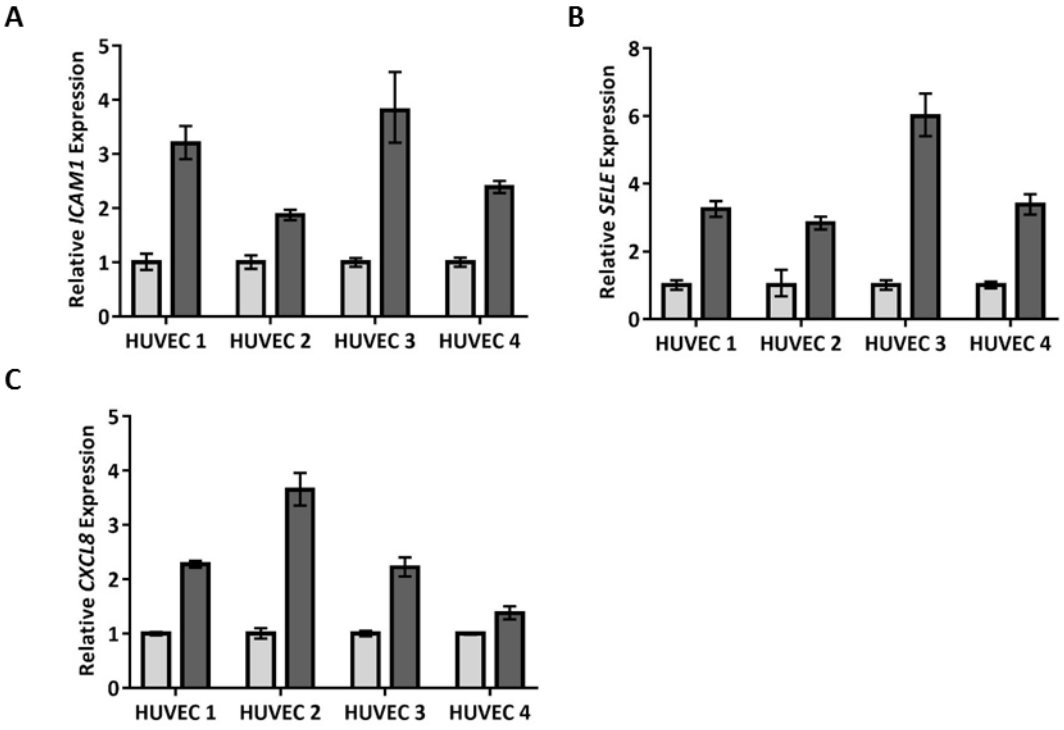

Figure 3.15: Validation of the upregulation of S1P target genes in HUVEC used for RNAseq analysis. qPCR analysis confirms the upregulation ICAM1 (A), SELE (B) and CXCL8 (C) in HUVECs treated with S1P for 4h (dark grey bars) relative to untreated cells (light grey bars) from four different donors (HUVEC 1-4). Samples were analysed in triplicate and are presented as $2^{-\Delta\Delta CT}$ values in comparison to corresponding control.

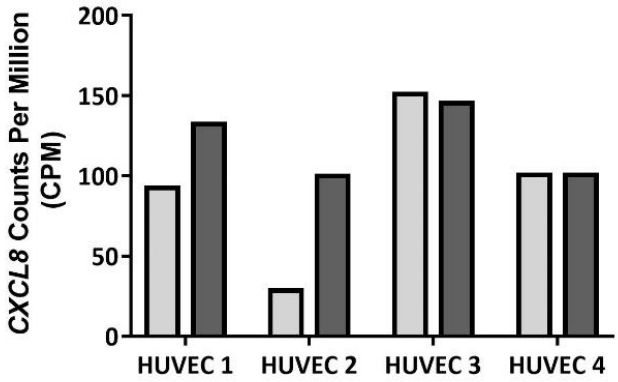

Figure 3.16: The RNAseq CPM values for CXCL8 in the four HUVEC control and S1P treated samples. The CPM values from the RNAseq analysis in four HUVEC samples treated with S1P (dark grey bars) and corresponding vehicle treated control (light grey bars). This shows that CXCL8 was detected as upregulated in two out of the four pairs of HUVEC.

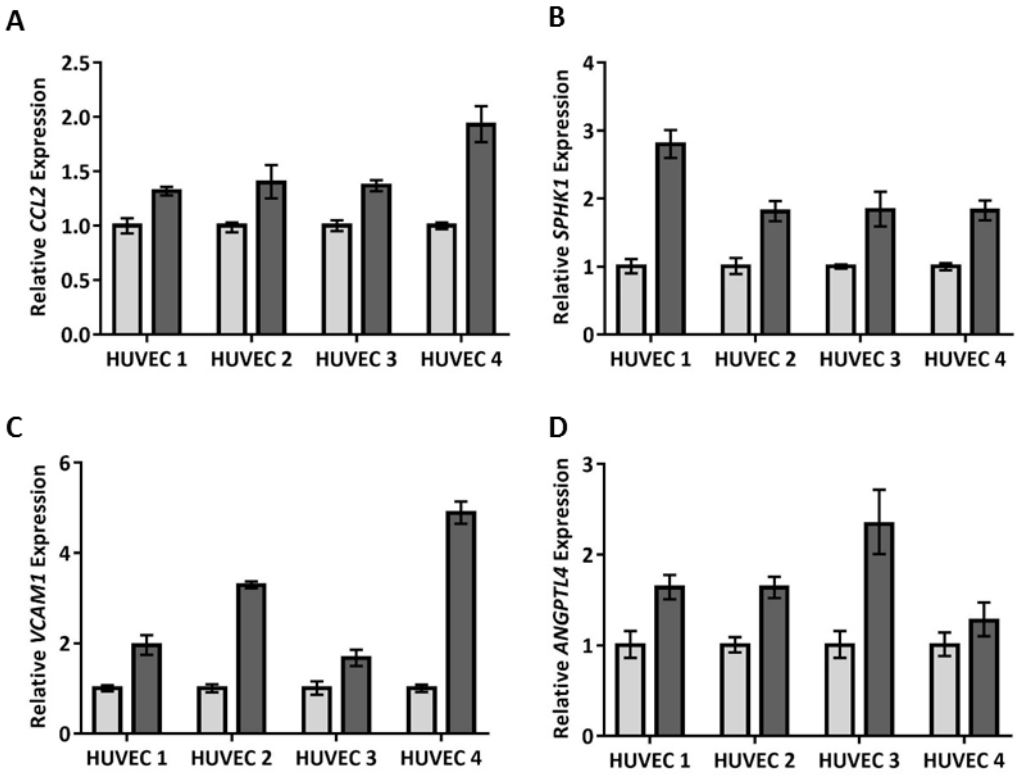

Figure 3.17: Validation of genes upregulated in HUVEC by S1P treatment identified by RNAseq analysis. qPCR was used to measure the relative quantity of CCL2 (A), SPHK1 (B), VCAM1 (C) and ANGPTL4 (D) in HUVECs treated with S1P for 4h (dark grey bars) relative to untreated cells (light grey bars) from four different donors (HUVEC 1-4). Samples were analysed in triplicate and are presented as $2^{-\Delta\Delta CT}$ values in comparison to corresponding control.

3.2.7 The S1P-endothelial cell gene signature is enriched in primary DLBCL

The genes differentially regulated in HUVEC following S1P stimulation constitute a potential S1P signalling endothelial cell signature. To determine if this signature is detectable in primary DLBCL, I used those genes that I previously showed to be correlated with SPHK1 expression in primary DLBCL (Section 3.2.2). Using only genes present on both platforms (Table 3.4), I compared the genes that were significantly correlated with SPHK1 expression in primary DLBCL with the genes regulated by S1P in HUVEC (Table 3.5). This analysis revealed that genes positively correlated with the expression of SPHK1 in primary DLBCL were significantly enriched for genes upregulated, but not genes downregulated, by S1P in HUVEC (chi-square=52.78, odds ratio =4.55, $p<0.0001$; chi-square=0.51, odds ratio =0.78, $p=0.48$; respectively. Table 3.6; Figure 3.18). It also revealed that genes negatively correlated with the expression of SPHK1 in primary DLBCL were significantly enriched for genes downregulated, but not genes upregulated, by S1P in HUVEC (chi-square=15.27, odds ratio =2.58, $p<0.0001$; chi-square=0.59, odds ratio =0.71, $p=0.44$; respectively. Table 3.6; Figure 3.18). These results provide strong evidence that an S1P-endothelial cell gene signature is present in SPHK1 expressing primary DLBCL.

Table 3.4.Number of genes positively and negatively correlated with SPHK1 expression in primary DLBCL and genes upregulated and downregulated by S1P in HUVEC including those used in the enrichment analyses.

	Total Number	Number of genes used in enrichment analysis (present on both DLBCL-SPHK1 correlated genes dataset and S1P regulated HUVEC genes dataset n=17446)
Genes positively correlated with SPHK1 expression in primary DLBCL	2236	2145
Genes negatively correlated with SPHK1 expression in primary DLBCL	1658	1537
Genes upregulated by S1P in HUVEC	117	93
Genes downregulated by S1P in HUVEC	126	111

Table 3.5. Number of genes upregulated or downregulated by S1P in HUVEC that were also found to be either positively or negatively correlated with the expression of SPHK1 in primary DLBCL.

	Genes up regulated in HUVECs treated with S1P (n=93)	Genes down regulated in HUVECs treated with S1P (n=111)
Genes positively correlated with SPHK1 expression in primary DLBCL (n=2145)	36	11
Genes negatively correlated with SPHK1 expression in primary DLBCL (n=1537)	6	22

Table 3.6: Chi-square test of the overlap between genes correlated with the expression of SPHK1 in primary DLBCL and those genes either upregulated or downregulated by S1P in HUVEC

	Observed (O)	Expected (E)	O-E	Chi square	Odds Ratio	P-Value
Genes positively correlated with SPHK1 expression in primary DLBCL and upregulated in S1P treated HUVEC	36	11.43	24.57	52.78	4.55	$p < 0.0001$
Genes negatively correlated with SPHK1 expression in primary DLBCL and upregulated in S1P treated HUVEC	6	8.19	-2.19	0.59	0.71	0.442
Genes positively correlated with SPHK1 expression in primary DLBCL and downregulated in S1P treated HUVEC	11	13.65	-2.65	0.51	0.78	0.475
Genes negatively correlated with SPHK1 expression in primary DLBCL and downregulated in S1P treated HUVEC	22	9.78	12.22	15.27	2.58	$p < 0.0001$

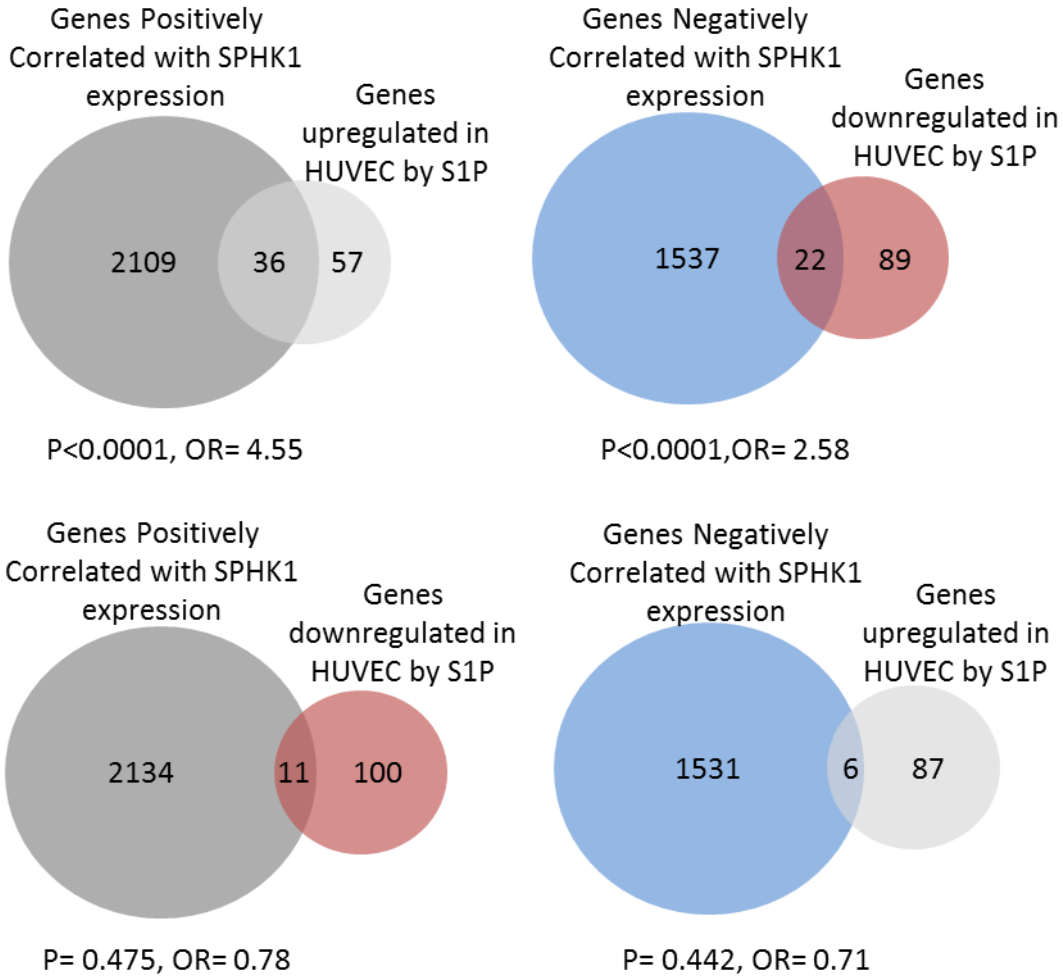

Figure 3.18: The S1P-endothelial cell gene signature is present in primary DLBCL. Venn diagrams showing the overlap between genes positively or negatively correlated with SPHK1 in primary DLBCL (dark grey and blue circles respectively) with those genes upregulated or downregulated in S1P treated HUVEC (light grey and red circles respectively). Genes positively correlated with the expression of SPHK1 in primary DLBCL were significantly enriched for genes upregulated, but not genes downregulated, by S1P in HUVEC (chi-square=52.78, odds ratio =4.55, p<0.0001; chi-square=0.51, odds ratio =0.78, p=0.48, respectively). It also revealed that genes negatively correlated with the expression of SPHK1 in primary DLBCL were significantly enriched for genes downregulated, but not genes upregulated, by S1P in HUVEC (chi-square=15.27, odds ratio =2.58, p<0.0001; chi-square=0.59, odds ratio =0.71, p=0.44). OR= odds ratio.

3.3 Discussion

Most of the oncogenic effects of SPHK1 are a consequence of its ability to produce the bioactive signalling lipid S1P (Pyne, 2012, Pyne and Pyne, 2010, Maceyka et al., 2012). SPHK1 is overexpressed in many cancer types such as kidney, lung, ovarian and pancreatic, and associated with an inferior survival in gastric, brain and breast cancer (French et al., 2003, Johnson et al., 2005, Guillermet-Guibert et al., 2009, Li et al., 2009, Van Brocklyn et al., 2005, Li et al., 2008b, Ruckhaberle et al., 2008). A previous study has documented the overexpression of SPHK1 in NHL. In this chapter I provide evidence that SPHK1 is overexpressed in the most common subtype of NHL, DLBCL (Bayerl et al., 2008). This was based on a reanalysis of two gene expression datasets which showed high levels of SPHK1 mRNA in DLBCL compared with GC B cells. Although SPHK1 IHC showed strong staining in DLBCL tumour cells I could not reliably quantify this due to the lack of an internal positive control. Quantification of SPHK1 expression in tumour cells of DLBCL sections will require an alternative assay such as RNAscope, an RNA in-situ hybridisation technology (Wang et al., 2012). At this time it is not technically feasible to measure S1P in tissue sections. Furthermore, the phospho-specific SPHK1 antibody used here is not specific in IHC. Therefore, I could only show that SPHK1 was constitutively phosphorylated in DLBCL lines.

I showed that SPHK1 expression is associated with the expression of angiogenic genes in primary DLBCL. This could be important because overall survival has been shown to be significantly poorer for those DLBCL patients with tumours displaying high blood vessel density compared to those with low blood vessel density (54% versus 78%, respectively, p=0.004)

(Cardesa-Salzmann et al., 2011). For this reason SPHK1-S1P signalling could be a novel anti-angiogenic target in DLBCL.

As a first step to investigate the contribution of SPHK1 to DLBCL angiogenesis I used HUVEC to define an S1P-endothelial cell gene signature. Having shown that HUVEC recapitulated the S1P receptor expression observed in DLBCL-associated endothelial cells I then optimised conditions which enabled me to reliably activate ERK and downstream transcription.

I showed that many of the transcriptional changes induced by the treatment of HUVEC with S1P were evident in SPHK1 expressing tumours, suggesting that S1P signalling is likely to be involved in DLBCL angiogenesis. This could be important because two studies have shown no association between microvessel density and VEGF expression in DLBCL (Gratzinger et al., 2008, Jorgensen et al., 2007). This suggests that another pathway independent of VEGF signalling, potentially the SPHK1-S1P pathway, is driving blood vessel growth in these tumours. Further studies are required to determine if SPHK1 expression is associated with microvessel density in primary DLBCL.

Although HUVEC proved useful in defining an S1P-endothelial cell gene signature, it should be noted that the S1P targets were defined following a single S1P stimulation which resulted in rapid and transient transcriptional changes. This almost certainly cannot completely recapitulate the *in vivo* steady state in which tumour-associated endothelial cells are likely to be chronically stimulated by S1P.

The observation that the S1P-endothelial cell gene signature was significantly associated with SPHK1 expression in primary tumours was based on the analysis of gene expression datasets

generated from whole tumour biopsies. Therefore, any correlations observed cannot be attributed with certainty to a given cell type. Equally, this method may not be sensitive enough to determine genes expressed by the tumour endothelial cells, as the endothelial cells make up a low percentage of the total cell count in tumour biopsies. Therefore, the total gene expression level of any given gene in endothelial cells may be affected by its expression in other cell types. This problem could be overcome by gene expression analysis of endothelial cells isolated from primary DLBCL samples.

CHAPTER FOUR

AN INVESTIGATION OF THE PHENOTYPIC EFFECTS OF THE S1P-ENDOTHELIAL CELL GENE SIGNATURE

4.1 Abstract

In the previous chapter I showed that genes co-expressed with SPHK1 in primary DLBCL are significantly enriched for angiogenic genes. Furthermore, I showed that S1P induces a gene expression programme in endothelial cells which is present in primary tumours. I hypothesise that in addition to increasing tumour angiogenesis, S1P might also induce other phenotypic effects on endothelial cells to promote tumour progression.

In this chapter I explore the impact of S1P on the transcription of other genes in endothelial cells, including those not directly associated with angiogenesis.

4.2 Results

4.2.1 Gene ontology analysis reveals that the S1P-endothelial cell gene signature is enriched for angiogenic, anti-apoptotic and leukocyte extravasation and migration functions

To explore the broader phenotypic effects of S1P signalling on endothelial cells, I initially performed a gene ontology analysis of the genes upregulated by S1P in HUVEC using an online functional classification tool, DAVID (https://david.ncifcrf.gov/) (Dennis et al., 2003). The significantly enriched gene ontology terms were grouped into functional categories and revealed a significant enrichment in angiogenic, anti-apoptotic, leukocyte extravasation and leukocyte chemotaxis functions (Figure 4.1).

4.2.2 Genes upregulated by S1P in endothelial cells are involved in the recruitment of monocytes and granulocytes

As the recruitment of stromal cells to the tumour microenvironment is increasingly recognised to play an important role in tumour progression, I chose to focus on the potential contribution of S1P-induced changes in the endothelial transcriptome to leukocyte recruitment (Lenz et al., 2008b).

The now firmly established process of leukocyte recruitment involves two main steps which have been extensively reviewed (reviewed in: Nourshargh and Alon, 2014, Hordijk, 2016, Vestweber, 2015, Muller, 2013). As part of the migration process, circulating leukocytes must first adhere to the endothelium. This association involves the expression of endothelial cell adhesion molecules. Secondly, the leukocytes are directed by chemoattractant gradients,

such as chemokines, to migrate across the endothelium (a process referred to as leukocyte extravasation) and into the tissue.

I interrogated the S1P regulated genes in HUVEC for chemokines and adhesion molecules. This gave me 7 chemokines and 3 adhesion molecules (Table 4.1). I validated the upregulation of several of the chemokine genes in HUVEC following S1P treatment by qPCR. In addition to those previously validated (CXCL8 Figure 3.15; CCL2 Figure 3.17) I confirmed the upregulation of CCL7, CXCL1, CXCL3 and CXCL12 mRNA (Figure 4.2). The adhesion molecule genes involved in leukocyte extravasation ICAM1, SELE and VCAM1 had previously been validated (ICAM1 and SELE Figure 3.15; VCAM1 Figure 3.17).

To further investigate the cell types that may be recruited by the chemokines and adhesion molecules regulated by S1P in HUVEC, I performed a PubMed search, (http://www.ncbi.nlm.nih.gov/pubmed), to identify the primary chemotactic/adhesion functions (Table 4.1). This literature search revealed that the chemokines and adhesion molecules regulated by S1P in HUVEC are primarily involved in the recruitment of monocytes and granulocytes.

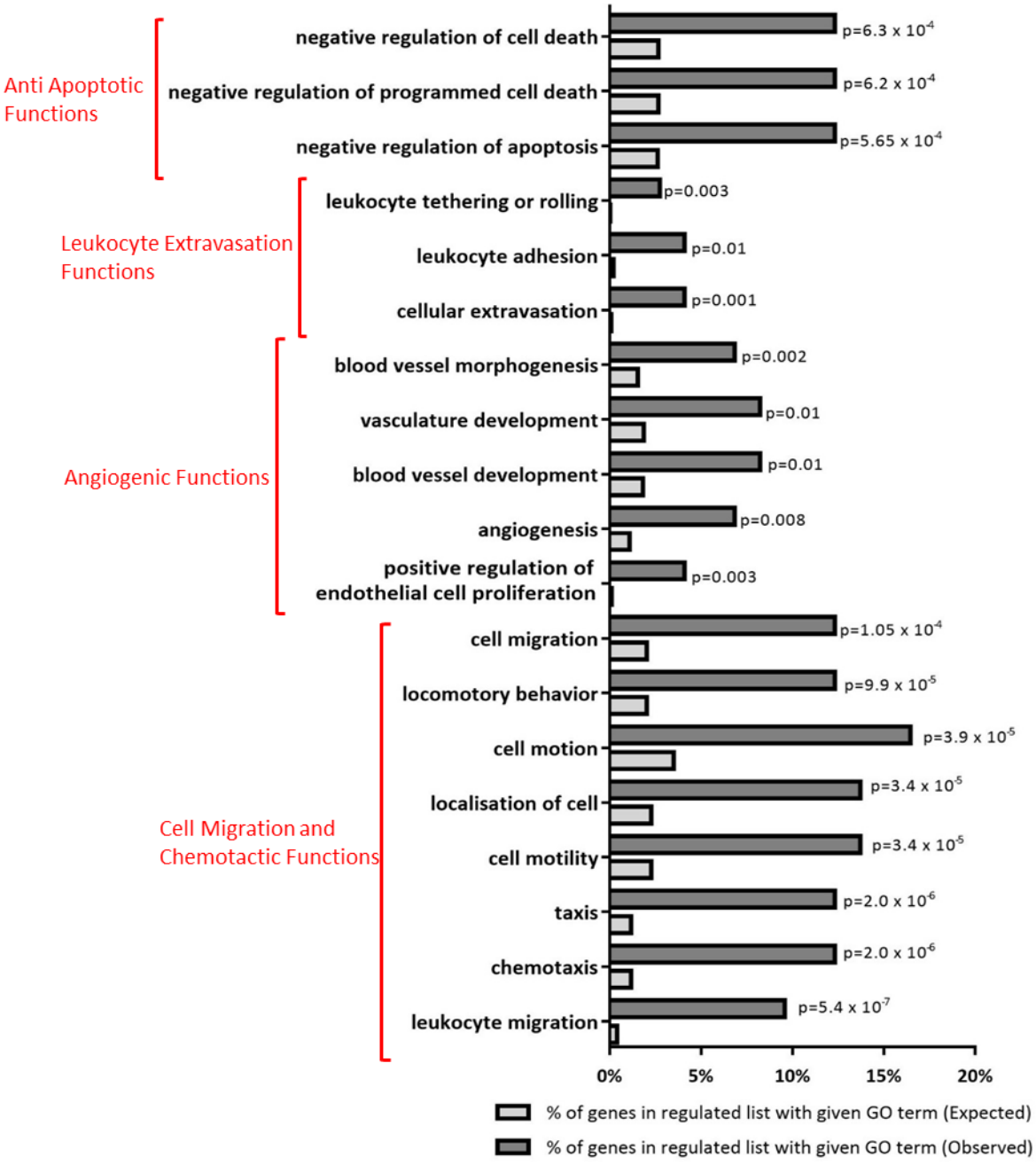

Figure 4.1: Gene ontology analysis of S1P target genes in HUVEC. GO analysis of genes upregulated by S1P in HUVEC revealed enrichment of genes with anti-apoptosis, leukocyte extravasation, angiogenesis and cell migration/chemotaxis functions. Dark grey bars represent the observed percentage of upregulated genes in a particular GO category, and light grey bars represent the expected percentage of upregulated genes in a particular GO category. P value of each term was determined using Fisher's exact test.

Table 4.1: A summary of the chemokines and endothelial cell adhesion molecules upregulated by S1P

	Official Gene Symbol	Official Gene Name	Other Gene Names	Primary Target Cell(s)	Reported endothelial cell S1P target gene? (Yes/No)	Significantly co-expressed with SPHK1? (Yes/No) (p-value)
Chemokines	CCL2	C-C motif chemokine ligand 2	Monocyte chemotactic protein 1 (MCP-1)	Monocytes (reviewed in: Deshmane et al., 2009)	Yes (Lin et al., 2007)	No p= 0.23
	CCL7	C-C motif chemokine ligand 7	Monocyte chemotactic protein 3 (MCP-3)	Monocytes (Van Damme et al., 1992)	No	Yes p= 0.03
	CX3CL1	C-X3-C motif chemokine ligand 1	Fractalkine	**Soluble:** Monocytes, T Cells (Bazan et al., 1997) **Endothelial Cell Bound**: Leukocyte Adhesion (Bazan et al., 1997)	No	No p= 0.054
	CXCL1	C-X-C motif chemokine ligand 1	GRO1 oncogene, Neutrophil activating protein-1 (NAP-3)	Neutrophils (Moser et al., 1990)	No	Yes p= 0.027
	CXCL3	C-X-C motif chemokine ligand 3	GRO3 oncogene, macrophage inflammatory protein-2-beta (MIP2b)	Granulocytes (Geiser et al., 1993)	No	No p= 0.076
	CXCL8	C-X-C motif chemokine ligand 8	Interleukin8 (IL8)	Granulocytes (Harada et al., 1994)	Yes (Lin et al., 2007)	Yes p= 0.005
	CXCL12	C-X-C motif chemokine ligand 12	Stromal cell derived factor 1 (SDF1)	Lymphocytes, endothelial progenitor cells: (Burger and Kipps, 2006)	No	No p= 0.061
Adhesion Molecules	ICAM1	intercellular adhesion molecule 1	CD54	Leukocytes (reviewed in: Etzioni, 1996)	Yes (Shimamura et al., 2004)	Yes p= 0.001
	SELE	Selectin E	E-selectin, CD62	Leukocytes (reviewed in: Etzioni, 1996)	Yes (Xia et al., 1998)	Yes p= 0.0008
	VCAM1	vascular cell adhesion molecule 1	CD106	lymphocytes, monocytes, eosinophils and basophils (reveiwed in: Etzioni, 1996)	Yes (Xia et al., 1998)	No p=0.177

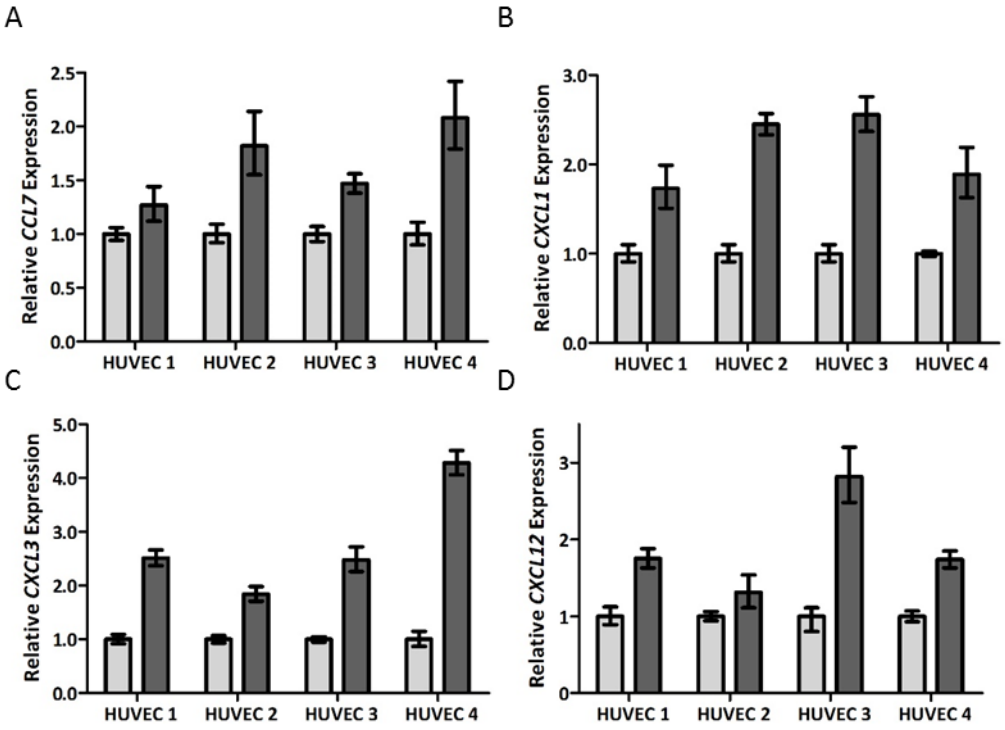

Figure 4.2: Upregulation of chemokines by S1P treated HUVEC. qPCR analysis confirms the upregulation of CCL7 (A), CXCL1 (B), CXCL3 (C) and CXCL12 (D) in HUVEC treated with S1P for 4 hours (dark grey bars) relative to untreated cells (light grey bars) from four different donors (HUVEC 1-4). Samples were analysed in triplicate and are presented as $2^{-\Delta\Delta CT}$ values in comparison to corresponding control.

4.2.3 Genes co-expressed with SPHK1 in primary DLBCL are enriched for a granulocyte and a tumour macrophage gene signature.

Following tissue recruitment, monocytes are polarised by the local environment and differentiate into macrophages, a process controlled by many tissue specific factors (Richards et al., 2013, Gordon and Taylor, 2005). Before investigating if S1P-induced changes on the endothelial transcriptome are involved in the recruitment of monocytes and granulocytes, I first wanted to confirm that macrophages and granulocytes were present in the microenvironment of the SPHK1-expressing DLBCL I had identified earlier (Section 3.2.1). To do this, macrophages and granulocytes were counted in 4 hpf (high power fields) and 10 hpf, respectively (performed by pathologist Dr Maha Ibrahim) using CD68 and CD15 as markers (Reid et al., 2011, Wada et al., 2012). Cells within vessels or necrotic areas were excluded. The average number of cells per hpf is shown in Table 4.2. Representative IHC stains are shown in Figure 4.3. I detected both macrophages and granulocytes in all tumours (mean: 157.6, 8.9; median 177.3, 4.9; range 48.3-298.3, 0.8-212.1, respectively). There was no correlation between the numbers of macrophages and granulocytes in these tumours (Figure 4.4).

Table 4.2: Average CD15 and CD68 counts from primary DLBCL cases. NA = not available

DLBCL case number	Average CD15 Count (10 hpf)	Average CD68 Count (4 hpf)
102	5.6	162.3
196	4.3	NA
204	0.8	NA
95	4.1	118.5
112	2.3	288.0
134	6.9	175.8
150	4.5	250.0
154	4.9	48.3
155	3.0	177.3
159	4.0	125.0
160	212.1	226.0
161	8.1	250.3
162	8.6	208.0
166	11.2	186.8
175	31.2	242.3
176	3.0	240.8
177	7.7	266.8
189	7.0	132.8
190	12.3	279.8
191	1.0	114.3
195	3.4	104.5
197	9.4	208.5
198	8.7	94.0
200	5.8	176.0
203	NA	298.3
207	15.5	192.8
208	1.5	183.3
209	3.9	NA
211	14.4	121.8
212	41.5	122.0
213	1.7	184.5
214	16.1	131.8
215	2.2	163.5
220	1.7	99.0
227	4.3	175.3
231	3.2	237.5
199	NA	125.3
182	NA	201.8

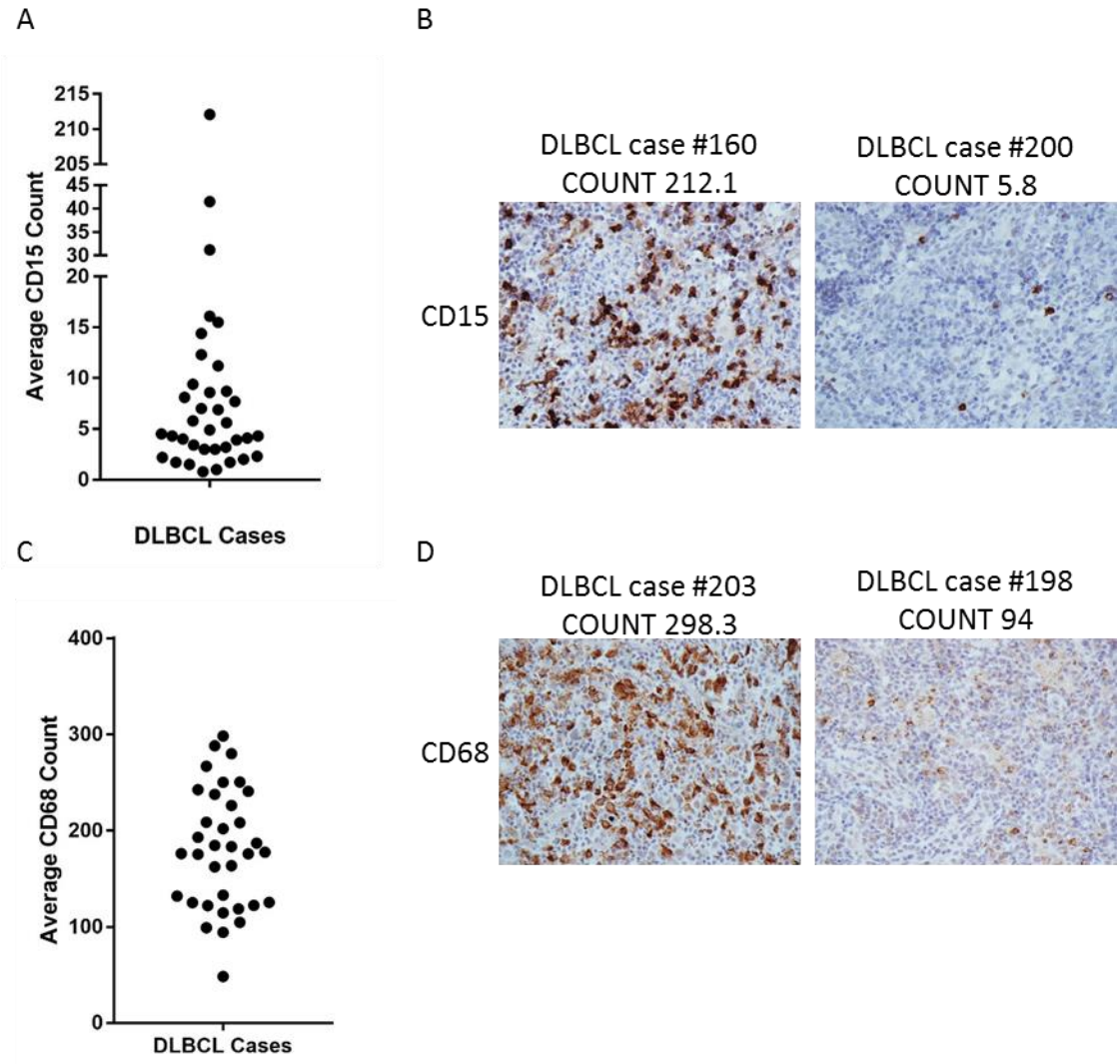

Figure 4.3: Frequency of CD15+ granulocytes and CD68+ macrophages in DLBCL. DLBCL cases were stained for CD15 and CD68 by IHC. The average number of cells per high power field for CD15 and CD68 for each case is shown (A and C, respectively). Representative IHC stains from two cases for both CD15 and CD68 are shown (B and D, respectively).

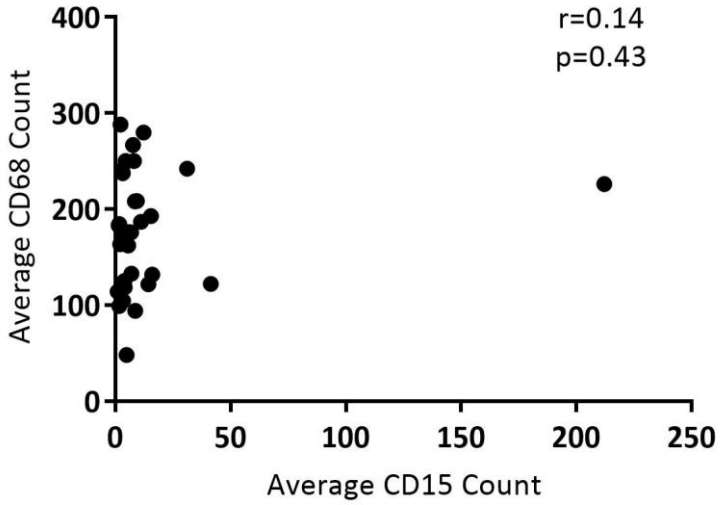

Figure 4.4: Correlation between average CD15 and CD68 counts in primary DLBCL. This analysis reveals that there was no significant correlation between average CD15 and CD68 counts. Pearson correlation, r=0.14, p=0.43.

As explained in Section 3.2.1, I could not accurately quantify the level of SPHK1 expression in these cases. However, to explore whether the presence of macrophages and granulocytes in the microenvironment of primary DLBCL is associated with the expression of SPHK1, I compared the genes significantly correlated with the expression of SPHK1 in primary DLBCL with published cell type specific gene signatures. I used a published tumour macrophage gene signature generated using a 3D network-based approach from a DLBCL gene expression dataset and shown to be conserved across multiple unrelated human cancer types (Doig et al., 2013). Using only genes present on both platforms, n= 17850 (Table 4.3), I compared the genes significantly correlated with SPHK1 expression with the tumour macrophage gene signature (Table 4.4). This analysis revealed that genes positively correlated with SPHK1 in primary DLBCL were significantly enriched for macrophage signature genes (chi-square=264.66, odds ratio=9.99, $p<0.0001$; Table 4.5; Figure 4.5), whereas genes negatively correlated with SPHK1 in primary DLBCL were significantly depleted for macrophage signature genes (chi-square= 13.42, odds ratio=0, $p=0.0002$; Table 4.5; Figure 4.5).

To confirm this observation, I used the re-analysis of a published RNAseq data set to show a significant positive correlation in the expression of SPHK1 and CD68 in primary DLBCL samples (n=86) (Figure 4.6).

Table 4.3. Number of genes positively and negatively correlated with SPHK1 expression in primary DLBCL, and present in the macrophage gene signature, including those used in the enrichment analyses.

	Total Number	Number of genes used in enrichment analysis (present on both DLBCL-SPHK1 correlated genes dataset and macrophage signature dataset n=17850)
Genes positively correlated with SPHK1 expression in primary DLBCL	2236	2150
Genes negatively correlated with SPHK1 expression in primary DLBCL	1658	1517
Macrophage gene signature	162	158

Table 4.4. Number of genes in the macrophage signature that were also found to be either positively or negatively correlated with the expression of SPHK1 in primary DLBCL.

	Macrophage gene signature (n=158)
Genes positively correlated with SPHK1 expression in primary DLBCL (n=2150)	90
Genes negatively correlated with SPHK1 expression in primary DLBCL (n=1517)	0

Table 4.5: Chi-square test of the overlap between genes correlated with the expression of SPHK1 in primary DLBCL and those present in the macrophage gene signature.

	Observed (O)	Expected (E)	O-E	Chi square	Odds Ratio	P-Value
Macrophage gene signature and genes positively correlated with SPHK1 expression in primary DLBCL	90	19.03	70.97	264.66	9.99	<0.0001
Macrophage gene signature and genes negatively correlated with SPHK1 expression in primary DLBCL	0	13.43	-13.43	13.42	0	0.0002

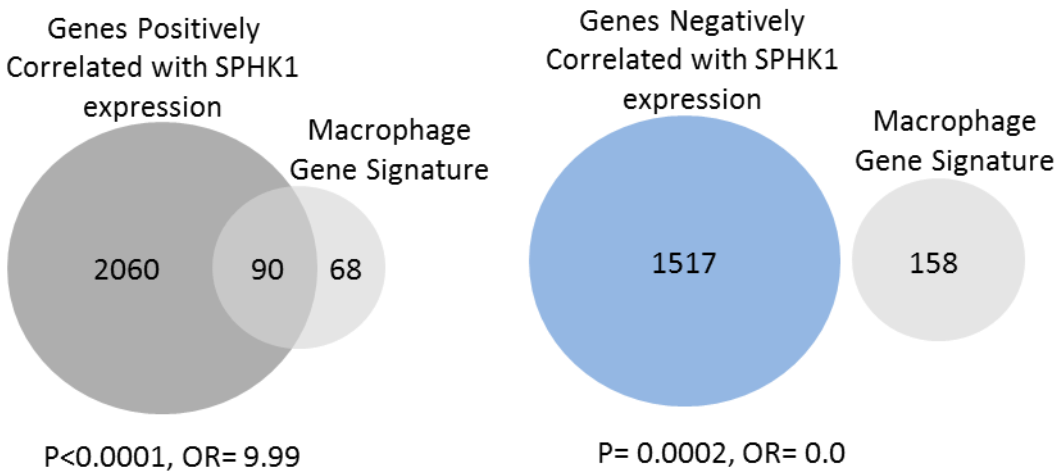

Figure 4.5: A macrophage gene signature is enriched in genes positively correlated with SPHK1 expression in primary DLBCL. Venn diagrams showing the overlap between genes positively and negatively correlated with SPHK1 expression in primary DLBCL (dark grey and blue circles respectively) with a macrophage gene signature (light grey circles). Genes positively correlated with the expression of SPHK1 in primary DLBCL were significantly enriched for macrophage signature genes (chi-square=264.66, odds ratio =9.99, p<0.0001). Genes negatively correlated with SPHK1 expression in primary DLBCL were significantly depleted for macrophage signature genes (chi-square=13.42, odds ratio =0.00, p=0.0002).

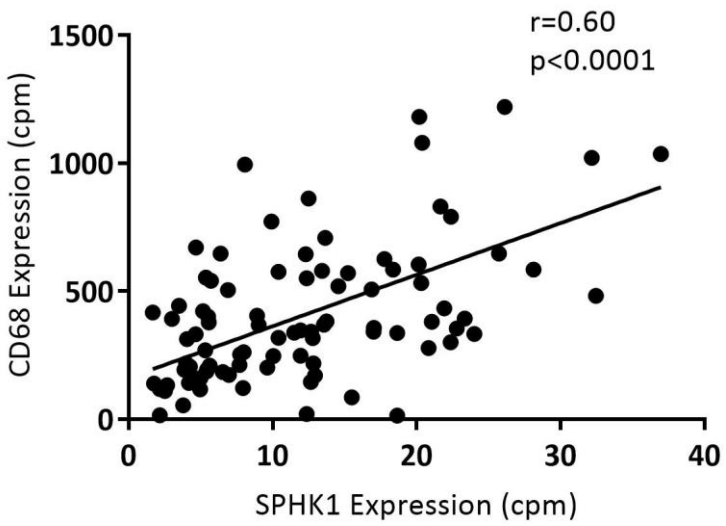

Figure 4.6: SPHK1 expression is correlated with the expression of CD68 in primary DLBCL. The reanalysis of RNAseq data shows a statistically significant correlation between SPHK1 expression and CD68 expression in 86 cases of primary DLBCL. Pearson correlation, r=0.60, p<0.0001.

Next I used a published granulocyte gene signature generated from cDNA microarray analysis of purified subpopulations of peripheral blood cells (Palmer et al., 2006). Using only genes present on both platforms, n=10042 (Table 4.6), I compared the genes significantly correlated with SPHK1 expression with the genes present in the granulocyte gene signature (Table 4.7). This analysis revealed that genes positively correlated with SPHK1 in primary DLBCL were significantly enriched for the granulocyte signature genes (chi-square=49.02, odds ratio =2.6, $p<0.0001$; Table 4.8; Figure 4.7), whereas the genes negatively correlated with SPHK1 in primary DLBCL were significantly depleted for the granulocyte signature genes (chi-square=12.02, odds ratio=3.3, $p=0.0005$; Table 4.8; Figure 4.7)

To confirm this observation, I used the re-analysis of a published RNAseq data set to show a significant positive correlation in the expression of SPHK1 and CD15 in primary DLBCL samples (n=86) (Figure 4.8).

Table 4.6. Number of genes positively and negatively correlated with SPHK1 expression in primary DLBCL and present in the granulocyte gene signature including those used in the enrichment analyses.

	Total Number	Number of genes used in enrichment analysis (present on both DLBCL-SPHK1 correlated genes dataset and granulocyte gene signature dataset n=10042)
Genes positively correlated with SPHK1 expression in primary DLBCL	2236	1543
Genes negatively correlated with SPHK1 expression in primary DLBCL	1658	1028
Granulocyte gene signature	304	293

Table 4.7. Number of genes in the granulocyte signature that were also found to be either positively or negatively correlated with the expression of SPHK1 in primary DLBCL.

	Granulocyte gene signature (n=293)
Genes positively correlated with SPHK1 expression in primary DLBCL (n=1543)	92
Genes negatively correlated with SPHK1 expression in primary DLBCL (n=1028)	11

Table 4.8: Chi-square test of the overlap between genes correlated with the expression of SPHK1 in primary DLBCL and those present in the granulocyte gene signature.

	Observed (O)	Expected (E)	O-E	Chi square	Odds Ratio	P-Value
Granulocyte gene signature and genes positively correlated with SPHK1 expression in primary DLBCL	92	45.02	46.98	49.02	2.59	<0.0001
Granulocyte gene signature and genes negatively Correlated with SPHK1 expression in primary DLBCL	11	29.99	-18.99	12.02	0.33	0.0005

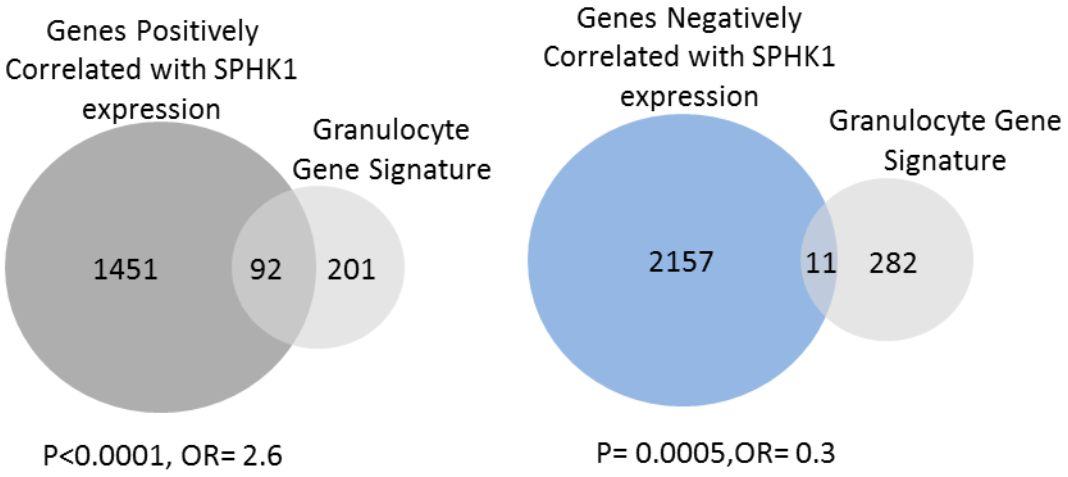

Figure 4.7: A granulocyte gene signature is enriched in genes positively correlated with SPHK1 expression in primary DLBCL. Venn diagrams showing the overlap between genes positively or negatively correlated with SPHK1 expression in primary DLBCL (dark grey and blue circles respectively) with a granulocyte gene signature (light grey circles). Genes positively correlated with the expression of SPHK1 in primary DLBCL were significantly enriched for granulocyte signature genes (chi-square=49.02, odds ratio =2.59, p<0.0001). Genes negatively correlated with SPHK1 expression in primary DLBCL were significantly depleted for the granulocyte signature genes (chi-square=12.02, odds ratio =0.33, p=0.0005).

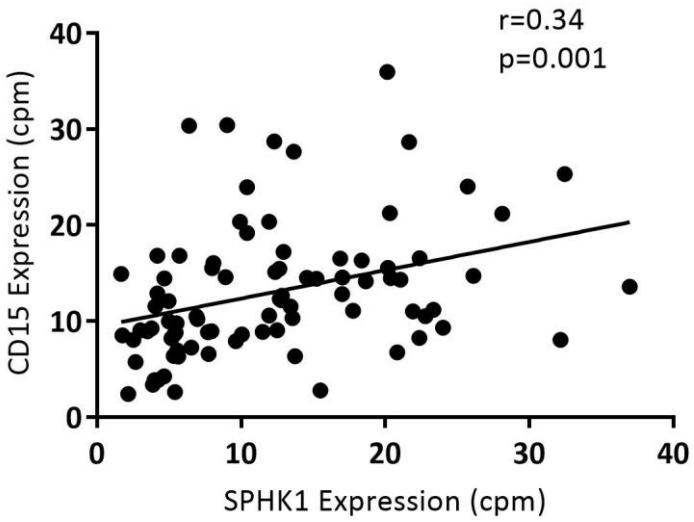

Figure 4.8: SPHK1 expression is correlated with the expression of CD15 in primary DLBCL. The reanalysis of RNAseq data shows a statistically significant correlation between SPHK1 expression and CD15 expression in 86 cases of primary DLBCL. Pearson correlation, r=0.34, p=0.001.

4.2.4 Investigating the S1P-induced chemotactic functions of endothelial cells *in vitro*

The validation of chemokine secretion from HUVEC following treatment with S1P

Having shown that S1P upregulates chemokines in HUVEC and that SPHK1 expression is enriched for macrophage and granulocyte gene signatures in primary DLBCL, I next explored the possibility that the chemokines upregulated by S1P in HUVEC recruit these cell types.

For these set of experiments, I chose to focus on the chemokines which I showed to be positively correlated with SPHK1 expression in DLBCL. They included, CCL7, CXCL1 and CXCL8 (Table 4.1). In the first instance I set out to confirm the upregulation and release of these chemokines from endothelial cells following S1P treatment. *In vivo* endothelial cells are exposed to S1P continually and having reflected on the S1P stimulation experiments (shown in Section 3.2.4) and the transient nature of the signal, I thought it might be possible to adjust the experimental conditions to better reflect what is seen *in vivo*. Two possible reasons for the transient nature of the ERK signal observed *in vitro* are that, S1PR1 surface expression is decreased following S1P exposure or alternatively that S1P is degraded in the cell media.

I first investigated whether the transient ERK signal was due to loss of sensitivity to S1P by re-challenging HUVEC with a second dose of S1P at 6 hours or 12 hours following the first. This analysis showed that those cells receiving a second stimulation activated ERK to the same level as control cells which had not received an initial stimulation (Figure 4.9), suggesting that cells remain sensitive to S1P after an initial stimulation 6 hours earlier.

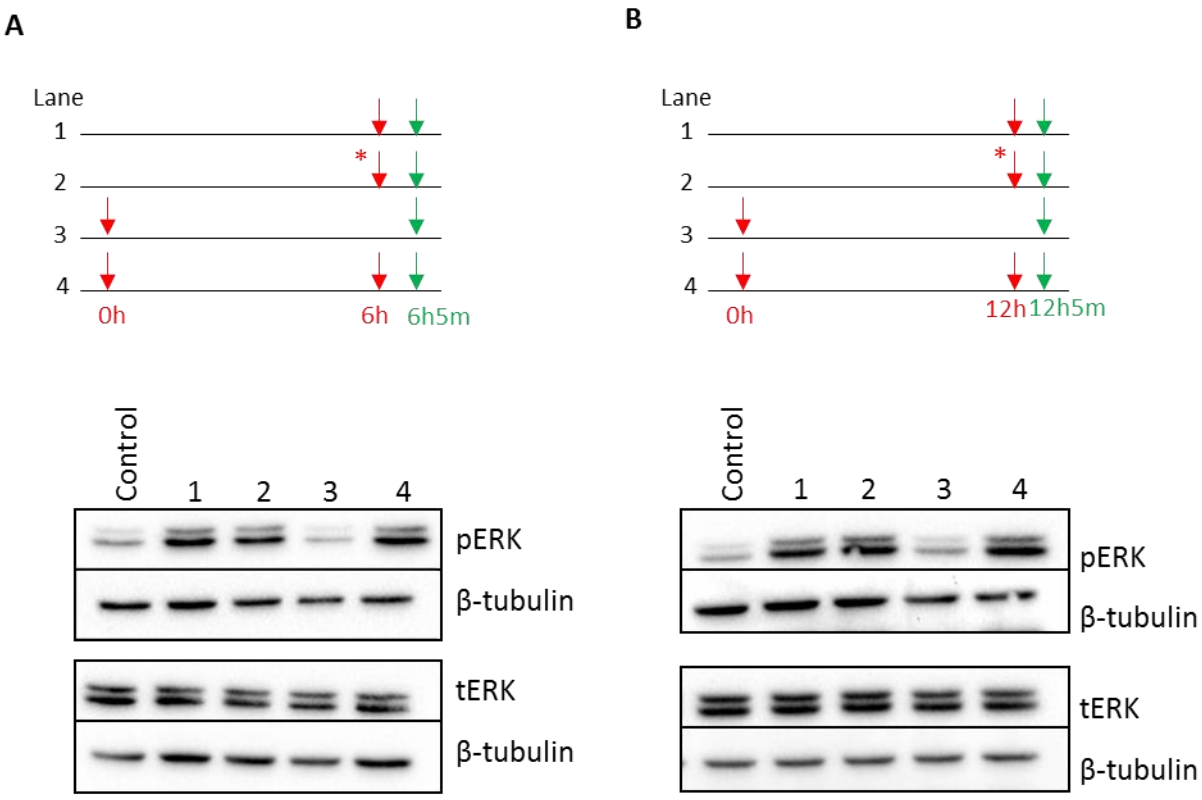

Figure 4.9: S1P treated HUVEC remain sensitive to restimulation with S1P. HUVEC were restimulated with S1P at 6 hours or 12 hours following an initial stimulation (A and B, respectively). Top panels show S1P stimulation times (red arrows) and the protein harvest times (green arrows) for each of the immunoblot samples, numbered by lane. Immunoblotting revealed that cells receiving a second dose of S1P (lanes 4) activate ERK to the same level as cells which received no prior stimulation (lanes 1 and 2). β-tubulin confirmed equal loading of sample. Data shown are representative of three independent experiments from three different HUVEC donors. *=double dose S1P.

I next investigated if S1P in the cell medium is degraded overtime. I took conditioned media from HUVEC that had been treated with S1P for different times and used this to treat unstimulated HUVEC. I found that the medium of S1P treated HUVEC conditioned for > 8 hours was no longer capable of activating ERK (Figure 4.10). These data indicate that S1P is degraded in media overtime. *In vitro* re-stimulation of HUVEC requires fresh S1P.

I used an ELISA to measure CCL7, CXCL1 and IL8 in the conditioned media from S1P treated HUVEC. For these experiments, in addition to depleting the HUVEC of growth factors for 16 hours prior to S1P stimulation, the medium was replaced again 1 hour prior to the initial S1P stimulation. I treated the HUVEC with one or two doses of S1P for up to 12h; the latter to potentially better mimic the effects seen *in vivo.* I chose the second dose time point of 6 hours, as I previously showed that HUVEC can re-activate ERK following a second stimulation 6h after the first (Figure 4.9). The conditioned medium was harvested 12 hours after the first S1P stimulation and subjected to ELISA analysis. Figure 4.11 shows that compared to controls, S1P induced a dose dependent increase in CXCL1 and IL8 levels in the cell supernatants. CCL7 levels were lower than the assay range standards and could therefore not be quantified.

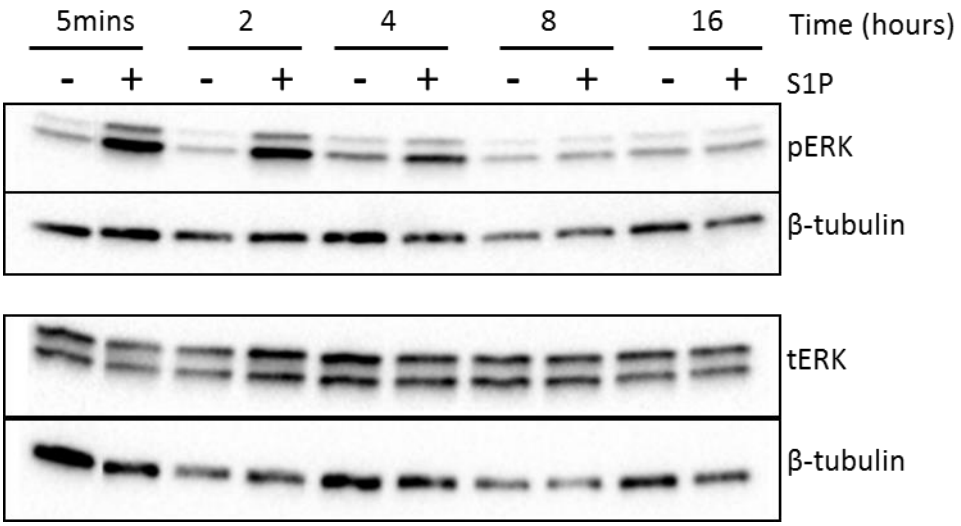

Figure 4.10: S1P is degraded in culture overtime. Media from S1P and control treated HUVEC was conditioned for the indicated time periods. Unstimulated HUVEC were treated with the conditioned media for 5 minutes. Immunoblotting revealed that media conditioned from S1P treated HUVEC for > 8 h was no longer capable of activating ERK. β-tubulin confirmed equal loading of samples. Data shown are representative of two independent experiments from two different HUVEC donors.

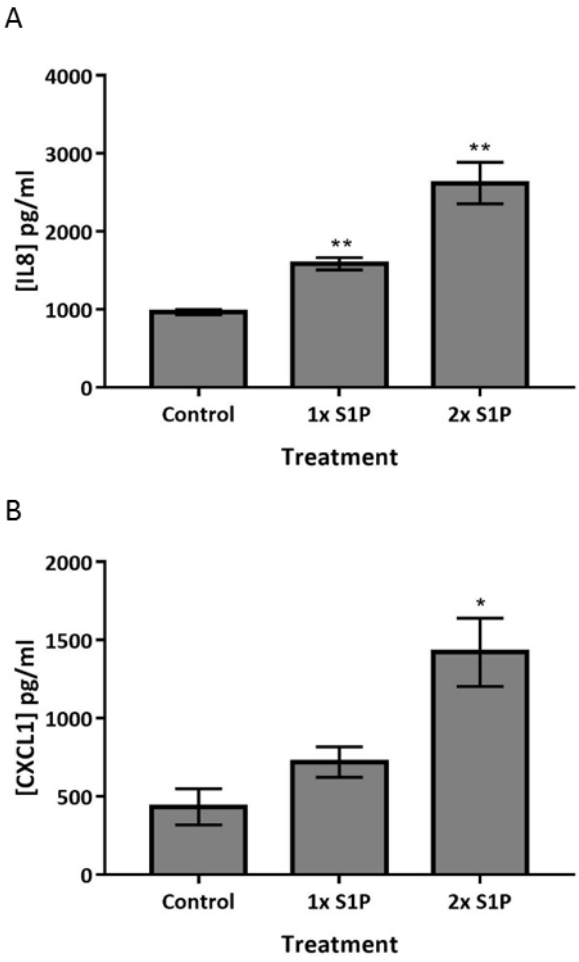

Figure 4.11: ELISA analysis for the production of chemokines by S1P treated HUVEC. An ELISA was used to measure the levels of IL8 (A) and CXCL1 (B) in the conditioned media of HUVEC treated with S1P for 12 hours. Cells were either untreated (control) or treated with 1 dose of S1P at 0 hours or 2 doses of S1P at 0h and 6h (1x S1P, 2x S1P, respectively). Analysis reveals the dose dependent upregulation of IL8 and CXCL1. Data are represented as mean ±SEM of three separate experiments. Students T-test. *p<0.05, **p<0.01.

Validation of monocyte migration to CXCL1: a chemokine secreted from HUVEC following treatment with S1P and co-expressed with SPHK1 in primary DLBCL

CXCL1 and IL8, the two validated chemokines that I showed were upregulated by S1P in HUVEC and which were co-expressed with SPHK1 in primary DLBCL, are thought to act predominantly on neutrophils (Table 4.1). Therefore I chose to focus my studies on the recruitment of monocytes. IL8 has already been reported to recruit monocytes (Gerszten et al., 1999), therefore, I chose to investigate the ability of CXCL1 to recruit monocytes.

To do this, I first wanted to establish an assay to measure the migration of monocytes to CXCL1. To do this I used the THP-1 human monocytic cell line which is derived from an acute monocytic leukaemia patient and is the most widely used monocyte cell line model. I exposed THP-1 cells to 50 ng/ml MCP1, one of the key chemokines that regulates migration of monocytes, in a transwell assay for 4 hours. Figure 4.12A shows a significant increase in THP-1 cell migration to MCP-1 compared to controls, confirming that my migration assay works.

Having optimised the THP-1 cell migration assay, I then tested the effects of CXCL1 on THP-1 cell migration using the same conditions. This assay revealed a significant and dose dependent increase in THP-1 cell migration to CXCL1 (Figure 4.12B).

Finally, I wanted to explore the effects of CXCL1 on the migration of primary human CD14+ monocytes as they are more representative of what is found *in vivo*. To do this I used CD14+ cells isolated from human peripheral blood (provided by Tracey Perry). Figure 4.13 shows that there was a significant increase in primary human CD14+ monocyte migration to MCP-1, however I observed no increase in primary human CD14+ monocytes to CXCL1 at 25 ng/ml or

50 ng/ml. Although this experiment indicates that primary human CD14+ monocyte migration do not migrate to CXCL1, repeated experiments from multiple donors would have to be performed for firm conclusions to be drawn, as donor variations in chemokine receptor expression have previously been described (Gerszten et al., 1999).

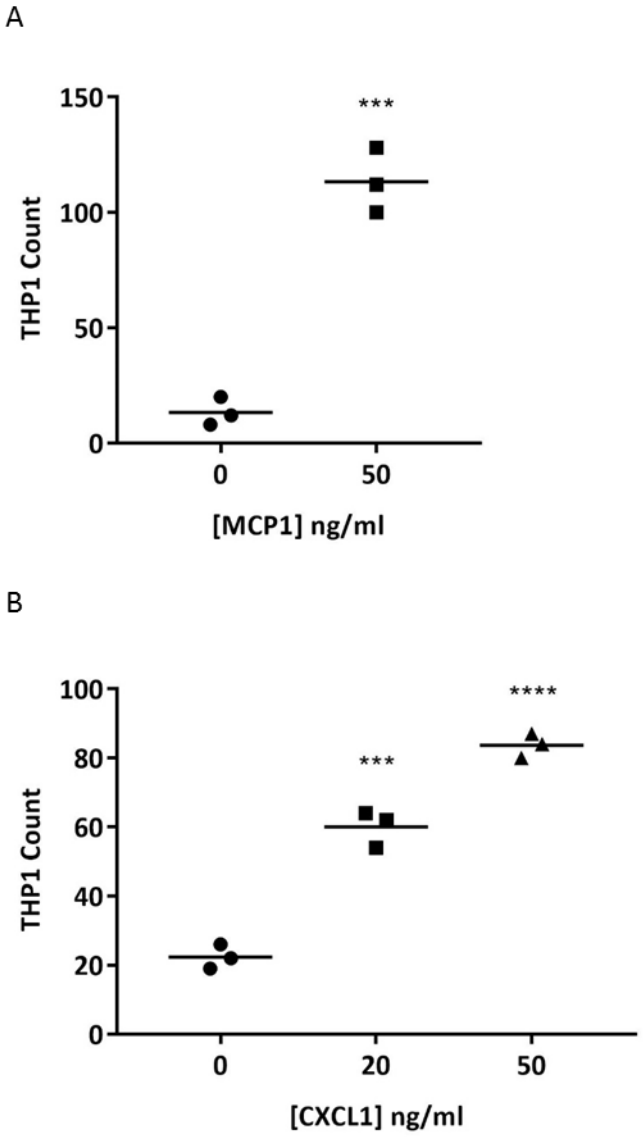

Figure 4.12: Increased migration of THP-1 cells to MCP1 and CXCL1. (A) THP-1 cells were exposed to 50 ng/ml MCP1 in a transwell assay. After 4 hours, the cells that had migrated through the membrane were counted using a flow cytometer from triplicate wells. Analysis revealed a significant increase in THP-1 cell migration in the presence of MCP1 compared to controls. (B) THP-1 cells were exposed to CXCL1 at the indicated concentration in a transwell assay. After 4 hours, the cells that had migrated through the membrane were counted using a flow cytometer from triplicate wells. Representative data are from one of four independent experiments. Analysis revealed the dose dependent migration of THP-1 cells to CXCL1. Student's T-test; ***p<0.001, ****p<0.0001.

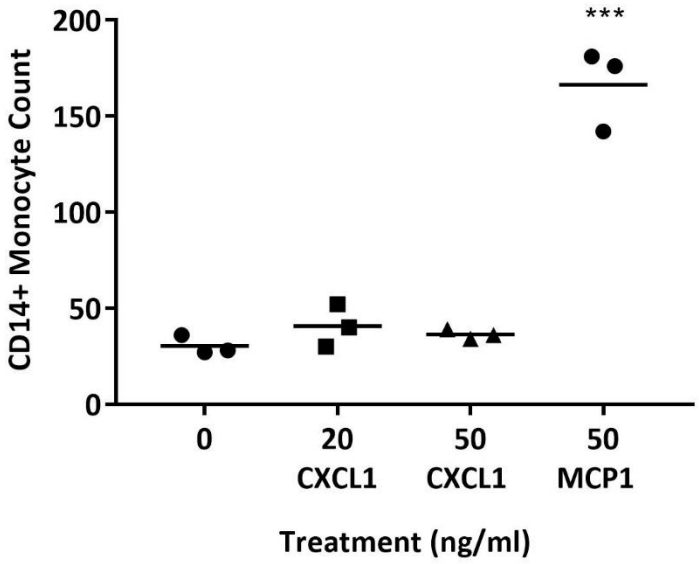

Figure 4.13: Increased migration of human CD14+ monocytes to MCP1, but not CXCL1. Purified human CD14+ monocytes from blood were exposed to CXCL1 and MCP1 in a transwell assay at the indicated concentrations. After 4 hours, cells that had migrated through the membrane were counted using a flow cytometer from triplicate wells. Analysis reveals a significant increase in CD14+ monocyte migration in the presence of MCP1 and no difference in the presence of CXCL1. Student's T-test; ***$p<0.001$, n=1.

4.4 Discussion

In this chapter I showed that genes upregulated by S1P in HUVEC are involved in the process of leukocyte recruitment. These genes include adhesion molecules and chemokines. In support of this finding, I showed that SPHK1 expression is correlated with the expression of a tumour macrophage gene signature and a granulocyte gene signature in primary DLBCL.

Macrophages, which differentiate from monocytes, are the main cell type in the tumour microenvironment of DLBCL (Scott and Gascoyne, 2014). Tumour-associated macrophages (TAMs), most commonly macrophages of the M2 phenotype, can enhance tumour cell proliferation and invasion, increase angiogenesis, and inhibit the T cell-mediated anti-tumour immune response thereby promoting tumour progression (Qian and Pollard, 2010). Two studies have reported that high numbers of M2 macrophages (defined as CD68+CD163+ cells), but not M1 macrophages are associated with an adverse outcome in R-CHOP treated patients (Wada et al., 2012, Marchesi et al., 2015).

Granulocytes have also been shown to be present in the DLBCL microenvironment and in one study were shown to express the B cell survival factor, APRIL (A Proliferating Inducing Ligand). In this study high expression of APRIL was associated with decreased overall patient survival (Schwaller et al., 2007). However, this study did not report the numbers of tumour infiltrating CD15+ cells. I observed very low numbers of infiltrating CD15+ cells in the microenvironment of DLBCL in the majority of cases, with an average of <10 cells per hpf. Even small numbers of cells producing soluble growth factors could be sufficient to promote DLBCL growth, but it would be of interest to determine if the numbers of infiltrating cells of the granulocytic lineage correlate with DLBCL survival.

It is not possible to determine from these analyses whether SPHK1 expression is responsible for the recruitment of monocytes/macrophages or granulocytes. Although the enrichment of macrophage and granulocyte gene signatures in the genes co-expressed with SPHK1 could be explained by other mechanisms, for example, the induction of SPHK1 expression on tumour cells by TAMs, two reports show that SPHK1-S1P signalling is responsible for macrophage recruitment *in vivo*. One of these studies showed that the inhibition of S1P signalling, by the S1P monoclonal antibody, Sphingomab, significantly reduced macrophage infiltration as well as neovascularisation in mice with oxygen induced ischemic retinopathy (Xie et al., 2009). In the second study, the numbers of macrophages were reduced in the livers and lungs of a mouse model of graft-versus-host disease (GVHD) in animals treated with an S1PR1 receptor-selective antagonist CYM-5442, which induces S1PR1 internalisation, phosphorylation, and ubiquitination (Cheng et al., 2015). An *in vivo* model of DLBCL will be required to determine whether SPHK1 expression contributes to stromal cell recruitment in DLBCL.

A previous study has shown that the expression of MCP1 and IL8 are upregulated following the treatment of HUVEC with S1P and that monocytes migrate towards conditioned media from S1P treated HUVEC (Lin et al., 2007). I have shown that S1P induces multiple chemokines in HUVEC, some of which may not be relevant to primary tumours. For this reason I focussed my initial experiments on those chemokines, IL8, CXCL1 and CCL7, upregulated by S1P in HUVEC *and* co-expressed with SPHK1 in primary DLBCL.

Although I observed the upregulation of CCL7 mRNA following S1P treatment, a finding which is supported by the previous observation that CCL7 mRNA is downregulated in HUVEC treated with an S1PR1 inhibitor (CYM-5442) (Cheng et al., 2015), I could not detect CCL7 in the

conditioned media of S1P treated HUVEC. At the present time it is not clear if this is due to the low sensitivity of the ELISA kit used (standards gave low signal) or to post transcriptional/translational regulation of CCL7 expression.

Although I was able to confirm the increased production of IL8 by HUVEC following S1P treatments, this chemokine has been shown to contribute to neutrophil and monocyte recruitment and I did not investigate its effects any further (Gerszten et al., 1999). I chose to focus on CXCL1 which is known to be involved in neutrophil, but not macrophage, recruitment. I optimised a migration assay using the THP-1 monocyte cell line and used this to show that CXCL1 promoted the migration of THP-1 cells. However, in one experiment I was unable to detect any change in migration of purified CD14+ monocytes to CXCL1. It has previously been shown that monocytes isolated from different donors vary in their migratory response to IL8 an observation that might be explained by different levels of IL8 receptors, C-X-C motif chemokine receptor 1 and 2 (CXCR1 and CXCR2), on primary monocytes (Gerszten et al., 1999). CXCR2 is the CXCL1 receptor. It remains to be seen if the failure of primary monocytes to migrate to CXCL1 in my experiment was due to low/absent expression of CXCR2 in these cells. Although my experiments mainly focused on migration it should be noted that both IL8 and CXCL1 can also support monocyte arrest and firm adhesion onto endothelium under flow conditions (Smith et al., 2005, Gerszten et al., 1999).

Tumour cells expressing chemokine receptors could be directed to the endothelial cell derived chemokines promoting intravasation of tumour cells from the primary site into the blood stream for dissemination and contributing to cancer metastasis. Adhesion molecules expressed on endothelial cells can facilitate the binding of tumour cells to the vasculature

(reviewed in: Kobayashi et al., 2007), for example E-selectin has been shown to regulate adhesion of a variety of cancer cell types, including lymphoma (Yoneda et al., 1994). In support of these studies, it has been shown that treatment with an SPHK1 inhibitor reduced metastases of a murine model of breast cancer to lymph nodes and lungs (Nagahashi et al., 2012). Therefore, the S1P-induced upregulation of endothelial cell adhesion molecules and chemokines may contribute to DLBCL spread as well as leukocyte recruitment.

In addition to angiogenesis and leukocyte recruitment, genes upregulated in HUVEC by S1P were also enriched for anti-apoptotic functions, these included BCL2 related protein A1 (BCL2A1). The anti-apoptotic effects of S1P in endothelial cells has previously been described. For example, it has been shown that S1P protects HUVEC from serum starvation (Hisano et al., 1999, Kwon et al., 2001).

CHAPTER FIVE

POTENTIAL THERAPEUTIC INHIBITION OF S1P-INDUCED ANGIOGENESIS AND STROMAL CELL RECRUITMENT IN DLBCL

5.1 Abstract

One third of patients with DLBCL have refractory disease or will relapse after current therapies and will eventually succumb to their disease. This highlights the necessity for the development of novel targeted therapies to treat DLBCL patients. In the preceding chapters I have shown that genes co-expressed with SPHK1 in primary DLBCL tumours are enriched for angiogenic gene signatures. *In vitro* I have provided evidence that in addition to the upregulation of angiogenic genes, the treatment of endothelial cells with S1P can mediate the increased secretion of chemokines known to be involved in monocyte and granulocyte migration. This is supported by the observation that macrophage and granulocyte gene signatures are enriched in genes co-expressed with SPHK1 in primary DLBCL.

Therefore, inhibiting S1P signalling could not only target angiogenesis but also reduce stromal cell recruitment. To date, targeting S1P signalling has not been explored to treat angiogenesis in patients with primary DLBCL. In this part of the work I set out to test the ability of two available S1P signalling targeting drugs, Sphingomab and FTY720, to inhibit S1P-mediated angiogenesis and stromal cell recruitment. Sphingomab is an anti-S1P monoclonal antibody which sequesters S1P, preventing it from binding to its receptors. FTY720 is an analogue of sphingosine which binds to S1PR1, 3, 4 and 5. FTY720 binding induces S1PR1 internalisation and degradation resulting in prolonged receptor downregulation (Matloubian et al., 2004).

Here I first explore, using these inhibitors, the potential inhibition of S1P-induced activation of signalling pathways and gene expression changes in endothelial cells *in vitro* before validating a relevant murine model in which to test the potential therapeutic effects of S1P inhibition.

5.2 Results

5.2.1 Inhibition of S1P-induced ERK activation in HUVEC by Sphingomab and FTY720

To test Sphingomab and FTY720 for their potential to inhibit S1P-mediated angiogenesis and stromal cell recruitment in DLBCL I first explored the ability of these drugs to inhibit S1P-induced activation of ERK in HUVEC. To do this I treated HUVEC with Sphingomab at a range of concentrations. These experiments showed that Sphingomab blocked S1P-induced ERK activation in HUVEC at both 40 μg/ml and 75 μg/ml (Figure 5.1A). Importantly, the S1P-induced ERK activation in HUVEC did occur in the presence of the same concentration of an isotype control antibody (Figure 5.1B). For all subsequent treatments I chose a concentration of 75 μg/ml of Sphingomab in the presence of 0.5 μM S1P to ensure efficient inhibition of S1P-induced signalling. This concentration is similar to those previously used by other studies (O'Brien et al., 2009).

Next, I explored the potential of FTY720 to inhibit the S1P-induced activation of ERK in HUVEC. I treated HUVEC with a range of concentrations of FTY720 for 1 hour prior to treatment with S1P. Figure 5.2 shows that 10 μM FTY720 blocked the S1P-induced activation of ERK.

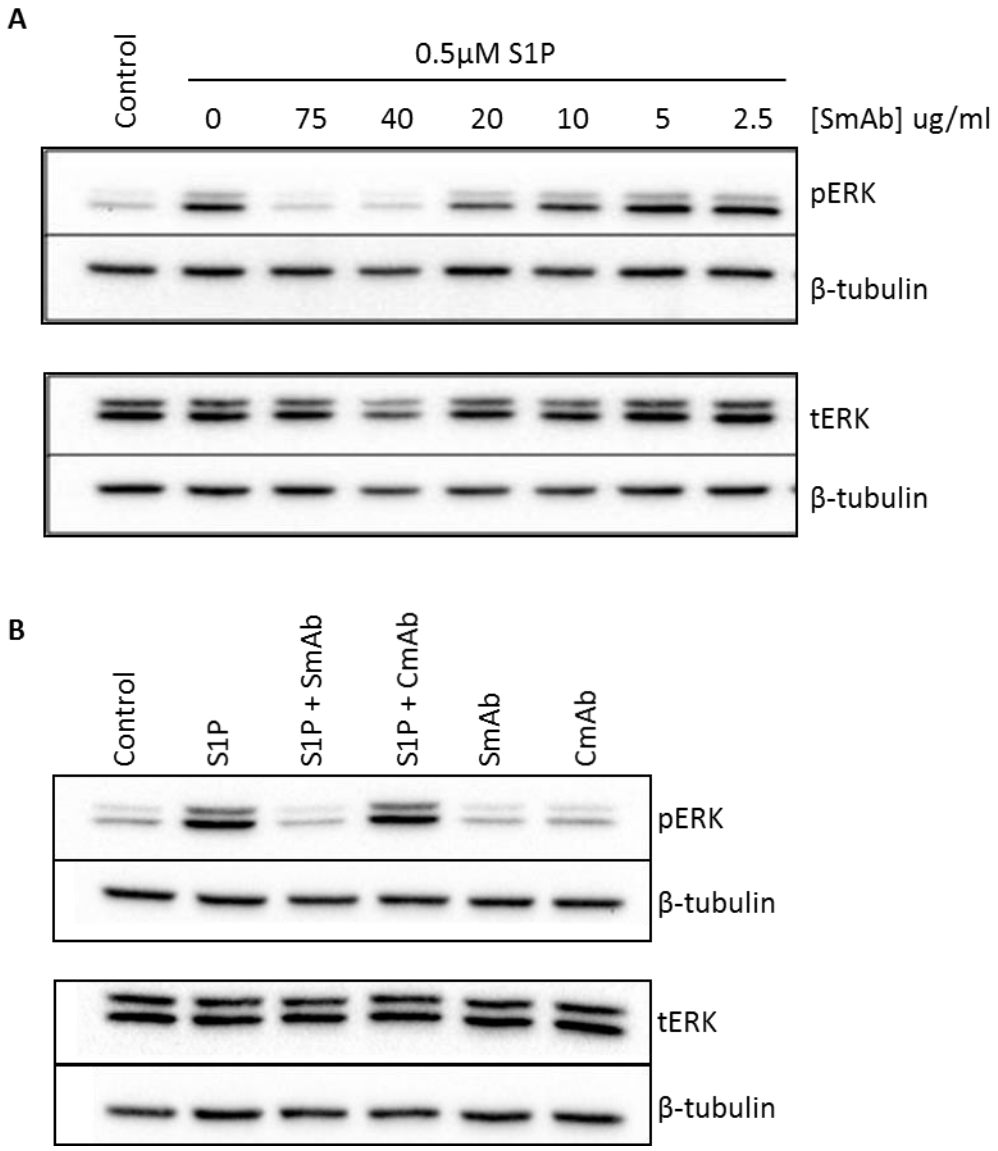

Figure 5.1: Sphingomab inhibits S1P-induced ERK activation in HUVEC. (A) HUVEC were stimulated with S1P in the presence of increasing concentrations of Sphingomab (SmAb) and harvested at 5 minutes. Immunoblotting revealed that compared to controls, Sphingomab blocked 0.5 µM S1P-induced ERK activation in a dose dependent manner with total reversal of ERK activation in the presence of 40 ug/ml and 75 ug/ml of Sphingomab. β-tubulin confirmed equal loading of samples. (B) HUVEC were stimulated with S1P in the presence of 75 ug/ml Sphingomab (SmAb) or isotype control antibody (CmAb) and harvested at 5 minutes. Immunblotting revealed that the S1P-induced ERK activation was completely inhibited with Sphingomab but not with the isotype control antibody. β-tubulin confirmed equal loading of samples. Data shown are representative of three independent experiments from three different HUVEC donors.

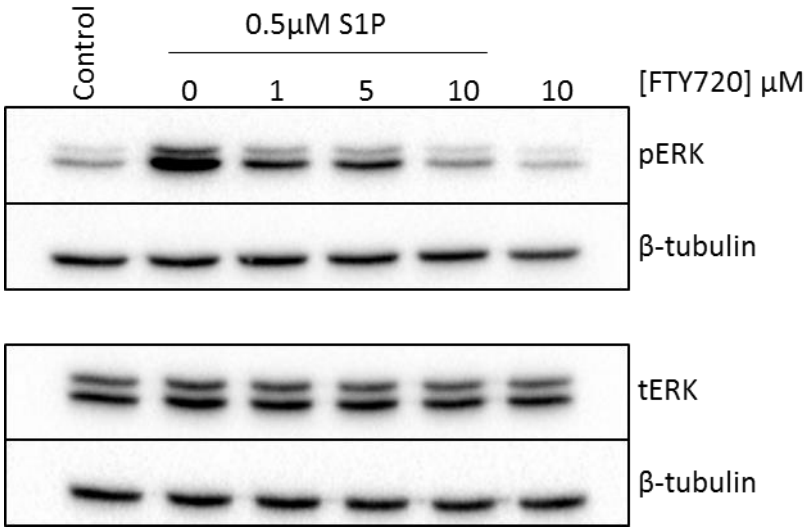

Figure 5.2: FTY720 inhibits S1P-induced ERK activation in HUVEC. HUVEC were pre-treated with increasing concentrations of FTY720 for 1 hour and then harvested following treatment with S1P for 5 minutes. Immunoblotting revealed that compared to control, FTY720 blocked S1P-induced ERK activation in a dose dependent manner with complete inhibition of ERK activation in the presence of 10 µM FTY720. 10 µM FTY720 treatment alone had no effect on ERK activation compared to control. β-tubulin confirmed equal loading of samples. Data shown are representative of three independent experiments from three different HUVEC donors.

5.2.2 Inhibition of S1P-induced gene upregulation in HUVEC

Having shown that both Sphingomab and FTY720 can block the S1P-induced activation of ERK in HUVEC, I next wanted to explore if these drugs could also block the induction of S1P-induced gene expression in HUVEC. I performed qPCR on HUVEC treated with S1P for 4 hours in the presence of Sphingomab, FTY720 or controls. Figure 5.3 shows that Sphingomab inhibited the S1P-induced upregulation of ICAM1, SELE, CXCL1, and CXCL8 mRNA whereas the isotype control antibody did not. However, FTY720 treatment resulted in the upregulation of these genes (Figure 5.4). In subsequent experiments I focussed only on Sphingomab.

5.2.3 Inhibition of S1P-induced chemokine release from HUVEC

I next studied if the S1P-induced release of CXCL1 and IL8 from HUVEC could be inhibited in the presence of Sphingomab. Cells were treated with two doses of S1P in the presence of either Sphingomab or isotype control antibody. Conditioned media was harvested after 12 hours and subjected to ELISA analysis. Figure 5.5 shows that in the presence of Sphingomab the S1P-induced increase in CXCL1 and IL8 levels from HUVEC was inhibited. By contrast, the isotype control antibody had no effect on the level of these chemokines following S1P treatment.

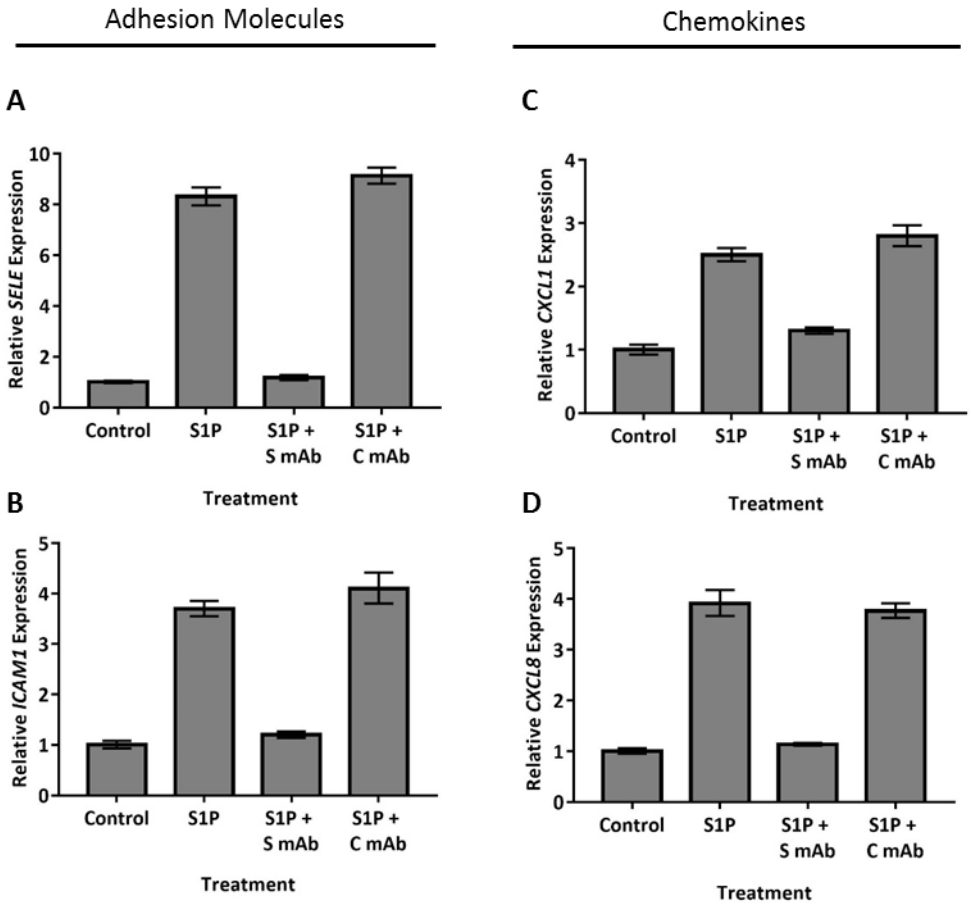

Figure 5.3: Sphingomab blocks the S1P-induced upregulation of adhesion molecules and chemokines in HUVEC. HUVEC were treated with S1P in the presence of Sphingomab (S mAb) or isotype control antibody (C mAb) for 4 hours. qPCR analysis shows that the S1P-induced upregulation of adhesion molecule genes ICAM1 (A) and SELE (B); and chemokine genes CXCL1 (C) and CXCL8 (D) was inhibited in the presence of Sphingomab, whereas isotype control antibody had no effect. Data shown are representative of three independent experiments from three different HUVEC donors. Samples were analysed in triplicate and are presented as $2^{-\Delta\Delta CT}$ values in comparison to corresponding control.

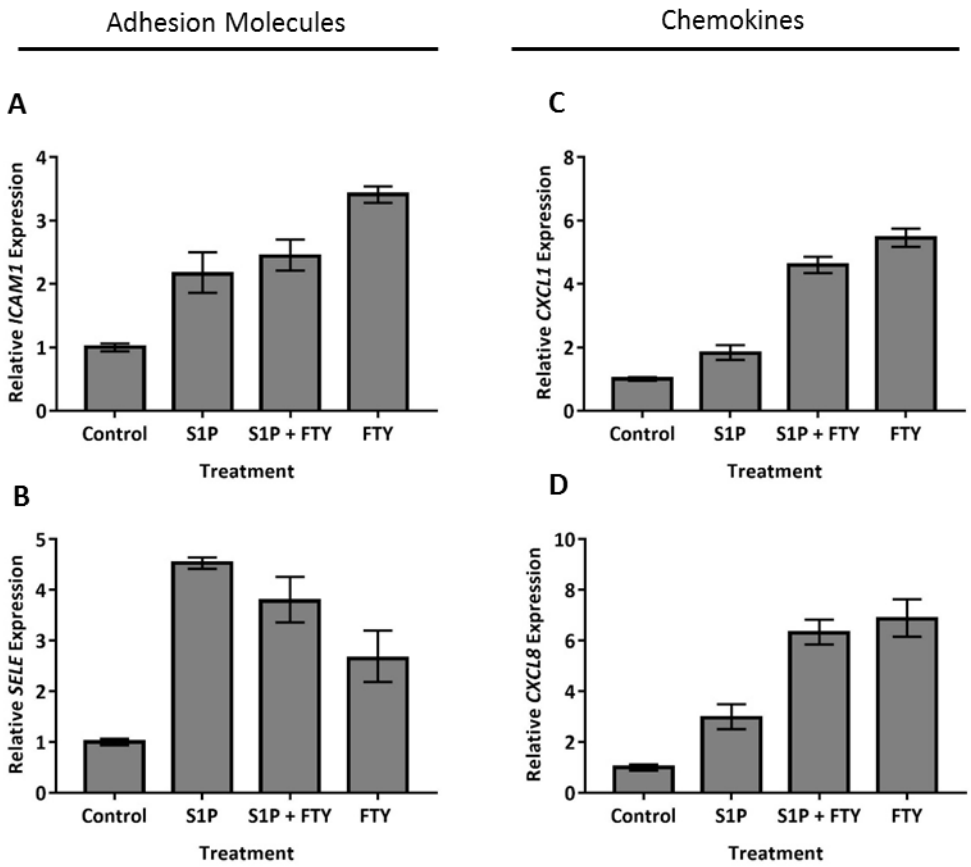

Figure 5.4: FTY720 induces the upregulation of adhesion molecules and chemokines in HUVEC. HUVEC were pre-treated with FTY720 (FTY) for 1 hour prior to S1P treatment for an additional four hours. qPCR analysis shows that FTY720 treatment alone induced upregulation of ICAM1 (A), SELE (B), CXCL1 (C) and CXCL8 (D). Data shown are representative of three independent experiments from three different HUVEC donors. Samples were analysed in triplicate and are presented as $2^{-\Delta\Delta CT}$ values in comparison to corresponding control.

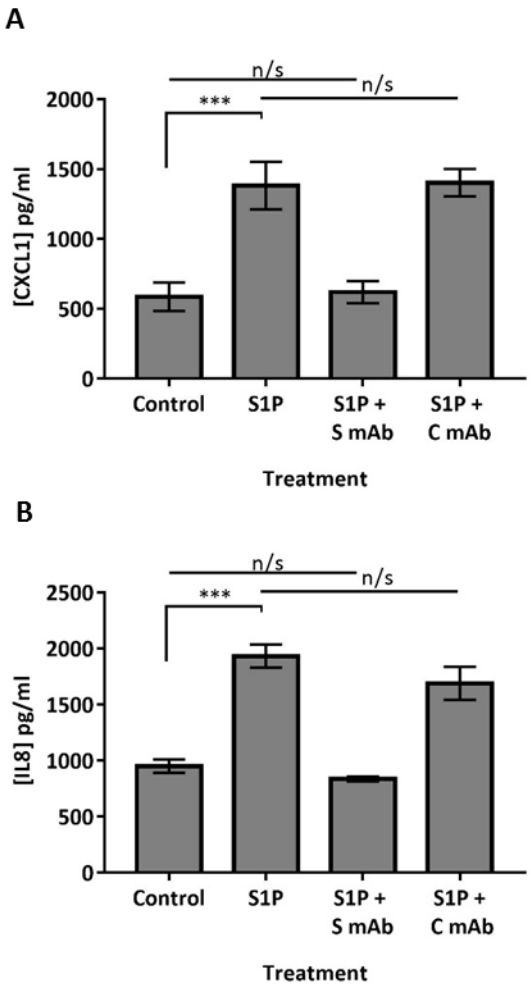

Figure 5.5: Sphingomab inhibits the S1P-induced increase in chemokine levels in HUVEC. An ELISA was used to measure the levels of CXCL1 (A) and IL8 (B) in the conditioned media of HUVEC treated with S1P in the presence of Sphingomab (S mAb) or isotype control antibody (C mAb) for 12 hours. Analysis reveals the inhibition of S1P-induced increase in CXCL1 and IL8 levels in the presence of Sphingomab, but not in the presence of isotype control antibody. Data are represented as mean ±SEM of four separate experiments. Students T-test.*** $p<0.001$. n/s = not significant.

5.2.4 *In vitro* studies for the validation of A20 BALB/c syngeneic model of DLBCL to test the potential therapeutic effects of SPHK1-S1P signalling targeting drugs

A20 Cell Line Expresses SPHK1

I chose to validate the A20 mouse model of lymphoma, in which immunocompetent BALB/c mice are injected with the A20 syngeneic B lymphoma cell line, to study the therapeutic effects of Sphingomab. This model has previously been used to study the microenvironment of DLBCL including the preclinical *in vivo* evaluation of immunotherapy against lymphoma (Briones et al., 2002, Siegel et al., 2003, Chaise et al., 2007, Serafini et al., 2008, Elpek et al., 2007). In the first instance I studied the expression of SPHK1 and its phosphorylation in the A20 cell line grown *in vitro* using immunoblotting. This suggests that A20 cells produce S1P like DLBCL primary tumours and is therefore a relevant cell model to study SPHK1-S1P signalling targeting drugs (Figure 5.6).

S1P activates ERK in mouse endothelial cells

For the next set of experiments I wanted to determine if S1P can also activate signalling in mouse endothelial cells. I was unable to successfully propagate mouse BALB/c endothelial cells in culture so I chose an extensively used murine endothelial cell line, sEnd-1 (Williams et al., 1989). I treated sEnd-1 cells with increasing concentrations of S1P and performed immunoblotting against pERK. Figure 5.7 reveals that sEnd-1 cells had a high basal level of pERK, attributed to the expression of polyoma middle T antigen, which mimics an activated growth receptor and activates many downstream signalling pathways (Schaffhausen and Roberts, 2009). A modest increase in pERK was detected by immunoblotting in those cells

treated with S1P. Due to this I performed densitometry to confirm the activation of ERK in those cells treated with S1P compared to control.

S1P upregulates expression of adhesion molecules and chemokines in mouse endothelial cells

Having shown that S1P activates ERK in mouse endothelial cells, I next wanted to determine if S1P can also upregulate adhesion molecules and chemokines in these cells. Mice do not express CXCL8, and CXCL1 is widely accepted as the functional homologue of CXCL8 in the mouse. I performed qPCR for ICAM1, SELE and CXCL1 on sEnd-1 cells treated with S1P for 4 hours. Figure 5.8 shows that the expression of all three genes was upregulated following S1P treatment.

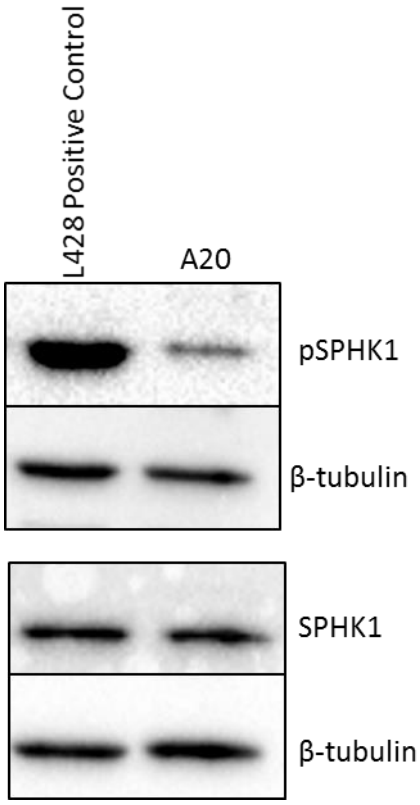

Figure 5.6: A20 cells express SPHK1. Immunoblotting confirmed the expression of SPHK1 and its phosphorylation in the A20 cell line grown *in vitro*. β-tubulin confirmed equal loading of sample. Data shown are representative of three independent experiments

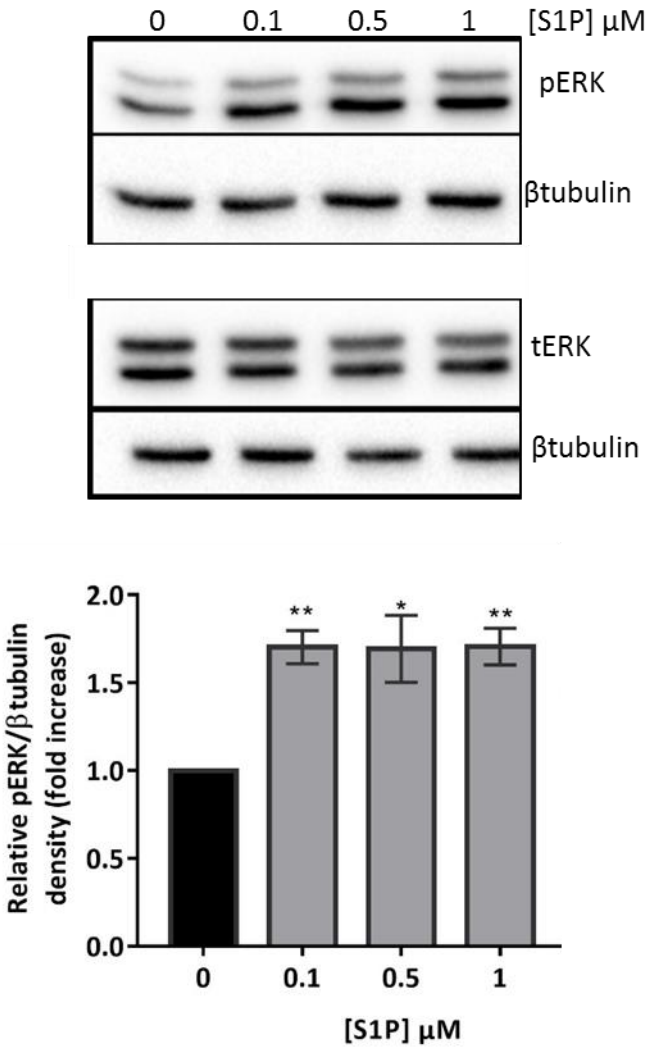

Figure 5.7: S1P activates ERK in sEnd-1 cells. sEnd-1 cells were treated with S1P at the indicated concentrations and harvested at 5 minutes. Immunoblotting reveals the S1P-induced activation of ERK compared to control cells. β-tubulin confirmed equal loading of sample. Data shown are representative of three independent experiments. Densitometry analysis of pERK expression is shown (bottom). Results were normalised by setting the densitometry of control cells to 1.0. Data shown are mean ±SEM of three separate experiments. Students T-test. *p<0.05, **p<0.01.

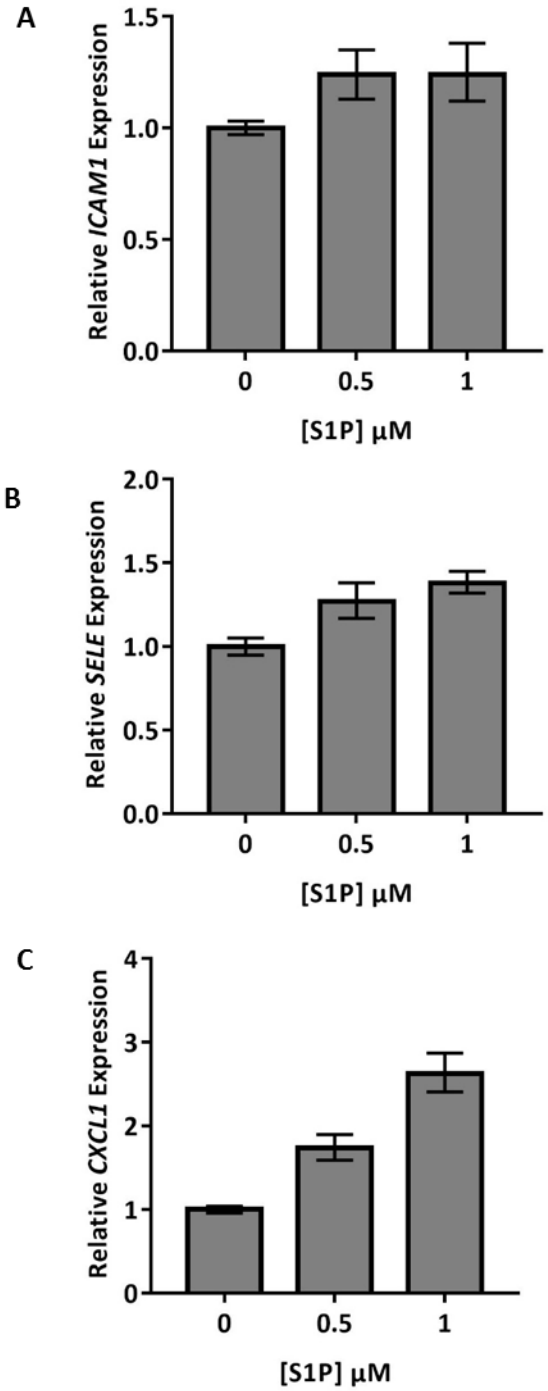

Figure 5.8: S1P treatment of sEnd-1 cells is followed by the upregulation of ICAM1, SELE and CXCL1. sEnd-1 cells were treated with S1P at the indicated concentrations for 4 hours and subjected to qPCR analysis. This analysis reveals the upregulation of murine ICAM1 (A), SELE (B) and CXCL1 (C) genes. Samples were analysed in triplicate and are presented as $2^{-\Delta\Delta CT}$ values in comparison to corresponding control.

5.2.5 *In vivo* studies for the validation of A20 BALB/c syngeneic model of DLBCL to test the potential therapeutic effects of SPHK1-S1P signalling targeting drugs

A pilot study was performed to study the growth kinetics and engraftment of A20 cells injected intravenously into two BALB/c mice. A20 engrafted mice were culled at a humane endpoint (day 28). Post mortem revealed that animals had enlarged spleens and livers indicating engraftment of tumours in these organs (Figure 5.9A). Tumour load was measured by weight of engrafted organs compared to organs from control animals (Figure 5.9B). H&E staining confirmed the engraftment of tumour cells in the spleens and livers which revealed multiple foci of rounded aggregates of tumour cells distributed throughout both organs (Figure 5.9C).

IHC was performed on sections from the A20 engrafted livers and spleens. A20 engrafted tumour cells were positive for SPHK1 in both the spleen and liver (Figure 5.8). Additionally tumours contained CD31+ endothelial cells, CD15+ granulocytes and CD68+ macrophages (Figure 5.10).

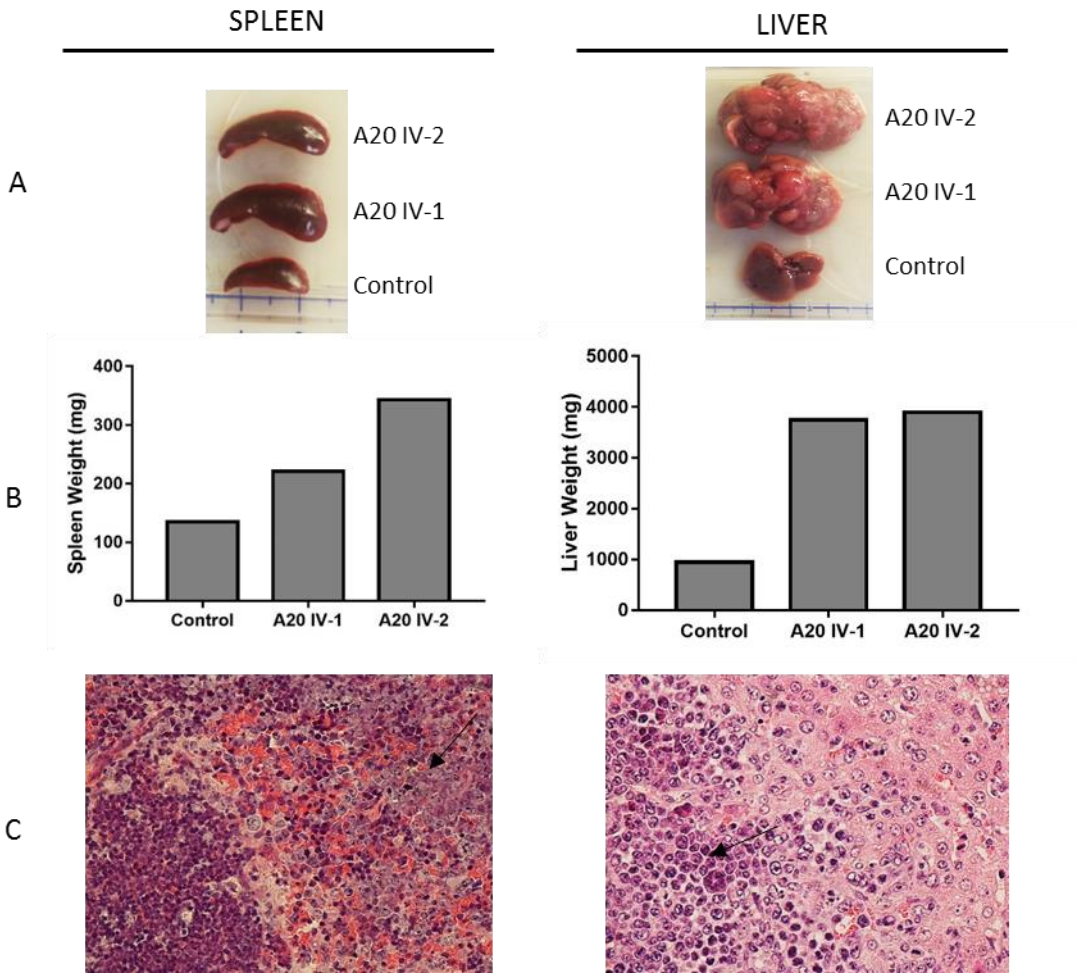

Figure 5.9. A20 lymphoma cell infiltration of mouse spleen and liver following intravenous injection. Two BALB/c mice were injected intravenously with A20 tumour cells (A20 IV-1 and A20 IV-2) and sacrificed after 28 days. Post mortem revealed enlarged spleens and livers in the A20 IV animals compared to corresponding organs from a control mouse (A, left and right panels, respectively). Spleen and liver weights of A20 IV animals was increased compared to control (B, left and right panels, respectively). H&E IHC sections confirmed the engraftment of A20 tumour cells (black arrows) in the spleen and liver (C, left and right panels, respectively).

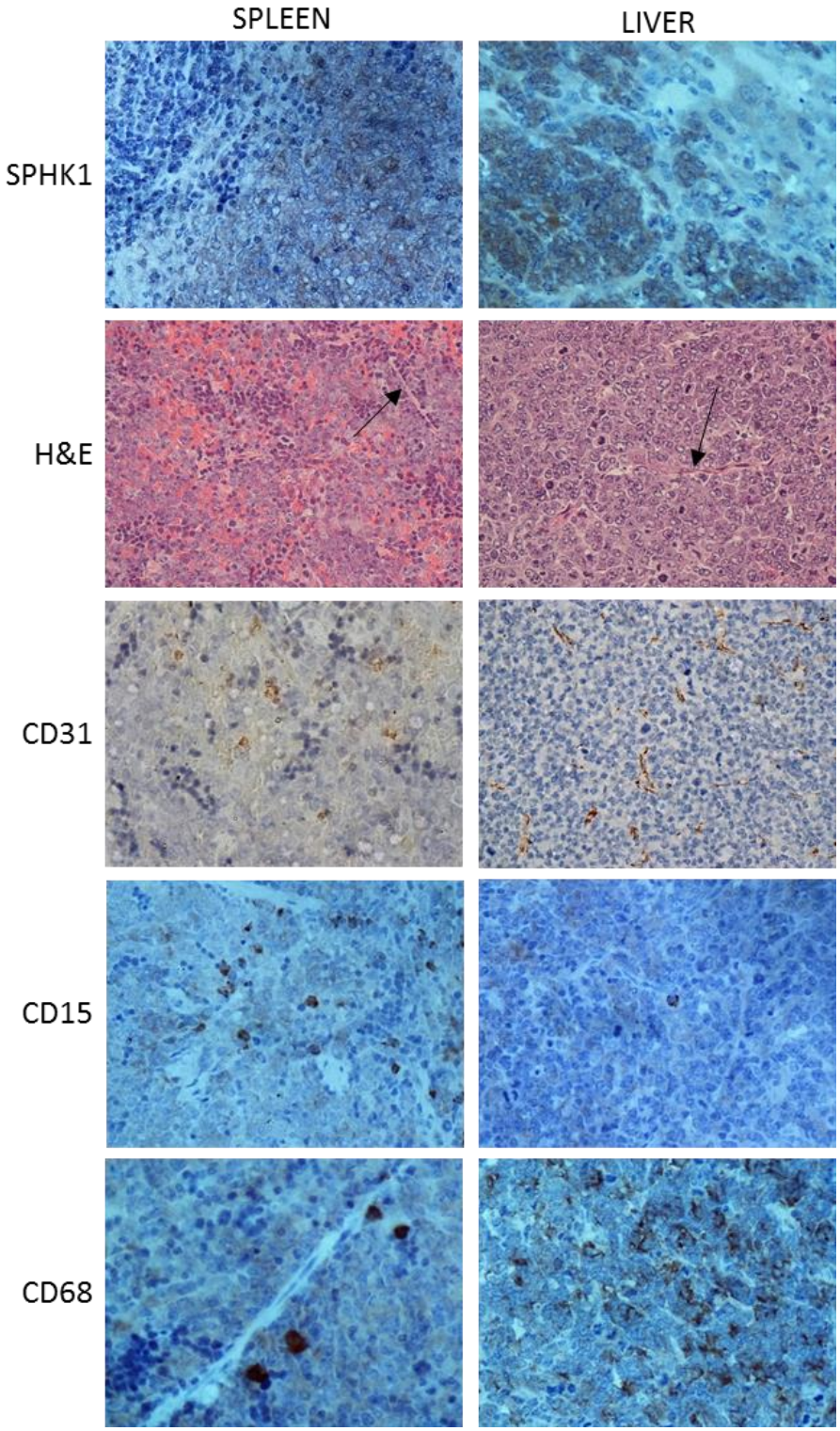

Figure 5.10: A20 tumours express SPHK1 and recruit stromal cell components *in vivo*. IHC analysis of sections from A20 engrafted spleen and liver (left and right panels, respectively) revealed A20 tumour cell expression of SPHK1, infiltration of tumour cells with endothelial cells (H&E black arrows and CD31), granulocytes (CD15) and macrophages (CD68).

5.3 Discussion

In this chapter I have shown that I can inhibit S1P-induced gene expression in HUVEC. I also demonstrated that the A20 syngeneic B-cell lymphoma mouse model can be used to study the therapeutic targeting of SPHK1-S1P signalling.

Sphingomab, a monoclonal antibody against S1P, blocked the S1P-induced activation of ERK, the upregulation of S1P targets and chemokine release in HUVEC. This supports *in vivo* studies which have shown that in the presence of Sphinomab, microvessel density was reduced in lung and ovarian tumour mouse models (Visentin et al., 2006). Previous studies have also shown that Sphingomab can significantly reduce macrophage infiltration and vascularisation in mice with oxygen induced ischemic retinopathy (Xie et al., 2009). Taken together, these observations could support the future testing of Sphingomab in preclinical models of DLBCL.

In contrast, treatment of HUVEC with FTY720 induced the upregulation of S1P target genes. FTY720 is an S1P receptor agonist, however these effects are followed by the prolonged downregulation of S1PR1 from the cell surface. It is possible that the upregulation of S1P target genes which I observed reflects the initial agonistic function of FTY720. It would be important to explore the effects of FTY720 on S1P-mediated upregulation of genes at a time point later than 4 hours. The inhibitory effects of FTY720 on S1P-mediated angiogenesis has been demonstrated in melanoma, lung and hepatocellular carcinoma mouse xenograft models, which showed reduction in blood vessel density following treatment with FTY720 (Schmid et al., 2005, LaMontagne et al., 2006, Ho et al., 2005).

The potential therapeutic effects of S1P signalling inhibitors on tumour angiogenesis and stromal cell recruitment have not been explored in a preclinical model of DLBCL. I have shown here that the A20 syngeneic model of DLBCL could be used to assess the efficacy of SPHK1-S1P targeting compounds *in vivo.* Furthermore I have shown using the sEnd-1 cell line that S1P can induce adhesion molecules and chemokines expression in mouse endothelial cells, albeit to a lesser extent than I observed in HUVEC. At the time of writing, experiments are underway to investigate if the S1P neutralising antibody, Sphingomab, can inhibit S1P target gene expression in the endothelial cells of A20 tumours. Furthermore it is important to note that differences exist in chemokine expression between the human and mouse. For example, IL8 is expressed in humans but not in the mouse.

A20 tumours displayed evidence of recruitment of macrophages, granulocytes and endothelial cells, further confirming the utility of this model to explore the effects of S1P on these stromal cells. To identify macrophages and granulocytes I used well established antibodies to detect CD68 and CD15 directed against human proteins. In preliminary experiments I showed that mouse cells with a morphology characteristic of macrophages and granulocytes were strongly stained with the anti-human CD68 and CD15, respectively. In future studies I plan to use reagents directed against mouse markers, for example, F4/80 which is expressed on most tissue macrophages in the mouse. Future work could also include the identification of the M1 and M2 phenotype of macrophages to assess the potential changes in the ratio of these macrophage types following treatment with SPHK-S1P targeting agents. Furthermore, the characterisation of the granulocytic cells infiltrating the tumour could be performed such as the identification of neutrophils by expression of Ly6G.

The multiplexed IHC technology analysed on multiplex biomarker imaging systems, such as the OPAL staining analysed on the Vectra quantitative imaging system (both; PerkinElmer Inc. Seer Green, United Kingdom), could be considered. In addition to a more sensitive and accurate analysis of the infiltrating stromal cells, this would allow for multiplex staining, which could include F4/80 and MHC class II staining to identify M1 macrophages and F4/80 and CD206 and/or CD163 to identify M2 macrophages.

CHAPTER SIX

CONCLUSIONS AND FUTURE PERSPECTIVES

DLBCL is a highly heterogeneous disease both molecularly and clinically. However, most patients are treated with the R-CHOP regimen. Although the addition of rituximab to CHOP saw great improvements in the survival of DLBCL patients, one-third of patients still relapse or have refractory disease and 5 year overall survival is only 60% (HMRN, 2016). Novel therapies that target components of the tumour microenvironment are being developed that might provide better, less toxic treatments.

In this thesis I have focussed on the potential contribution of S1P signalling to the phenotype of the tumour microenvironment. My data show that expression of SPHK1, the major enzyme that produces S1P, is associated with the expression of angiogenic genes in DLBCL. Furthermore, my studies also showed that many of the transcriptional changes induced by the treatment of endothelial cells with S1P *in vitro* were evident in SPHK1-expressing tumours, suggesting that tumour-derived S1P is likely to be involved in tumour angiogenesis in DLBCL.

Clinical trials of angiogenesis inhibitors have so far produced disappointing results. However this may have been because some tumours show less evidence of an angiogenic phenotype and therefore might be less susceptible to anti-angiogenic drugs. Alternatively, the angiogenic phenotype may be driven by another signalling pathway to VEGF, such as SPHK1-S1P. Stratification of patients up front before therapy should be considered before anti-angiogenic treatments. In this regard it is noteworthy that a phase two clinical trials of Sphingomab in renal cell carcinoma patients was terminated as the overall median time to progression was less than two months in 39 patients. However, this clinical trial did not stratify patients to identify which would benefit from Sphingomab treatment. Seven patients were progression

free for at least six months and three of which were for over 20 months. Six patients still received treatment at the date of the report (PRnewswire, 2015)

To identify patients who might benefit from SPHK1-S1P signalling targeting therapies, future studies could identify or develop useful biomarkers which would enable stratification of patients. Considerations could be to identify those patients with tumours which express high levels of SPHK1 and/or tumours with high microvessel density, both of which could be identified from tumour biopsies. Another possibility could be the development of a test to identify whether serum S1P levels are a useful biomarker. Furthermore, with the ever advancing technology in the field of diagnostics, the presence of an S1P signalling expression profile, determined by gene expression profiling of patient samples, could be used to identify those patients which would potentially benefit from SPHK1-S1P signalling targeting agents.

As well as having direct effects on the expression of angiogenesis-associated genes in endothelial cells, my data also point to important contributions of S1P-induced endothelial cell-derived chemokines, to the pathogenesis of DLBCL. My preliminary studies and the work of other groups suggest that the induction of these chemokines by S1P is likely to be important for endothelial cell mediated recruitment of stromal cells including monocytes/macrophages and granulocytes, to DLBCL. These cell types are known to contribute to tumour cell survival and immune escape (Qian and Pollard, 2010, Schwaller et al., 2007).

I was able to block S1P-induced ERK activation and gene expression changes in HUVEC, suggesting that drugs such as Sphingomab might reverse S1P-induced tumour angiogenesis and endothelial cell mediated stromal cell recruitment. In addition to Sphingomab, further work could also include FTY720. FTY720, which has also been shown to be an effective agent

in many types of cancer in animal models, is already being used clinically for the treatment of multiple sclerosis (Brinkmann et al., 2010, Kappos et al., 2006). Focussing on an agent which is already FDA approved, could mean getting FTY720 into DLBCL treatment regimens faster.

Pre-clinical studies on the feasibility of using SPHK1-S1P targeting compounds to treat DLBCL are necessary before clinical trials can be considered. I have shown that the A20 syngeneic model of DLBCL would seem to be a relevant model with which to assess the efficacy of SPHK1-S1P targeting compounds *in vivo.* It would be especially desirable to study the effects of inhibiting SPHK-S1P signalling using either humanised mouse models with human B cell lymphoma cells implanted, or patient derived xenografts (PDX) models. PDX models, which are based on the transfer of primary tumours directly from the patient into an immunodeficient mouse, are reported to maintain more similarities to the parental tumour such as histology and gene expression profiling (Siolas and Hannon, 2013).

Although some way off a clinical trial, it is worth considering where in the care pathway drugs that target SPHK1-S1P signalling might be positioned. It seems likely that in the first instance they will be tested in patients treated unsuccessfully with front-line and salvage therapies. If successful in this scenario then trials with and without these new drugs in combination with R-CHOP could be considered.

APPENDICES

Appendix 1: SPHK1 and S1P receptor IHC staining results of primary DLBCL cases

+ = positive, - = negative, NA = not available, yellow shading = no internal positive control.

Case Number	SPHK1 Tumour expression	S1PR1 Endothelial cell expression	S1PR2 Endothelial cell expression	S1PR3 Endothelial cell expression
95	+	+	-	-
102	-	+	-	-
112	+	+	-	-
134	+	+	-	-
138	CRUSHED	CRUSHED	CRUSHED	CRUSHED
150	+	+	-	-
154	+	+	-	-
155	+	+	-	-
159	+	+	-	-
160	+	+	-	-
161	+	+	-	-
162	+	+	-	-
166	+	+	-	-
175	+	+	-	-
176	+	+	-	-
177	+	+	-	-
182	+	+	-	NA
189	+	+	-	-
190	+	+	-	-
191	+	+	-	-
195	+	+	NA	-
196	-	+	-	-
197	+	NA	-	-
198	+	+	-	-
199	+	NA	-	NA
200	+	+	-	-
203	+	+	NA	-
204	+	+	-	-
207	+	+	-	-
208	+	+	-	-
209	+	+	-	-
211	+	+	-	-
212	+	+	-	-
213	+	+	-	-
214	+	+	NA	-
215	+	+	-	-
220	+	+	-	-
227	+	+	-	-
231	+	+	-	-

Appendix 2: Genes regulated by S1P in HUVEC

Genes downregulated by S1P in HUVEC			Genes upregulated by S1P in HUVEC		
Gene Symbol	Fold Change	P-Value	Gene Symbol	Fold Change	P-Value
NELL2	-3.18	0.010	CSF2	3.39	1.87E-07
ZNF888	-2.80	0.000	BCL2A1	3.37	7.38E-05
CSNK1E	-2.70	0.000	CSF3	3.34	3.66E-07
CMPK2	-2.65	0.039	NBPF25P	3.00	0.026
NEU3	-2.54	0.030	CCL7	2.80	0.001
TBC1D3P1-DHX40P1	-2.45	0.028	TRAF1	2.48	0.000
GPRASP1	-2.42	0.001	MORN3	2.43	0.002
LOC441155	-2.39	0.046	COL1A1	2.29	0.001
CEP170P1	-2.36	0.037	KCNN2	2.22	0.027
FLRT3	-2.28	0.001	CX3CL1	2.20	0.002
CCNE2	-2.20	0.003	PXN-AS1	2.18	0.004
ZNF808	-2.19	0.003	CXCL3	2.14	0.000
PLCL1	-2.17	0.027	MRS2P2	2.14	0.002
CRYBG3	-2.15	0.030	SELE	2.08	0.002
MKRN9P	-2.08	0.014	CYSRT1	2.03	0.042
HIST2H2BE	-2.06	0.004	PTPN7	2.00	0.003
SERPINI1	-2.05	0.016	PWARSN	1.99	0.003
ULBP3	-1.96	0.040	LOC100506076	1.96	0.009
CEP152	-1.96	0.000	S100A3	1.96	0.031
GALNT15	-1.94	0.021	RRAD	1.94	0.001
ZNF680	-1.92	0.013	CCNI2	1.93	0.016
DOCK3	-1.92	0.049	C19orf18	1.93	0.022
FOXF1	-1.92	0.028	ZP3	1.91	0.020
FAM156A	-1.92	0.028	LTB	1.89	0.026
NHS	-1.89	0.034	POU2F2	1.83	0.008
FSTL5	-1.87	0.001	CD83	1.82	0.006
MANEA	-1.87	0.002	BIRC3	1.81	0.001
ZNF488	-1.87	0.017	VSIG2	1.80	0.007
ZNF549	-1.84	0.047	UFSP1	1.79	0.035
CNTN1	-1.83	0.022	RASSF8-AS1	1.78	0.033
CYP26B1	-1.83	0.011	VCAM1	1.77	0.022
RAB43	-1.83	0.017	PDE8B	1.77	0.022
DNAJB4	-1.78	0.043	MIR17HG	1.76	0.012
PYGO1	-1.78	0.022	LOC101929709	1.75	0.007
RFXAP	-1.77	0.002	EIF4EBP3	1.75	0.035
E2F8	-1.77	0.021	ANKHD1-EIF4EBP3	1.74	0.012
SENP7	-1.77	0.044	LOC100128398	1.74	0.012
SATB2	-1.76	0.042	LOC286437	1.73	0.037
PFKFB2	-1.76	0.045	MEI1	1.73	0.025

HSPA4L	-1.75	0.014	MT1X	1.72	0.023
CYB5R4	-1.74	0.007	LOC101926963	1.72	0.007
PKNOX2	-1.72	0.017	MYEOV	1.71	0.028
ZNF92	-1.71	0.011	LOC100131564	1.71	0.007
PCGF6	-1.71	0.027	PSORS1C1	1.70	0.026
DDX60	-1.70	0.023	ADM2	1.70	0.027
CMTR2	-1.69	0.034	ANG	1.68	0.010
KIAA1109	-1.69	0.002	HIST1H2BD	1.67	0.015
FREM3	-1.69	0.048	RND1	1.67	0.008
IGFBP5	-1.68	0.022	TNFAIP2	1.65	0.001
RECQL	-1.68	0.029	PRSS53	1.64	0.009
APC	-1.65	0.001	CXCL12	1.64	0.041
UPRT	-1.64	0.005	RELB	1.64	0.002
RNFT1	-1.64	0.033	MYADM	1.64	0.001
TSPAN12	-1.62	0.022	MFI2-AS1	1.63	0.017
UBE2V1	-1.61	0.043	RNF207	1.63	0.043
GRAMD1C	-1.61	0.032	TFPT	1.62	0.046
SESN3	-1.60	0.023	KANSL1-AS1	1.60	0.028
USP53	-1.60	0.014	ARL17A	1.59	0.047
CFAP44	-1.59	0.013	SPHK1	1.59	0.013
CEP128	-1.59	0.010	PPM1J	1.59	0.025
C1orf226	-1.58	0.023	ICOSLG	1.58	0.004
CHML	-1.58	0.017	ANKRD18B	1.58	0.021
ARHGAP28	-1.58	0.009	LOC102724434	1.57	0.038
REV3L	-1.58	0.028	ICAM1	1.57	0.005
WNK3	-1.58	0.044	SPOCD1	1.57	0.011
TEF	-1.58	0.027	ISG20	1.56	0.036
LOC727896	-1.57	0.029	LRP2BP	1.56	0.019
KIF14	-1.57	0.019	ZBED3	1.56	0.010
ZBTB41	-1.56	0.032	C11orf80	1.55	0.014
SNX16	-1.55	0.021	DNAH5	1.55	0.044
ZSCAN31	-1.55	0.050	IFI27L1	1.54	0.028
TFEC	-1.54	0.019	PET100	1.54	0.024
CNTRL	-1.54	0.013	C8orf76	1.54	0.048
ZNF644	-1.54	0.029	C2CD4B	1.53	0.020
PDIK1L	-1.54	0.037	LINC00152	1.53	0.037
EGR1	-1.53	0.030	PIN1P1	1.53	0.042
FAM117B	-1.53	0.029	PRNCR1	1.51	0.011
ZNF112	-1.52	0.017	C11orf91	1.50	0.034
ZNF765	-1.52	0.023	DNPH1	1.50	0.049
ZNF215	-1.52	0.041	MAP1B	1.49	0.033
ETNK1	-1.51	0.022	SDC4	1.49	0.002
XRN1	-1.51	0.047	STAG3L1	1.49	0.039
ZNF678	-1.51	0.034	GATA2-AS1	1.48	0.017

ZDHHC17	-1.50	0.044	CASC10	1.48	0.031
INCA1	-1.50	0.049	NFKB2	1.48	0.009
RNF182	-1.50	0.046	POLR2J3	1.48	0.049
USP32P1	-1.50	0.050	DHRS4L2	1.48	0.044
MIS18BP1	-1.49	0.026	FTH1P3	1.48	0.039
GJA5	-1.49	0.049	MSX1	1.47	0.043
AHCTF1P1	-1.48	0.031	TRIM47	1.46	0.015
TMEM79	-1.48	0.047	SOX4	1.43	0.035
SEMA6A	-1.47	0.032	CCL2	1.43	0.011
TBK1	-1.47	0.008	DAPK3	1.43	0.031
LACTB2	-1.47	0.038	UPP1	1.43	0.045
ZNF100	-1.47	0.045	MIR155HG	1.42	0.042
USP45	-1.47	0.043	FGGY	1.41	0.037
ZNF117	-1.47	0.041	LINC-PINT	1.41	0.036
TTK	-1.46	0.014	CEBPD	1.40	0.027
CDKN2C	-1.46	0.018	ANGPTL4	1.40	0.025
NRROS	-1.45	0.016	HLX	1.40	0.033
ZCCHC11	-1.45	0.029	C10orf54	1.39	0.026
TOP1P1	-1.45	0.043	GFPT2	1.39	0.031
KIAA1551	-1.45	0.028	RASAL3	1.39	0.050
TRMT1L	-1.45	0.027	FSTL3	1.38	0.032
HLTF	-1.44	0.035	PDGFA	1.38	0.019
MAF	-1.44	0.039	MED18	1.37	0.043
DLL4	-1.44	0.029	PLAUR	1.37	0.022
EVI2B	-1.43	0.049	TMEM217	1.37	0.025
DNAJB14	-1.43	0.031	KLF6	1.35	0.023
RANBP2	-1.43	0.025	PHF20	1.35	0.023
FERMT1	-1.43	0.042	RSPO3	1.33	0.035
IFT80	-1.43	0.040	COL27A1	1.33	0.038
ATG4C	-1.42	0.044	ITSN2	1.32	0.038
GMFB	-1.42	0.022	CALD1	1.30	0.037
DDX26B	-1.41	0.042	CXCL1	1.30	0.041
TBC1D31	-1.41	0.045	RUNX1T1	1.30	0.018
FAR1	-1.41	0.016			
TTC37	-1.41	0.028			
LRRC40	-1.40	0.039			
BRWD3	-1.40	0.033			
USO1	-1.40	0.037			
MPHOSPH9	-1.39	0.032			
SMCHD1	-1.39	0.043			
MSH2	-1.38	0.031			
STAG2	-1.38	0.030			
CRY2	-1.35	0.034			

LIST OF REFERENCES

AKAO, Y., BANNO, Y., NAKAGAWA, Y., et al. 2006. High expression of sphingosine kinase 1 and S1P receptors in chemotherapy-resistant prostate cancer PC3 cells and their camptothecin-induced up-regulation. *Biochemical and Biophysical Research Communications,* 342**,** 1284-1290.

ALIZADEH, A. A., EISEN, M. B., DAVIS, R. E., et al. 2000. Distinct types of diffuse large B-cell lymphoma identified by gene expression profiling. *Nature,* 403**,** 503-511.

ALVAREZ, S. E., HARIKUMAR, K. B., HAIT, N. C., et al. 2010. Sphingosine-1-phosphate is a missing cofactor for the E3 ubiquitin ligase TRAF2. *Nature,* 465**,** 1084-8.

ALVAREZ, S. E., MILSTIEN, S. & SPIEGEL, S. 2007. Autocrine and paracrine roles of sphingosine-1-phosphate. *Trends Endocrinol Metab,* 18**,** 300-7.

ANELLI, V., GAULT, C. R., CHENG, A. B. & OBEID, L. M. 2008. Sphingosine kinase 1 is up-regulated during hypoxia in U87MG glioma cells. Role of hypoxia-inducible factors 1 and 2. *J Biol Chem,* 283**,** 3365-75.

ANELLI, V., GAULT, C. R., SNIDER, A. J. & OBEID, L. M. 2010. Role of sphingosine kinase-1 in paracrine/transcellular angiogenesis and lymphangiogenesis in vitro. *FASEB J,* 24**,** 2727-38.

AVERY, K., AVERY, S., SHEPHERD, J., HEATH, P. R. & MOORE, H. 2008. Sphingosine-1-phosphate mediates transcriptional regulation of key targets associated with survival, proliferation, and pluripotency in human embryonic stem cells. *Stem Cells Dev,* 17**,** 1195-205.

AZUMA, H., TAKAHARA, S., HORIE, S., et al. 2003. Induction of apoptosis in human bladder cancer cells in vitro and in vivo caused by FTY720 treatment. *J Urol,* 169**,** 2372-7.

AZUMA, H., TAKAHARA, S., ICHIMARU, N., et al. 2002. Marked Prevention of Tumor Growth and Metastasis by a Novel Immunosuppressive Agent, FTY720, in Mouse Breast Cancer Models. *Cancer Research,* 62**,** 1410-1419.

BARAN, Y., SALAS, A., SENKAL, C. E., et al. 2007. Alterations of ceramide/sphingosine 1-phosphate rheostat involved in the regulation of resistance to imatinib-induced apoptosis in K562 human chronic myeloid leukemia cells. *J Biol Chem,* 282**,** 10922-34.

BASSO, K. & DALLA-FAVERA, R. 2010. BCL6: master regulator of the germinal center reaction and key oncogene in B cell lymphomagenesis. *Adv Immunol,* 105**,** 193-210.

BASSO, K. & DALLA-FAVERA, R. 2012. Roles of BCL6 in normal and transformed germinal center B cells. *Immunol Rev,* 247**,** 172-83.

BAYERL, M. G., BRUGGEMAN, R. D., CONROY, E. J., et al. 2008. Sphingosine kinase 1 protein and mRNA are overexpressed in non-Hodgkin lymphomas and are attractive targets for novel pharmacological interventions. *Leukemia & Lymphoma,* 49**,** 948-954.

BAZAN, J. F., BACON, K. B., HARDIMAN, G., et al. 1997. A new class of membrane-bound chemokine with a CX3C motif. *Nature,* 385**,** 640-4.

BEGUELIN, W., POPOVIC, R., TEATER, M., et al. 2013. EZH2 is required for germinal center formation and somatic EZH2 mutations promote lymphoid transformation. *Cancer Cell,* 23**,** 677-92.

BRINKMANN, V. 2007. Sphingosine 1-phosphate receptors in health and disease: mechanistic insights from gene deletion studies and reverse pharmacology. *Pharmacol Ther,* 115**,** 84-105.

BRINKMANN, V., BILLICH, A., BAUMRUKER, T., et al. 2010. Fingolimod (FTY720): discovery and development of an oral drug to treat multiple sclerosis. *Nat Rev Drug Discov,* 9**,** 883-97.

BRIONES, J., TIMMERMAN, J. & LEVY, R. 2002. In vivo antitumor effect of CD40L-transduced tumor cells as a vaccine for B-cell lymphoma. *Cancer Res,* 62**,** 3195-9.

BRUNE, V., TIACCI, E., PFEIL, I., et al. 2008. Origin and pathogenesis of nodular lymphocyte–predominant Hodgkin lymphoma as revealed by global gene expression analysis. *The Journal of Experimental Medicine,* 205**,** 2251-2268.

BURGER, J. A. & KIPPS, T. J. 2006. CXCR4: a key receptor in the crosstalk between tumor cells and their microenvironment. *Blood,* 107**,** 1761-7.

CAGANOVA, M., CARRISI, C., VARANO, G., et al. 2013. Germinal center dysregulation by histone methyltransferase EZH2 promotes lymphomagenesis. *J Clin Invest,* 123**,** 5009-22.

CARDESA-SALZMANN, T. M., COLOMO, L., GUTIERREZ, G., et al. 2011. High microvessel density determines a poor outcome in patients with diffuse large B-cell lymphoma treated with rituximab plus chemotherapy. *Haematologica,* 96**,** 996-1001.

CARE, M. A., WESTHEAD, D. R. & TOOZE, R. M. 2015. Gene expression meta-analysis reveals immune response convergence on the IFNgamma-STAT1-IRF1 axis and adaptive immune resistance mechanisms in lymphoma. *Genome Med,* 7**,** 15-218.

CARMELIET, P. & JAIN, R. K. 2000. Angiogenesis in cancer and other diseases. *Nature,* 407**,** 249-57.

CATTORETTI, G., MANDELBAUM, J., LEE, N., et al. 2009. Targeted Disruption of the S1P2 Sphingosine 1-Phosphate Receptor Gene Leads to Diffuse Large B-Cell Lymphoma Formation. *Cancer Research,* 69**,** 8686-8692.

CHAE, S. S., PAIK, J. H., FURNEAUX, H. & HLA, T. 2004. Requirement for sphingosine 1-phosphate receptor-1 in tumor angiogenesis demonstrated by in vivo RNA interference. *J Clin Invest,* 114**,** 1082-9.

CHAISE, C., ITTI, E., PETEGNIEF, Y., et al. 2007. [F-18]-Fluoro-2-deoxy-D: -glucose positron emission tomography as a tool for early detection of immunotherapy response in a murine B cell lymphoma model. *Cancer Immunol Immunother,* 56**,** 1163-71.

CHENG, Q., MA, S., LIN, D., et al. 2015. The S1P1 receptor-selective agonist CYM-5442 reduces the severity of acute GVHD by inhibiting macrophage recruitment. *Cell Mol Immunol,* 12**,** 681-91.

CHIBA, K., YANAGAWA, Y., MASUBUCHI, Y., et al. 1998. FTY720, a novel immunosuppressant, induces sequestration of circulating mature lymphocytes by acceleration of lymphocyte homing in rats. I. FTY720 selectively decreases the number of circulating mature lymphocytes by acceleration of lymphocyte homing. *J Immunol,* 160**,** 5037-44.

CHUA, C.-W., LEE, D. T.-W., LING, M.-T., et al. 2005. FTY720, a fungus metabolite, inhibits in vivo growth of androgen-independent prostate cancer. *International Journal of Cancer,* 117**,** 1039-1048.

CHUN, J. 2013. *Lysophospholipid receptors : signaling and biochemistry,* Hoboken, N.J., Wiley.

CHUN, J., HLA, T., LYNCH, K. R., SPIEGEL, S. & MOOLENAAR, W. H. 2010. International Union of Basic and Clinical Pharmacology. LXXVIII. Lysophospholipid receptor nomenclature. *Pharmacol Rev,* 62**,** 579-87.

COIFFIER, B., LEPAGE, E., BRIÈRE, J., et al. 2002. CHOP Chemotherapy plus Rituximab Compared with CHOP Alone in Elderly Patients with Diffuse Large-B-Cell Lymphoma. *New England Journal of Medicine,* 346**,** 235-242.

COIFFIER, B., THIEBLEMONT, C., VAN DEN NESTE, E., et al. 2010. Long-term outcome of patients in the LNH-98.5 trial, the first randomized study comparing rituximab-CHOP to standard CHOP chemotherapy in DLBCL patients: a study by the Groupe d'Etudes des Lymphomes de l'Adulte. *Blood,* 116**,** 2040-5.

COMPAGNO, M., LIM, W. K., GRUNN, A., et al. 2009. Mutations of multiple genes cause deregulation of NF-[kgr]B in diffuse large B-cell lymphoma. *Nature,* 459**,** 717-721.

CRUK. 2013. *Different types of non hodgkin lymphoma* [Online]. Available: Available from: http://www.cancerresearchuk.org/about-cancer/type/non-hodgkins-lymphoma/about/types/the-most-common-types-of-non-hodgkins-lymphoma [Accessed 9th April 2016].

CUVILLIER, O., ADER, I., BOUQUEREL, P., et al. 2010. Activation of sphingosine kinase-1 in cancer: implications for therapeutic targeting. *Curr Mol Pharmacol,* 3**,** 53-65.

CUVILLIER, O. & LEVADE, T. 2001. Sphingosine 1-phosphate antagonizes apoptosis of human leukemia cells by inhibiting release of cytochrome c and Smac/DIABLO from mitochondria. *Blood,* 98**,** 2828-36.

CUVILLIER, O., PIRIANOV, G., KLEUSER, B., et al. 1996. Suppression of ceramide-mediated programmed cell death by sphingosine-1-phosphate. *Nature,* 381**,** 800-803.

CYSTER, J. G. 2005. Chemokines, sphingosine-1-phosphate, and cell migration in secondary lymphoid organs. *Annu Rev Immunol,* 23**,** 127-59.

CYSTER, J. G. & SCHWAB, S. R. 2012. Sphingosine-1-phosphate and lymphocyte egress from lymphoid organs. *Annu Rev Immunol,* 30**,** 69-94.

DAVIS, R. E., BROWN, K. D., SIEBENLIST, U. & STAUDT, L. M. 2001. Constitutive Nuclear Factor κB Activity Is Required for Survival of Activated B Cell–like Diffuse Large B Cell Lymphoma Cells. *The Journal of Experimental Medicine,* 194**,** 1861-1874.

DAVIS, R. E., NGO, V. N., LENZ, G., et al. 2010. Chronic active B-cell-receptor signalling in diffuse large B-cell lymphoma. *Nature,* 463**,** 88-92.

DENNIS, G., JR., SHERMAN, B. T., HOSACK, D. A., et al. 2003. DAVID: Database for Annotation, Visualization, and Integrated Discovery. *Genome Biol,* 4**,** 3.

DESHMANE, S. L., KREMLEV, S., AMINI, S. & SAWAYA, B. E. 2009. Monocyte Chemoattractant Protein-1 (MCP-1): An Overview. *Journal of Interferon & Cytokine Research,* 29**,** 313-326.

DING, B. B., YU, J. J., YU, R. Y.-L., et al. 2008. Constitutively activated STAT3 promotes cell proliferation and survival in the activated B-cell subtype of diffuse large B-cell lymphomas. *Blood,* 111**,** 1515-1523.

DING, G., SONODA, H., YU, H., et al. 2007. Protein kinase D-mediated phosphorylation and nuclear export of sphingosine kinase 2. *J Biol Chem,* 282**,** 27493-502.

DOIG, T. N., HUME, D. A., THEOCHARIDIS, T., et al. 2013. Coexpression analysis of large cancer datasets provides insight into the cellular phenotypes of the tumour microenvironment. *BMC Genomics,* 14**,** 469.

DORTH, J. A., PROSNITZ, L. R., BROADWATER, G., et al. 2012. Impact of consolidation radiation therapy in stage III-IV diffuse large B-cell lymphoma with negative post-chemotherapy radiologic imaging. *Int J Radiat Oncol Biol Phys,* 84**,** 762-7.

DUDLEY, D. D., CHAUDHURI, J., BASSING, C. H. & ALT, F. W. 2005. Mechanism and control of V(D)J recombination versus class switch recombination: similarities and differences. *Adv Immunol,* 86**,** 43-112.

DUNLEAVY, K., PITTALUGA, S., CZUCZMAN, M. S., et al. 2009. Differential efficacy of bortezomib plus chemotherapy within molecular subtypes of diffuse large B-cell lymphoma. *Blood,* 113**,** 6069-76.

ELPEK, K. G., LACELLE, C., SINGH, N. P., YOLCU, E. S. & SHIRWAN, H. 2007. CD4+CD25+ T regulatory cells dominate multiple immune evasion mechanisms in early but not late phases of tumor development in a B cell lymphoma model. *J Immunol,* 178**,** 6840-8.

ENDO, K., IGARASHI, Y., NISAR, M., ZHOU, Q. H. & HAKOMORI, S. 1991. Cell membrane signaling as target in cancer therapy: inhibitory effect of N,N-dimethyl and N,N,N-trimethyl sphingosine derivatives on in vitro and in vivo growth of human tumor cells in nude mice. *Cancer Res,* 51**,** 1613-8.

ENGLISH, D., KOVALA, A. T., WELCH, Z., et al. 1999. Induction of endothelial cell chemotaxis by sphingosine 1-phosphate and stabilization of endothelial monolayer barrier function by lysophosphatidic acid, potential mediators of hematopoietic angiogenesis. *J Hematother Stem Cell Res,* 8**,** 627-34.

ESTRADA, R., ZENG, Q., LU, H., et al. 2008. Up-regulating sphingosine 1-phosphate receptor-2 signaling impairs chemotactic, wound-healing, and morphogenetic responses in senescent endothelial cells. *J Biol Chem,* 283**,** 30363-75.

ETZIONI, A. 1996. Adhesion Molecules-Their Role in Health and Disease. *Pediatr Res,* 39**,** 191-198.

FISHER , R. I., GAYNOR , E. R., DAHLBERG , S., et al. 1993. Comparison of a Standard Regimen (CHOP) with Three Intensive Chemotherapy Regimens for Advanced Non-Hodgkin's Lymphoma. *New England Journal of Medicine,* 328**,** 1002-1006.

FOLKMAN, J. 1971. Tumor Angiogenesis: Therapeutic Implications. *New England Journal of Medicine,* 285**,** 1182-1186.

FRENCH, K. J., SCHRECENGOST, R. S., LEE, B. D., et al. 2003. Discovery and Evaluation of Inhibitors of Human Sphingosine Kinase. *Cancer Research,* 63**,** 5962-5969.

FRIEDBERG, J. W. 2011. Relapsed/refractory diffuse large B-cell lymphoma. *Hematology Am Soc Hematol Educ Program,* 2011**,** 498-505.

FUGMANN S, L. A., SHOCKETT P, VILLEY I, AND SCHATZ D 2000. The RAG Proteins and V(D)J Recombination: Complexes, Ends, and Transposition. *Annual Review of Immunology,* 18**,** 495-527.

FURMAN , R. R., SHARMAN , J. P., COUTRE , S. E., et al. 2014. Idelalisib and Rituximab in Relapsed Chronic Lymphocytic Leukemia. *New England Journal of Medicine,* 370**,** 997-1007.

GANJOO, K. N., AN, C. S., ROBERTSON, M. J., et al. 2006. Rituximab, bevacizumab and CHOP (RA-CHOP) in untreated diffuse large B-cell lymphoma: safety, biomarker and pharmacokinetic analysis. *Leuk Lymphoma,* 47**,** 998-1005.

GEARHART, P. J. & BOGENHAGEN, D. F. 1983. Clusters of point mutations are found exclusively around rearranged antibody variable genes. *Proc Natl Acad Sci U S A,* 80**,** 3439-43.

GEISER, T., DEWALD, B., EHRENGRUBER, M. U., CLARK-LEWIS, I. & BAGGIOLINI, M. 1993. The interleukin-8-related chemotactic cytokines GRO alpha, GRO beta, and GRO gamma activate human neutrophil and basophil leukocytes. *J Biol Chem,* 268**,** 15419-24.

GERSZTEN, R. E., GARCIA-ZEPEDA, E. A., LIM, Y. C., et al. 1999. MCP-1 and IL-8 trigger firm adhesion of monocytes to vascular endothelium under flow conditions. *Nature,* 398**,** 718-23.

GLICKMAN, M., MALEK, R. L., KWITEK-BLACK, A. E., JACOB, H. J. & LEE, N. H. 1999. Molecular cloning, tissue-specific expression, and chromosomal localization of a novel nerve growth factor-regulated G-protein- coupled receptor, nrg-1. *Mol Cell Neurosci,* 14**,** 141-52.

GOETZL, E. J., WANG, W., MCGIFFERT, C., HUANG, M. C. & GRALER, M. H. 2004. Sphingosine 1-phosphate and its G protein-coupled receptors constitute a multifunctional immunoregulatory system. *J Cell Biochem,* 92**,** 1104-14.

GONDA, K., OKAMOTO, H., TAKUWA, N., et al. 1999. The novel sphingosine 1-phosphate receptor AGR16 is coupled via pertussis toxin-sensitive and -insensitive G-proteins to multiple signalling pathways. *Biochem J,* 337 (Pt 1)**,** 67-75.

GOOSSENS, T., KLEIN, U. & KÜPPERS, R. 1998. Frequent occurrence of deletions and duplications during somatic hypermutation: Implications for oncogene translocations and heavy chain disease. *Proceedings of the National Academy of Sciences,* 95**,** 2463-2468.

GOPAL , A. K., KAHL , B. S., DE VOS , S., et al. 2014. PI3Kδ Inhibition by Idelalisib in Patients with Relapsed Indolent Lymphoma. *New England Journal of Medicine,* 370**,** 1008-1018.

GORDON, S. & TAYLOR, P. R. 2005. Monocyte and macrophage heterogeneity. *Nat Rev Immunol,* 5**,** 953-964.

GRALER, M. H. & GOETZL, E. J. 2004. The immunosuppressant FTY720 down-regulates sphingosine 1-phosphate G-protein-coupled receptors. *FASEB J,* 18**,** 551-3.

GRATZINGER, D., ZHAO, S., TIBSHIRANI, R. J., et al. 2008. Prognostic significance of VEGF, VEGF receptors, and microvessel density in diffuse large B cell lymphoma treated with anthracycline-based chemotherapy. *Lab Invest,* 88**,** 38-47.

GREEN, J. A. & CYSTER, J. G. 2012. S1PR2 links germinal center confinement and growth regulation. *Immunol Rev,* 247**,** 36-51.

GREEN, T. M., YOUNG, K. H., VISCO, C., et al. 2012. Immunohistochemical double-hit score is a strong predictor of outcome in patients with diffuse large B-cell lymphoma treated with rituximab plus cyclophosphamide, doxorubicin, vincristine, and prednisone. *J Clin Oncol,* 30**,** 3460-7.

GUILLERMET-GUIBERT, J., DAVENNE, L., PCHEJETSKI, D., et al. 2009. Targeting the sphingolipid metabolism to defeat pancreatic cancer cell resistance to the chemotherapeutic gemcitabine drug. *Mol Cancer Ther,* 8**,** 809-20.

HABERMANN, T. M., WELLER, E. A., MORRISON, V. A., et al. 2006. Rituximab-CHOP versus CHOP alone or with maintenance rituximab in older patients with diffuse large B-cell lymphoma. *J Clin Oncol,* 24**,** 3121-7.

HAIT, N. C., ALLEGOOD, J., MACEYKA, M., et al. 2009. Regulation of histone acetylation in the nucleus by sphingosine-1-phosphate. *Science,* 325**,** 1254-7.

HAIT, N. C., BELLAMY, A., MILSTIEN, S., KORDULA, T. & SPIEGEL, S. 2007. Sphingosine kinase type 2 activation by ERK-mediated phosphorylation. *J Biol Chem,* 282**,** 12058-65.

HANNUN, Y. A. & OBEID, L. M. 2008. Principles of bioactive lipid signalling: lessons from sphingolipids. *Nat Rev Mol Cell Biol,* 9**,** 139-50.

HANS, C. P., WEISENBURGER, D. D., GREINER, T. C., et al. 2004. Confirmation of the molecular classification of diffuse large B-cell lymphoma by immunohistochemistry using a tissue microarray. *Blood,* 103**,** 275-282.

HARADA, A., SEKIDO, N., AKAHOSHI, T., et al. 1994. Essential involvement of interleukin-8 (IL-8) in acute inflammation. *J Leukoc Biol,* 56**,** 559-64.

HEFFERNAN-STROUD, L. A., HELKE, K. L., JENKINS, R. W., et al. 2012. Defining a role for sphingosine kinase 1 in p53-dependent tumors. *Oncogene,* 31**,** 1166-75.

HEINRICH, M., WICKEL, M., WINOTO-MORBACH, S., et al. 2000. Ceramide as an activator lipid of cathepsin D. *Adv Exp Med Biol,* 477**,** 305-15.

HELD, G., MURAWSKI, N., ZIEPERT, M., et al. 2014. Role of radiotherapy to bulky disease in elderly patients with aggressive B-cell lymphoma. *J Clin Oncol,* 32**,** 1112-8.

HISANO, N., YATOMI, Y., SATOH, K., et al. 1999. Induction and suppression of endothelial cell apoptosis by sphingolipids: a possible in vitro model for cell-cell interactions between platelets and endothelial cells. *Blood,* 93**,** 4293-9.

HISANO, Y., KOBAYASHI, N., KAWAHARA, A., YAMAGUCHI, A. & NISHI, T. 2011. The sphingosine 1-phosphate transporter, SPNS2, functions as a transporter of the phosphorylated form of the immunomodulating agent FTY720. *J Biol Chem,* 286**,** 1758-66.

HITZ, F., CONNORS, J. M., GASCOYNE, R. D., et al. 2015. Outcome of patients with primary refractory diffuse large B cell lymphoma after R-CHOP treatment. *Ann Hematol,* 94**,** 1839-43.

HLA, T. & MACIAG, T. 1990. An abundant transcript induced in differentiating human endothelial cells encodes a polypeptide with structural similarities to G-protein-coupled receptors. *Journal of Biological Chemistry,* 265**,** 9308-9313.

HMRN. 2016. *HMRN Survival Diffuse large B-cell lymphoma* [Online]. Available: https://www.hmrn.org/statistics/survival [Accessed 10/08/2016].

HO, J. W., MAN, K., SUN, C. K., et al. 2005. Effects of a novel immunomodulating agent, FTY720, on tumor growth and angiogenesis in hepatocellular carcinoma. *Mol Cancer Ther,* 4**,** 1430-8.

HORDIJK, P. L. 2016. Recent insights into endothelial control of leukocyte extravasation. *Cell Mol Life Sci,* 73**,** 1591-608.

HU, S., XU-MONETTE, Z. Y., TZANKOV, A., et al. 2013. MYC/BCL2 protein coexpression contributes to the inferior survival of activated B-cell subtype of diffuse large B-cell lymphoma and demonstrates high-risk gene expression signatures: a report from The International DLBCL Rituximab-CHOP Consortium Program. *Blood,* 121**,** 4021-31; quiz 4250.

IGARASHI, N., OKADA, T., HAYASHI, S., et al. 2003. Sphingosine kinase 2 is a nuclear protein and inhibits DNA synthesis. *J Biol Chem,* 278**,** 46832-9.

IQBAL, J., MEYER, P. N., SMITH, L. M., et al. 2011. BCL2 predicts survival in germinal center B-cell-like diffuse large B-cell lymphoma treated with CHOP-like therapy and rituximab. *Clin Cancer Res,* 17**,** 7785-95.

ISHII, I., FUKUSHIMA, N., YE, X. & CHUN, J. 2004. Lysophospholipid receptors: signaling and biology. *Annu Rev Biochem,* 73**,** 321-54.

JAFFE, E. A., NACHMAN, R. L., BECKER, C. G. & MINICK, C. R. 1973. Culture of human endothelial cells derived from umbilical veins. Identification by morphologic and immunologic criteria. *J Clin Invest,* 52**,** 2745-56.

JARMAN, K. E., MORETTI, P. A., ZEBOL, J. R. & PITSON, S. M. 2010. Translocation of sphingosine kinase 1 to the plasma membrane is mediated by calcium- and integrin-binding protein 1. *J Biol Chem,* 285**,** 483-92.

JOHNSON, K. R., JOHNSON, K. Y., CRELLIN, H. G., et al. 2005. Immunohistochemical distribution of sphingosine kinase 1 in normal and tumor lung tissue. *J Histochem Cytochem,* 53**,** 1159-66.

JOHNSON, N. A., SLACK, G. W., SAVAGE, K. J., et al. 2012. Concurrent expression of MYC and BCL2 in diffuse large B-cell lymphoma treated with rituximab plus cyclophosphamide, doxorubicin, vincristine, and prednisone. *J Clin Oncol,* 30**,** 3452-9.

JORGENSEN, J. M., SORENSEN, F. B., BENDIX, K., et al. 2007. Angiogenesis in non-Hodgkin's lymphoma: clinico-pathological correlations and prognostic significance in specific subtypes. *Leuk Lymphoma,* 48**,** 584-95.

KAPITONOV, D., ALLEGOOD, J. C., MITCHELL, C., et al. 2009. Targeting sphingosine kinase 1 inhibits Akt signaling, induces apoptosis, and suppresses growth of human glioblastoma cells and xenografts. *Cancer Res,* 69**,** 6915-23.

KAPPOS, L., ANTEL, J., COMI, G., et al. 2006. Oral fingolimod (FTY720) for relapsing multiple sclerosis. *N Engl J Med,* 355**,** 1124-40.

KAWAMORI, T., KANESHIRO, T., OKUMURA, M., et al. 2009. Role for sphingosine kinase 1 in colon carcinogenesis. *FASEB J,* 23**,** 405-14.

KEDDERIS, L. B., BOZIGIAN, H. P., KLEEMAN, J. M., et al. 1995. Toxicity of the protein kinase C inhibitor safingol administered alone and in combination with chemotherapeutic agents. *Fundam Appl Toxicol,* 25**,** 201-17.

KLEIN, U., CASOLA, S., CATTORETTI, G., et al. 2006. Transcription factor IRF4 controls plasma cell differentiation and class-switch recombination. *Nat Immunol,* 7**,** 773-782.

KLEIN, U. & DALLA-FAVERA, R. 2008. Germinal centres: role in B-cell physiology and malignancy. *Nat Rev Immunol,* 8**,** 22-33.

KOBAYASHI, H., BOELTE, K. C. & LIN, P. C. 2007. Endothelial cell adhesion molecules and cancer progression. *Curr Med Chem,* 14**,** 377-86.

KOCKS, C. & RAJEWSKY, K. 1989. Stable expression and somatic hypermutation of antibody V regions in B-cell developmental pathways. *Annu Rev Immunol,* 7**,** 537-59.

KOHAMA, T., OLIVERA, A., EDSALL, L., et al. 1998. Molecular Cloning and Functional Characterization of Murine Sphingosine Kinase. *Journal of Biological Chemistry,* 273**,** 23722-23728.

KRITHARIS, A., COYLE, M., SHARMA, J. & EVENS, A. M. 2015. Lenalidomide in non-Hodgkin lymphoma: biological perspectives and therapeutic opportunities. *Blood,* 125**,** 2471-2476.

KWON, Y. G., MIN, J. K., KIM, K. M., et al. 2001. Sphingosine 1-phosphate protects human umbilical vein endothelial cells from serum-deprived apoptosis by nitric oxide production. *J Biol Chem,* 276**,** 10627-33.

LAMONTAGNE, K., LITTLEWOOD-EVANS, A., SCHNELL, C., et al. 2006. Antagonism of sphingosine-1-phosphate receptors by FTY720 inhibits angiogenesis and tumor vascularization. *Cancer Res,* 66**,** 221-31.

LEE, H., DENG, J., KUJAWSKI, M., et al. 2010. STAT3-induced S1PR1 expression is crucial for persistent STAT3 activation in tumors. *Nat Med,* 16**,** 1421-1428.

LEE, O. H., KIM, Y. M., LEE, Y. M., et al. 1999. Sphingosine 1-phosphate induces angiogenesis: its angiogenic action and signaling mechanism in human umbilical vein endothelial cells. *Biochem Biophys Res Commun,* 264**,** 743-50.

LENZ, G., DAVIS, R. E., NGO, V. N., et al. 2008a. Oncogenic CARD11 Mutations in Human Diffuse Large B Cell Lymphoma. *Science,* 319**,** 1676-1679.

LENZ, G., WRIGHT, G., DAVE, S. S., et al. 2008b. Stromal Gene Signatures in Large-B-Cell Lymphomas. *New England Journal of Medicine,* 359**,** 2313-2323.

LENZ, G., WRIGHT, G. W., EMRE, N. C. T., et al. 2008c. Molecular subtypes of diffuse large B-cell lymphoma arise by distinct genetic pathways. *Proceedings of the National Academy of Sciences,* 105**,** 13520-13525.

LI, J., GUAN, H.-Y., GONG, L.-Y., et al. 2008a. Clinical Significance of Sphingosine Kinase-1 Expression in Human Astrocytomas Progression and Overall Patient Survival. *Clinical Cancer Research,* 14**,** 6996-7003.

LI, J., GUAN, H. Y., GONG, L. Y., et al. 2008b. Clinical significance of sphingosine kinase-1 expression in human astrocytomas progression and overall patient survival. *Clin Cancer Res,* 14**,** 6996-7003.

LI, Q. F., WU, C. T., GUO, Q., WANG, H. & WANG, L. S. 2008c. Sphingosine 1-phosphate induces Mcl-1 upregulation and protects multiple myeloma cells against apoptosis. *Biochem Biophys Res Commun,* 371**,** 159-62.

LI, W., YU, C.-P., XIA, J.-T., et al. 2009. Sphingosine Kinase 1 Is Associated with Gastric Cancer Progression and Poor Survival of Patients. *Clinical Cancer Research,* 15**,** 1393-1399.

LIAO, Y., SMYTH, G. K. & SHI, W. 2013. The Subread aligner: fast, accurate and scalable read mapping by seed-and-vote. *Nucleic Acids Res,* 41**,** e108.

LIN, C.-I., CHEN, C.-N., LIN, P.-W. & LEE, H. 2007. Sphingosine 1-phosphate regulates inflammation-related genes in human endothelial cells through S1P1 and S1P3. *Biochemical and Biophysical Research Communications,* 355**,** 895-901.

LIN, C. I., CHEN, C. N., CHEN, J. H. & LEE, H. 2006. Lysophospholipids increase IL-8 and MCP-1 expressions in human umbilical cord vein endothelial cells through an IL-1-dependent mechanism. *J Cell Biochem,* 99**,** 1216-32.

LIU, H., SUGIURA, M., NAVA, V. E., et al. 2000a. Molecular Cloning and Functional Characterization of a Novel Mammalian Sphingosine Kinase Type 2 Isoform. *Journal of Biological Chemistry,* 275**,** 19513-19520.

LIU, H., TOMAN, R. E., GOPARAJU, S. K., et al. 2003. Sphingosine kinase type 2 is a putative BH3-only protein that induces apoptosis. *J Biol Chem,* 278**,** 40330-6.

LIU, Y., DENG, J., WANG, L., et al. 2012. S1PR1 is an effective target to block STAT3 signaling in activated B cell–like diffuse large B-cell lymphoma. *Blood,* 120**,** 1458-1465.

LIU, Y., WADA, R., YAMASHITA, T., et al. 2000b. Edg-1, the G protein–coupled receptor for sphingosine-1-phosphate, is essential for vascular maturation. *The Journal of Clinical Investigation,* 106**,** 951-961.

LIVAK, K. J. & SCHMITTGEN, T. D. 2001. Analysis of Relative Gene Expression Data Using Real-Time Quantitative PCR and the 2−ΔΔCT Method. *Methods,* 25**,** 402-408.

MACEYKA, M., HARIKUMAR, K. B., MILSTIEN, S. & SPIEGEL, S. 2012. Sphingosine-1-phosphate signaling and its role in disease. *Trends in Cell Biology,* 22**,** 50-60.

MACEYKA, M., PAYNE, S. G., MILSTIEN, S. & SPIEGEL, S. 2002. Sphingosine kinase, sphingosine-1-phosphate, and apoptosis. *Biochim Biophys Acta,* 1585**,** 193-201.

MACEYKA, M., SANKALA, H., HAIT, N. C., et al. 2005. SphK1 and SphK2, sphingosine kinase isoenzymes with opposing functions in sphingolipid metabolism. *J Biol Chem,* 280**,** 37118-29.

MACLENNAN 1994. Germinal Centers. *Annual Review of Immunology,* 12**,** 117-139.

MALEK, R. L., TOMAN, R. E., EDSALL, L. C., et al. 2001. Nrg-1 belongs to the endothelial differentiation gene family of G protein-coupled sphingosine-1-phosphate receptors. *J Biol Chem,* 276**,** 5692-9.

MANDALA, S., HAJDU, R., BERGSTROM, J., et al. 2002. Alteration of lymphocyte trafficking by sphingosine-1-phosphate receptor agonists. *Science,* 296**,** 346-9.

MARCHESI, F., CIRILLO, M., BIANCHI, A., et al. 2015. High density of CD68+/CD163+ tumour-associated macrophages (M2-TAM) at diagnosis is significantly correlated to unfavorable prognostic factors and to poor clinical outcomes in patients with diffuse large B-cell lymphoma. *Hematol Oncol,* 33**,** 110-2.

MASIERO, M., SIMOES, F. C., HAN, H. D., et al. 2013. A core human primary tumor angiogenesis signature identifies the endothelial orphan receptor ELTD1 as a key regulator of angiogenesis. *Cancer Cell,* 24**,** 229-41.

MATLOUBIAN, M., LO, C. G., CINAMON, G., et al. 2004. Lymphocyte egress from thymus and peripheral lymphoid organs is dependent on S1P receptor 1. *Nature,* 427**,** 355-60.

MEYER, P. N., FU, K., GREINER, T. C., et al. 2011. Immunohistochemical methods for predicting cell of origin and survival in patients with diffuse large B-cell lymphoma treated with rituximab. *J Clin Oncol,* 29**,** 200-7.

MITRA, P., OSKERITZIAN, C. A., PAYNE, S. G., et al. 2006. Role of ABCC1 in export of sphingosine-1-phosphate from mast cells. *Proc Natl Acad Sci U S A,* 103**,** 16394-9.

MIZUGISHI, K., YAMASHITA, T., OLIVERA, A., et al. 2005. Essential role for sphingosine kinases in neural and vascular development. *Mol Cell Biol,* 25**,** 11113-21.

MORIN, R. D., JOHNSON, N. A., SEVERSON, T. M., et al. 2010. Somatic mutations altering EZH2 (Tyr641) in follicular and diffuse large B-cell lymphomas of germinal-center origin. *Nat Genet,* 42**,** 181-185.

MORIN, R. D., MENDEZ-LAGO, M., MUNGALL, A. J., et al. 2011. Frequent mutation of histone-modifying genes in non-Hodgkin lymphoma. *Nature,* 476**,** 298-303.

MORIN, R. D., MUNGALL, K., PLEASANCE, E., et al. 2013. Mutational and structural analysis of diffuse large B-cell lymphoma using whole-genome sequencing. *Blood,* 122**,** 1256-65.

MOSER, B., CLARK-LEWIS, I., ZWAHLEN, R. & BAGGIOLINI, M. 1990. Neutrophil-activating properties of the melanoma growth-stimulatory activity. *J Exp Med,* 171**,** 1797-802.

MULLER, W. A. 2013. Getting leukocytes to the site of inflammation. *Vet Pathol,* 50**,** 7-22.

MURAMATSU, M., KINOSHITA, K., FAGARASAN, S., et al. 2000. Class Switch Recombination and Hypermutation Require Activation-Induced Cytidine Deaminase (AID), a Potential RNA Editing Enzyme. *Cell,* 102**,** 553-563.

MURATA, N., SATO, K., KON, J., et al. 2000. Interaction of sphingosine 1-phosphate with plasma components, including lipoproteins, regulates the lipid receptor-mediated actions. *Biochem J,* 352 Pt 3**,** 809-15.

MURDOCH, C., MUTHANA, M., COFFELT, S. B. & LEWIS, C. E. 2008. The role of myeloid cells in the promotion of tumour angiogenesis. *Nat Rev Cancer,* 8**,** 618-31.

NAGAHASHI, M., RAMACHANDRAN, S., KIM, E. Y., et al. 2012. Sphingosine-1-phosphate produced by sphingosine kinase 1 promotes breast cancer progression by stimulating angiogenesis and lymphangiogenesis. *Cancer Res,* 72**,** 726-35.

NAVA, V. E., CUVILLIER, O., EDSALL, L. C., et al. 2000. Sphingosine enhances apoptosis of radiation-resistant prostate cancer cells. *Cancer Res,* 60**,** 4468-74.

NGO, V. N., YOUNG, R. M., SCHMITZ, R., et al. 2011. Oncogenically active MYD88 mutations in human lymphoma. *Nature,* 470**,** 115-9.

NIU, H., YE, B. H. & DALLA-FAVERA, R. 1998. Antigen receptor signaling induces MAP kinase-mediated phosphorylation and degradation of the BCL-6 transcription factor. *Genes & Development,* 12**,** 1953-1961.

NOURSHARGH, S. & ALON, R. 2014. Leukocyte migration into inflamed tissues. *Immunity,* 41**,** 694-707.

NOVELLI, S., BRIONES, J. & SIERRA, J. 2013. Epidemiology of lymphoid malignancies: last decade update. *SpringerPlus,* 2**,** 70.

NOWAKOWSKI, G. S., LAPLANT, B., HABERMANN, T. M., et al. 2011. Lenalidomide can be safely combined with R-CHOP (R2CHOP) in the initial chemotherapy for aggressive B-cell lymphomas: phase I study. *Leukemia,* 25**,** 1877-81.

NOWAKOWSKI, G. S., LAPLANT, B., MACON, W. R., et al. 2015. Lenalidomide combined with R-CHOP overcomes negative prognostic impact of non-germinal center B-cell phenotype in newly diagnosed diffuse large B-Cell lymphoma: a phase II study. *J Clin Oncol,* 33**,** 251-7.

O'BRIEN, N., JONES, S. T., WILLIAMS, D. G., et al. 2009. Production and characterization of monoclonal anti-sphingosine-1-phosphate antibodies. *Journal of Lipid Research,* 50**,** 2245-2257.

OBEID, L. M., LINARDIC, C. M., KAROLAK, L. A. & HANNUN, Y. A. 1993. Programmed cell death induced by ceramide. *Science,* 259**,** 1769-71.

OGRETMEN, B. & HANNUN, Y. A. 2001. Updates on functions of ceramide in chemotherapy-induced cell death and in multidrug resistance. *Drug Resistance Updates,* 4**,** 368-377.

OKAMOTO, H., TAKUWA, N., GONDA, K., et al. 1998. EDG1 is a functional sphingosine-1-phosphate receptor that is linked via a Gi/o to multiple signaling pathways, including phospholipase C activation, Ca2+ mobilization, Ras-mitogen-activated protein kinase activation, and adenylate cyclase inhibition. *J Biol Chem,* 273**,** 27104-10.

OKAMOTO, H., TAKUWA, N., YATOMI, Y., et al. 1999. EDG3 is a functional receptor specific for sphingosine 1-phosphate and sphingosylphosphorylcholine with signaling characteristics distinct from EDG1 and AGR16. *Biochem Biophys Res Commun,* 260**,** 203-8.

OKAMOTO, H., TAKUWA, N., YOKOMIZO, T., et al. 2000. Inhibitory Regulation of Rac Activation, Membrane Ruffling, and Cell Migration by the G Protein-Coupled Sphingosine-1-Phosphate Receptor EDG5 but Not EDG1 or EDG3. *Molecular and Cellular Biology,* 20**,** 9247-9261.

OKAZAKI, H., ISHIZAKA, N., SAKURAI, T., et al. 1993. Molecular cloning of a novel putative G protein-coupled receptor expressed in the cardiovascular system. *Biochem Biophys Res Commun,* 190**,** 1104-9.

OKOSHI, H., HAKOMORI, S., NISAR, M., et al. 1991. Cell membrane signaling as target in cancer therapy. II: Inhibitory effect of N,N,N-trimethylsphingosine on metastatic potential of

murine B16 melanoma cell line through blocking of tumor cell-dependent platelet aggregation. *Cancer Res,* 51**,** 6019-24.

PACKARD, T. A. & CAMBIER, J. C. 2013. B lymphocyte antigen receptor signaling: initiation, amplification, and regulation. *F1000Prime Rep,* 5**,** 40.

PALMER, C., DIEHN, M., ALIZADEH, A. A. & BROWN, P. O. 2006. Cell-type specific gene expression profiles of leukocytes in human peripheral blood. *BMC Genomics,* 7**,** 115.

PAPPU, R., SCHWAB, S. R., CORNELISSEN, I., et al. 2007. Promotion of lymphocyte egress into blood and lymph by distinct sources of sphingosine-1-phosphate. *Science,* 316**,** 295-8.

PARK, K. S., KIM, M. K., LEE, H. Y., et al. 2007. S1P stimulates chemotactic migration and invasion in OVCAR3 ovarian cancer cells. *Biochem Biophys Res Commun,* 356**,** 239-44.

PCHEJETSKI, D., GOLZIO, M., BONHOURE, E., et al. 2005. Sphingosine Kinase-1 as a Chemotherapy Sensor in Prostate Adenocarcinoma Cell and Mouse Models. *Cancer Research,* 65**,** 11667-11675.

PERRY, A. M., ALVARADO-BERNAL, Y., LAURINI, J. A., et al. 2014. MYC and BCL2 protein expression predicts survival in patients with diffuse large B-cell lymphoma treated with rituximab. *British Journal of Haematology,* 165**,** 382-391.

PFEIFER, M., GRAU, M., LENZE, D., et al. 2013. PTEN loss defines a PI3K/AKT pathway-dependent germinal center subtype of diffuse large B-cell lymphoma. *Proc Natl Acad Sci U S A,* 110**,** 12420-5.

PFREUNDSCHUH, M., SCHUBERT, J., ZIEPERT, M., et al. 2008. Six versus eight cycles of bi-weekly CHOP-14 with or without rituximab in elderly patients with aggressive CD20+ B-cell lymphomas: a randomised controlled trial (RICOVER-60). *Lancet Oncol,* 9**,** 105-16.

PFREUNDSCHUH, M., TRUMPER, L., OSTERBORG, A., et al. 2006. CHOP-like chemotherapy plus rituximab versus CHOP-like chemotherapy alone in young patients with good-prognosis diffuse large-B-cell lymphoma: a randomised controlled trial by the MabThera International Trial (MInT) Group. *Lancet Oncol,* 7**,** 379-91.

PHAN, J., MAZLOOM, A., MEDEIROS, L. J., et al. 2010. Benefit of consolidative radiation therapy in patients with diffuse large B-cell lymphoma treated with R-CHOP chemotherapy. *J Clin Oncol,* 28**,** 4170-6.

PITSON, S. M., MORETTI, P. A., ZEBOL, J. R., et al. 2003a. Activation of sphingosine kinase 1 by ERK1/2-mediated phosphorylation. *EMBO J,* 22**,** 5491-500.

PITSON, S. M., MORETTI, P. A. B., ZEBOL, J. R., et al. 2003b. Activation of sphingosine kinase 1 by ERK1/2-mediated phosphorylation. *The EMBO Journal,* 22**,** 5491-5500.

PITSON, S. M., XIA, P., LECLERCQ, T. M., et al. 2005. Phosphorylation-dependent translocation of sphingosine kinase to the plasma membrane drives its oncogenic signalling. *J Exp Med,* 201**,** 49-54.

PRNEWSWIRE. 2015. *Lpath Reports Results for ASONEP Phase 2a Study in Renal Cell Carcinoma* [Online]. Available: http://www.prnewswire.com/news-releases/lpath-reports-results-for-asonep-phase-2a-study-in-renal-cell-carcinoma-300053872.html [Accessed 08/08/2016].

PROJECT, T. N.-H. S. L. C. 1997. A Clinical Evaluation of the International Lymphoma Study Group Classification of Non-Hodgkin's Lymphoma. *Blood,* 89**,** 3909-3918.

PYNE, F. T., KENG GAT LIM, JACLYN S. LONG, JOANNE EDWARDS AND SUSAN PYNE 2012. Sphingosine 1-phosphate signalling in cancer. *Biochemical Society Transactions* 40**,** 94-100.

PYNE, N. J. & PYNE, S. 2010. Sphingosine 1-phosphate and cancer. *Nat Rev Cancer,* 10**,** 489-503.

PYNE, N. J., TONELLI, F., LIM, K. G., et al. 2012. Sphingosine 1-phosphate signalling in cancer. *Biochem Soc Trans,* 40**,** 94-100.

PYNE, S. & PYNE, N. J. 2000. Sphingosine 1-phosphate signalling in mammalian cells. *Biochem J,* 349**,** 385-402.

QIAN, B. Z. & POLLARD, J. W. 2010. Macrophage diversity enhances tumor progression and metastasis. *Cell,* 141**,** 39-51.

REID, M. D., BASTURK, O., THIRABANJASAK, D., et al. 2011. Tumor-infiltrating neutrophils in pancreatic neoplasia. *Mod Pathol,* 24**,** 1612-9.

RICHARDS, D. M., HETTINGER, J. & FEUERER, M. 2013. Monocytes and macrophages in cancer: development and functions. *Cancer Microenviron,* 6**,** 179-91.

RICKERT, R. C. 2013. New insights into pre-BCR and BCR signalling with relevance to B cell malignancies. *Nat Rev Immunol,* 13**,** 578-91.

RIVERA, R. & CHUN, J. 2008. Biological effects of lysophospholipids. *Rev Physiol Biochem Pharmacol,* 160**,** 25-46.

ROBINSON, M. D., MCCARTHY, D. J. & SMYTH, G. K. 2010. edgeR: a Bioconductor package for differential expression analysis of digital gene expression data. *Bioinformatics,* 26**,** 139-40.

ROSENWALD, A., WRIGHT, G., CHAN, W. C., et al. 2002. The Use of Molecular Profiling to Predict Survival after Chemotherapy for Diffuse Large-B-Cell Lymphoma. *New England Journal of Medicine,* 346**,** 1937-1947.

ROSENWALD, A., WRIGHT, G., LEROY, K., et al. 2003. Molecular Diagnosis of Primary Mediastinal B Cell Lymphoma Identifies a Clinically Favorable Subgroup of Diffuse Large B Cell Lymphoma Related to Hodgkin Lymphoma. *The Journal of Experimental Medicine,* 198**,** 851-862.

ROUSSEAU, H., LANDRY AND HUOT 1997. p38 MAP kinase activation by vascular endothelial growth factor mediates actin reorganization and cell migration in human endothelial cells. *Oncogene,* 15**,** 2169-2177.

RUCKHABERLE, E., RODY, A., ENGELS, K., et al. 2008. Microarray analysis of altered sphingolipid metabolism reveals prognostic significance of sphingosine kinase 1 in breast cancer. *Breast Cancer Res Treat,* 112**,** 41-52.

SABBADINI, R. A. 2011. Sphingosine-1-phosphate antibodies as potential agents in the treatment of cancer and age-related macular degeneration. *Br J Pharmacol,* 162**,** 1225-38.

SAITO, M., GAO, J., BASSO, K., et al. 2007. A Signaling Pathway Mediating Downregulation of BCL6 in Germinal Center B Cells Is Blocked by BCL6 Gene Alterations in B Cell Lymphoma. *Cancer Cell,* 12**,** 280-292.

SANCHEZ, T., ESTRADA-HERNANDEZ, T., PAIK, J. H., et al. 2003. Phosphorylation and action of the immunomodulator FTY720 inhibits vascular endothelial cell growth factor-induced vascular permeability. *J Biol Chem,* 278**,** 47281-90.

SANCHEZ, T., THANGADA, S., WU, M.-T., et al. 2005. PTEN as an effector in the signaling of antimigratory G protein-coupled receptor. *Proceedings of the National Academy of Sciences of the United States of America,* 102**,** 4312-4317.

SANKALA, H. M., HAIT, N. C., PAUGH, S. W., et al. 2007. Involvement of sphingosine kinase 2 in p53-independent induction of p21 by the chemotherapeutic drug doxorubicin. *Cancer Res,* 67**,** 10466-74.

SATO, K., MALCHINKHUU, E., HORIUCHI, Y., et al. 2007. Critical role of ABCA1 transporter in sphingosine 1-phosphate release from astrocytes. *J Neurochem,* 103**,** 2610-9.

SAUER, B., GONSKA, H., MANGGAU, M., et al. 2005. Sphingosine 1-phosphate is involved in cytoprotective actions of calcitriol in human fibroblasts and enhances the intracellular Bcl-2/Bax rheostat. *Pharmazie,* 60**,** 298-304.

SCHAFFHAUSEN, B. S. & ROBERTS, T. M. 2009. Lessons from polyoma middle T antigen on signaling and transformation: A DNA tumor virus contribution to the war on cancer. *Virology,* 384**,** 304-16.

SCHMID, G., GUBA, M., PAPYAN, A., et al. 2005. FTY720 inhibits tumor growth and angiogenesis. *Transplant Proc,* 37**,** 110-1.

SCHUPPEL, M., KURSCHNER, U., KLEUSER, U., SCHAFER-KORTING, M. & KLEUSER, B. 2008. Sphingosine 1-phosphate restrains insulin-mediated keratinocyte proliferation via inhibition of Akt through the S1P2 receptor subtype. *J Invest Dermatol,* 128**,** 1747-56.

SCHWAB, S. R., PEREIRA, J. P., MATLOUBIAN, M., et al. 2005. Lymphocyte sequestration through S1P lyase inhibition and disruption of S1P gradients. *Science,* 309**,** 1735-9.

SCHWALLER, J., SCHNEIDER, P., MHAWECH-FAUCEGLIA, P., et al. 2007. Neutrophil-derived APRIL concentrated in tumor lesions by proteoglycans correlates with human B-cell lymphoma aggressiveness. *Blood,* 109**,** 331-8.

SCHWALM, S., DOLL, F., ROMER, I., et al. 2008. Sphingosine kinase-1 is a hypoxia-regulated gene that stimulates migration of human endothelial cells. *Biochem Biophys Res Commun,* 368**,** 1020-5.

SCHWICKERT, T. A., LINDQUIST, R. L., SHAKHAR, G., et al. 2007. In vivo imaging of germinal centres reveals a dynamic open structure. *Nature,* 446**,** 83-87.

SCOTT, D. W. & GASCOYNE, R. D. 2014. The tumour microenvironment in B cell lymphomas. *Nat Rev Cancer,* 14**,** 517-34.

SCOTT, D. W., MOTTOK, A., ENNISHI, D., et al. 2015. Prognostic Significance of Diffuse Large B-Cell Lymphoma Cell of Origin Determined by Digital Gene Expression in Formalin-Fixed Paraffin-Embedded Tissue Biopsies. *J Clin Oncol,* 33**,** 2848-56.

SCOTT, D. W., WRIGHT, G. W., WILLIAMS, P. M., et al. 2014. Determining cell-of-origin subtypes of diffuse large B-cell lymphoma using gene expression in formalin-fixed paraffin-embedded tissue. *Blood,* 123**,** 1214-7.

SEHN, L. H., DONALDSON, J., CHHANABHAI, M., et al. 2005. Introduction of combined CHOP plus rituximab therapy dramatically improved outcome of diffuse large B-cell lymphoma in British Columbia. *J Clin Oncol,* 23**,** 5027-33.

SERAFINI, P., MGEBROFF, S., NOONAN, K. & BORRELLO, I. 2008. Myeloid-derived suppressor cells promote cross-tolerance in B-cell lymphoma by expanding regulatory T cells. *Cancer Res,* 68**,** 5439-49.

SEYMOUR, J. F., GERECITANO, J. F., KAHL, B. S., et al. 2013. The Single-Agent Bcl-2 Inhibitor ABT-199 (GDC-0199) In Patients With Relapsed/Refractory (R/R) Non-Hodgkin

Lymphoma (NHL): Responses Observed In All Mantle Cell Lymphoma (MCL) Patients. *Blood,* 122**,** 1789-1789.

SEYMOUR, J. F., PFREUNDSCHUH, M., TRNĚNÝ, M., et al. 2014. R-CHOP with or without bevacizumab in patients with previously untreated diffuse large B-cell lymphoma: final MAIN study outcomes. *Haematologica,* 99**,** 1343-1349.

SHAFFER, A. L., SHAPIRO-SHELEF, M., IWAKOSHI, N. N., et al. 2004. XBP1, downstream of Blimp-1, expands the secretory apparatus and other organelles, and increases protein synthesis in plasma cell differentiation. *Immunity,* 21**,** 81-93.

SHAFFER, A. L., YU, X., HE, Y., et al. 2000. BCL-6 Represses Genes that Function in Lymphocyte Differentiation, Inflammation, and Cell Cycle Control. *Immunity,* 13**,** 199-212.

SHAFFER, E., ROMESSER AND STAUDT. 2009. IRF4: Immunity. Malignancy! Therapy? *Clinical Cancer Research,* 15**,** 2954-2961.

SHIMAMURA, K., TAKASHIRO, Y., AKIYAMA, N., HIRABAYASHI, T. & MURAYAMA, T. 2004. Expression of adhesion molecules by sphingosine 1-phosphate and histamine in endothelial cells. *Eur J Pharmacol,* 486**,** 141-50.

SHIPP, M., HARRINGTON, DP, ANDERSON, JR, ARMITAGE,JO, BONADONNA, G, B. G., CABANILLAS F, CANELLOS GP, COIFFIER B,, CONNORS JM, C. R., CROWTHER D, DAHLBERG S, ENGELHARD M,, et al. 1993. A Predictive Model for Aggressive Non-Hodgkin's Lymphoma. *New England Journal of Medicine,* 329**,** 987-994.

SIEGEL, S., WAGNER, A., KABELITZ, D., et al. 2003. Induction of cytotoxic T-cell responses against the oncofetal antigen-immature laminin receptor for the treatment of hematologic malignancies. *Blood,* 102**,** 4416-23.

SIOLAS, D. & HANNON, G. J. 2013. Patient-derived tumor xenografts: transforming clinical samples into mouse models. *Cancer Res,* 73**,** 5315-9.

SMITH, D. F., GALKINA, E., LEY, K. & HUO, Y. 2005. GRO family chemokines are specialized for monocyte arrest from flow. *Am J Physiol Heart Circ Physiol,* 289**,** H1976-84.

SNEERINGER, C. J., SCOTT, M. P., KUNTZ, K. W., et al. 2010. Coordinated activities of wild-type plus mutant EZH2 drive tumor-associated hypertrimethylation of lysine 27 on histone H3 (H3K27) in human B-cell lymphomas. *Proc Natl Acad Sci U S A,* 107**,** 20980-5.

SOBUE, S., MURAKAMI, M., BANNO, Y., et al. 2008a. v-Src oncogene product increases sphingosine kinase 1 expression through mRNA stabilization: alteration of AU-rich element-binding proteins. *Oncogene,* 27**,** 6023-33.

SOBUE, S., NEMOTO, S., MURAKAMI, M., et al. 2008b. Implications of sphingosine kinase 1 expression level for the cellular sphingolipid rheostat: relevance as a marker for daunorubicin sensitivity of leukemia cells. *Int J Hematol,* 87**,** 266-75.

SOUERS, A. J., LEVERSON, J. D., BOGHAERT, E. R., et al. 2013. ABT-199, a potent and selective BCL-2 inhibitor, achieves antitumor activity while sparing platelets. *Nat Med,* 19**,** 202-8.

SPIEGEL, S. 1999. Sphingosine 1-phosphate: a prototype of a new class of second messengers. *J Leukoc Biol,* 65**,** 341-4.

SPIEGEL, S. & MILSTIEN, S. 2003. Sphingosine-1-phosphate: an enigmatic signalling lipid. *Nat Rev Mol Cell Biol,* 4**,** 397-407.

STOPECK, A. T., UNGER, J. M., RIMSZA, L. M., et al. 2009. A phase II trial of single agent bevacizumab in patients with relapsed, aggressive non-Hodgkin lymphoma: Southwest oncology group study S0108. *Leuk Lymphoma,* 50**,** 728-35.

STRUB, G. M., PAILLARD, M., LIANG, J., et al. 2011. Sphingosine-1-phosphate produced by sphingosine kinase 2 in mitochondria interacts with prohibitin 2 to regulate complex IV assembly and respiration. *FASEB J,* 25**,** 600-12.

SWERDLOW, S. H., CAMPO, E., PILERI, S. A., et al. 2016. The 2016 revision of the World Health Organization classification of lymphoid neoplasms. *Blood,* 127**,** 2375-90.

SWERDLOW, S. H., CAMPO, E., HARRIS, N.L., JAFFE, E.S., PILERI, S.A., STEIN, H., THIELE, J., VARDIMAN, J.W 2008. *WHO Classification of Tumours of Haematopoietic and Lymphoid Tissues, Fourth Edition*, Lyon.

TAHA, T. A., HANNUN, Y. A. & OBEID, L. M. 2006a. Sphingosine kinase: biochemical and cellular regulation and role in disease. *J Biochem Mol Biol,* 39**,** 113-31.

TAHA, T. A., KITATANI, K., EL-ALWANI, M., et al. 2006b. Loss of sphingosine kinase-1 activates the intrinsic pathway of programmed cell death: modulation of sphingolipid levels and the induction of apoptosis. *FASEB J,* 20**,** 482-4.

TAKABE, K., PAUGH, S. W., MILSTIEN, S. & SPIEGEL, S. 2008. "Inside-out" signaling of sphingosine-1-phosphate: therapeutic targets. *Pharmacol Rev,* 60**,** 181-95.

TAKUWA, N., DU, W., KANEKO, E., et al. 2011. Tumor-suppressive sphingosine-1-phosphate receptor-2 counteracting tumor-promoting sphingosine-1-phosphate receptor-1 and sphingosine kinase 1 - Jekyll Hidden behind Hyde. *American journal of cancer research,* 1**,** 460-481.

TAKUWA, Y. 2002. Subtype-specific differential regulation of Rho family G proteins and cell migration by the Edg family sphingosine-1-phosphate receptors. *Biochimica et Biophysica Acta (BBA) - Molecular and Cell Biology of Lipids,* 1582**,** 112-120.

TAKUWA, Y., OKAMOTO, H., TAKUWA, N., et al. 2001. Subtype-specific, differential activities of the EDG family receptors for sphingosine-1-phosphate, a novel lysophospholipid mediator. *Mol Cell Endocrinol,* 177**,** 3-11.

TAKUWA, Y., TAKUWA, N. & SUGIMOTO, N. 2002. The Edg family G protein-coupled receptors for lysophospholipids: their signaling properties and biological activities. *J Biochem,* 131**,** 767-71.

TAM, W., GOMEZ, M., CHADBURN, A., et al. 2006. Mutational analysis of PRDM1 indicates a tumor-suppressor role in diffuse large B-cell lymphomas. *Blood,* 107**,** 4090-4100.

TENG, G. & PAPAVASILIOU, F. N. 2007. Immunoglobulin somatic hypermutation. *Annu Rev Genet,* 41**,** 107-20.

TERAI, K., SOGA, T., TAKAHASHI, M., et al. 2003. Edg-8 receptors are preferentially expressed in oligodendrocyte lineage cells of the rat CNS. *Neuroscience,* 116**,** 1053-1062.

TONINI, T., ROSSI, F. & CLAUDIO, P. P. 2003. Molecular basis of angiogenesis and cancer. *Oncogene,* 22**,** 6549-56.

TURNER, C. A., MACK, D. H. & DAVIS, M. M. 1994. Blimp-1, a novel zinc finger-containing protein that can drive the maturation of B lymphocytes into immunoglobulin-secreting cells. *Cell,* 77**,** 297-306.

UBAI, T., AZUMA, H., KOTAKE, Y., et al. 2007. FTY720 induced Bcl-associated and Fas-independent apoptosis in human renal cancer cells in vitro and significantly reduced in vivo tumor growth in mouse xenograft. *Anticancer Res,* 27**,** 75-88.

VAN BROCKLYN, J. R., JACKSON, C. A., PEARL, D. K., et al. 2005. Sphingosine kinase-1 expression correlates with poor survival of patients with glioblastoma multiforme:

roles of sphingosine kinase isoforms in growth of glioblastoma cell lines. *J Neuropathol Exp Neurol,* 64**,** 695-705.

VAN DAMME, J., PROOST, P., LENAERTS, J. P. & OPDENAKKER, G. 1992. Structural and functional identification of two human, tumor-derived monocyte chemotactic proteins (MCP-2 and MCP-3) belonging to the chemokine family. *J Exp Med,* 176**,** 59-65.

VENKATARAMAN, K., LEE, Y.-M., MICHAUD, J., et al. 2008. Vascular Endothelium As a Contributor of Plasma Sphingosine 1-Phosphate. *Circulation Research,* 102**,** 669-676.

VESTWEBER, D. 2015. How leukocytes cross the vascular endothelium. *Nat Rev Immunol,* 15**,** 692-704.

VISENTIN, B., VEKICH, J. A., SIBBALD, B. J., et al. 2006. Validation of an anti-sphingosine-1-phosphate antibody as a potential therapeutic in reducing growth, invasion, and angiogenesis in multiple tumor lineages. *Cancer Cell,* 9**,** 225-238.

VITOLO, U., CHIAPPELLA, A., FRANCESCHETTI, S., et al. 2014. Lenalidomide plus R-CHOP21 in elderly patients with untreated diffuse large B-cell lymphoma: results of the REAL07 open-label, multicentre, phase 2 trial. *Lancet Oncol,* 15**,** 730-7.

WADA, N., ZAKI, M. A., HORI, Y., et al. 2012. Tumour-associated macrophages in diffuse large B-cell lymphoma: a study of the Osaka Lymphoma Study Group. *Histopathology,* 60**,** 313-9.

WANG, F., FLANAGAN, J., SU, N., et al. 2012. RNAscope: a novel in situ RNA analysis platform for formalin-fixed, paraffin-embedded tissues. *J Mol Diagn,* 14**,** 22-9.

WANG, G., SILVA, J., KRISHNAMURTHY, K., et al. 2005. Direct binding to ceramide activates protein kinase Czeta before the formation of a pro-apoptotic complex with PAR-4 in differentiating stem cells. *J Biol Chem,* 280**,** 26415-24.

WILLIAMS, R. L., RISAU, W., ZERWES, H. G., et al. 1989. Endothelioma cells expressing the polyoma middle T oncogene induce hemangiomas by host cell recruitment. *Cell,* 57**,** 1053-63.

WILSON, W. H. 2013. Treatment strategies for aggressive lymphomas: what works? *Hematology Am Soc Hematol Educ Program,* 2013**,** 584-90.

WILSON, W. H., YOUNG, R. M., SCHMITZ, R., et al. 2015. Targeting B cell receptor signaling with ibrutinib in diffuse large B cell lymphoma. *Nat Med,* 21**,** 922-926.

WINDH, R. T., LEE, M. J., HLA, T., et al. 1999. Differential coupling of the sphingosine 1-phosphate receptors Edg-1, Edg-3, and H218/Edg-5 to the G(i), G(q), and G(12) families of heterotrimeric G proteins. *J Biol Chem,* 274**,** 27351-8.

WITZIG, T. E., VOSE, J. M., ZINZANI, P. L., et al. 2011. An international phase II trial of single-agent lenalidomide for relapsed or refractory aggressive B-cell non-Hodgkin's lymphoma. *Ann Oncol,* 22**,** 1622-7.

WRIGHT, G., TAN, B., ROSENWALD, A., et al. 2003. A gene expression-based method to diagnose clinically distinct subgroups of diffuse large B cell lymphoma. *Proc Natl Acad Sci U S A,* 100**,** 9991-6.

XIA, P., GAMBLE, J. R., RYE, K. A., et al. 1998. Tumor necrosis factor-alpha induces adhesion molecule expression through the sphingosine kinase pathway. *Proc Natl Acad Sci U S A,* 95**,** 14196-201.

XIA, P., GAMBLE, J. R., WANG, L., et al. 2000. An oncogenic role of sphingosine kinase. *Current Biology,* 10**,** 1527-1530.

XIA, P., WANG, L., GAMBLE, J. R. & VADAS, M. A. 1999. Activation of sphingosine kinase by tumor necrosis factor-alpha inhibits apoptosis in human endothelial cells. *J Biol Chem,* 274**,** 34499-505.

XIAO, C., SRINIVASAN, L., CALADO, D. P., et al. 2008. Lymphoproliferative disease and autoimmunity in mice with increased miR-17-92 expression in lymphocytes. *Nat Immunol,* 9**,** 405-414.

XIE, B., SHEN, J., DONG, A., et al. 2009. Blockade of sphingosine-1-phosphate reduces macrophage influx and retinal and choroidal neovascularization. *J Cell Physiol,* 218**,** 192-8.

YAGI, H., KAMBA, R., CHIBA, K., et al. 2000. Immunosuppressant FTY720 inhibits thymocyte emigration. *Eur J Immunol,* 30**,** 1435-44.

YAMASHITA, H., KITAYAMA, J., SHIDA, D., et al. 2006. Sphingosine 1-Phosphate Receptor Expression Profile in Human Gastric Cancer Cells: Differential Regulation on the Migration and Proliferation1. *Journal of Surgical Research,* 130**,** 80-87.

YATOMI, Y., OZAKI, Y., OHMORI, T. & IGARASHI, Y. 2001. Sphingosine 1-phosphate: synthesis and release. *Prostaglandins Other Lipid Mediat,* 64**,** 107-22.

YONEDA, J., SAIKI, I., KOBAYASHI, H., et al. 1994. Inhibitory effect of recombinant fibronectin polypeptides on the adhesion of liver-metastatic lymphoma cells to hepatic sinusoidal endothelial cells and tumor invasion. *Jpn J Cancer Res,* 85**,** 723-34.

ZHANG, H., DESAI, N. N., OLIVERA, A., et al. 1991. Sphingosine-1-phosphate, a novel lipid, involved in cellular proliferation. *The Journal of Cell Biology,* 114**,** 155-167.

ZHOU, Z., SEHN, L. H., RADEMAKER, A. W., et al. 2014. An enhanced International Prognostic Index (NCCN-IPI) for patients with diffuse large B-cell lymphoma treated in the rituximab era. *Blood,* 123**,** 837-42.

ZIEPERT, M., HASENCLEVER, D., KUHNT, E., et al. 2010. Standard International prognostic index remains a valid predictor of outcome for patients with aggressive CD20+ B-cell lymphoma in the rituximab era. *J Clin Oncol,* 28**,** 2373-80.